

SALINITY TRENDS IN SUISUN BAY AND THE WESTERN DELTA: OCTOBER 1921 – SEPTEMBER 2012



Prepared for:

**San Luis and Delta Mendota Water Authority
P.O. Box 2157, Los Banos, CA 93635**

AND

**State Water Contractors
1121 L. Street, Suite 1050, Sacramento, CA 95814**

Technical Representative:

**Paul Hutton, Ph.D., P.E.
Metropolitan Water District of Southern California
1121 L Street, Suite 900, Sacramento CA 95814-3974**

Prepared by:

**Sujoy Roy, John Rath, Limin Chen, Michael Ungs, and Miguel Guerrero
Tetra Tech, Inc.
3746 Mt. Diablo Blvd, Suite 300, Lafayette, CA 94549**

January 16, 2014

TABLE OF CONTENTS

Acknowledgements	vii
Executive Summary	ix
1. Introduction	1-1
2. Background	2-1
3. Data Summary	3-1
3.1. Compilation of Historical Data Sources	3-1
3.2. Compilation of Electronic Data Sources	3-1
3.3. Supporting Data	3-2
4. Procedures for Cleaning Data and Isohaline Computation	4-1
4.1. Unit Conversions	4-1
4.2. Accounting for Tidal Effects	4-1
4.3. Screening EC Data with Erroneous Values	4-3
4.4. Pairwise Station Cross-checking	4-3
4.5. Data Filling	4-4
4.6. Isohaline Calculations	4-4
4.6.1 Station Distances	4-5
4.6.2 Other Isohalines	4-5
4.6.3 Review of Interpolated Isohaline Positions	4-6
5. Patterns and Trends in Isohalines	5-1
5.1. Time Series of X2	5-1
5.2. Monthly Behavior of X2 Position	5-3
5.3. X2 Position as a Function of Water Year Type	5-3
5.4. Comparison of Interpolated X2 to Daily KM X2	5-3
5.5. Comparison of Interpolated and Modeled X2	5-4
5.6. Trend Evaluation of X2	5-7
5.7. Comparison of Isohaline Positions in Water Year Types	5-8
5.8. Relationship of X2 to Long Term Trends in Delta Outflow and Mean Sea Level	5-8
5.9. Structure of Salinity Gradient in the Estuary	5-8
5.10. Summary of Evaluation	5-9
6. Discussion	6-1
7. References	7-1
Appendix A: Creation of Historical Salinity Observations Database	
Appendix B: Procedures for Cleaning Data and Calculating Isohalines	
Appendix C: Supporting Plots for All Isohalines	
Appendix D: Statistical Procedures Used	

Appendix E: Mann-Kendall Trend Test and Wilcoxon Rank-Sum Test for
All Isohalines

LIST OF TABLES

Table 3-1	DPW or DWR Bulletin Site Information	3-4
Table 3-2	Bulletin 23 Data Summary of Data Used	3-5
Table 3-3	CDEC Summary of Data Used	3-6
Table 5-1	Recalibration of KM-equation with Monthly Interpolated X2s.....	5-12
Table 5-2	Sacramento X2 Mann-Kendall Test Results, WY 1922–1944.....	5-12
Table 5-3	Sacramento X2 Mann-Kendall Test Results, WY 1945–1967.....	5-13
Table 5-4	Sacramento X2 Mann-Kendall Test Results, WY 1968–1999.....	5-13
Table 5-5	Sacramento X2 Mann-Kendall Test Results, WY 2000-2012	5-14
Table 5-6	Sacramento X2 Mann-Kendall Test Results, WY 1922–1967.....	5-14
Table 5-7	Sacramento X2 Mann-Kendall Test Results, WY 1968–2012.....	5-15
Table 5-8	Sacramento X2 Mann-Kendall Test Results, WY 1922–2012.....	5-15
Table 5-9	San Joaquin X2 Mann-Kendall Test Results, WY 1922–1944	5-16
Table 5-10	San Joaquin X2 Mann-Kendall Test Results, WY 1945–1967	5-16
Table 5-11	San Joaquin X2 Mann-Kendall Test Results, WY 1968–1999	5-17
Table 5-12	San Joaquin X2 Mann-Kendall Test Results, WY 2000–2012	5-17
Table 5-13	San Joaquin X2 Mann-Kendall Test Results, WY 1922–1967	5-18
Table 5-14	San Joaquin X2 Mann-Kendall Test Results, WY 1968–2012.....	5-18
Table 5-15	San Joaquin X2 Mann-Kendall Test Results, WY 1922–2012	5-19
Table 5-16	Sacramento X2 Wilcoxon Rank Sum Test Results	5-19
Table 5-17	San Joaquin X2 Wilcoxon Rank Sum Test Results	5-19
Table 5-18	Fitted Slopes and Intercepts for Bias-correction of DSG Model.....	5-20
Table 5-19	Fitted Slopes and Intercepts for Bias-correction of K-M Model.....	5-20
Table 5-20	Fitted Slopes and Intercepts for Bias-correction of K-M Model.....	5-21

LIST OF FIGURES

Figure 3-1 CDEC and Bulletin 23 stations providing salinity data for this analysis..... 3-9

Figure 3-2 All Bulletin 23 stations with grab sample salinity data..... 3-11

Figure 3-3 Stations in the CDEC dataset 3-13

Figure 4-1 Comparison of salinity from Bulletin 23 source data with CDEC data from the same day, where overlapping data were available. 4-7

Figure 4-2 Example of usual isohaline calculation 4-8

Figure 4-3 Example of leaving isohaline uncalculated 4-8

Figure 4-4 Example of heavy weighting toward western isohaline bounding pair..... 4-9

Figure 4-5 Bulletin 23 derived monthly average EC values after cleaning and filling with 5-year moving average..... 4-10

Figure 4-6 CDEC monthly average EC values after cleaning and filling with 5-year moving average. 4-11

Figure 5-1 Time series of Sacramento X2 from October 1921– September 2012..... 5-22

Figure 5-2 Time series of San Joaquin X2 from October 1921– September 2012..... 5-23

Figure 5-3 Box plots of X2 for various time intervals 5-24

Figure 5-4 Variation in X2 over the period of record..... 5-25

Figure 5-5 Line and scatter plots of X2 by month and by water year type..... 5-26

Figure 5-6 Comparison of daily interpolated X2 from this report and X2 from Kimmerer and Monismith at daily time resolution 5-27

Figure 5-7 Boxplots of coefficient of variations of Delta outflow, with whiskers extending to the most extreme data points no further than 1.5 times the interquartile range from the box edges 5-28

Figure 5-8 Time series of coefficient of variations of Delta outflow, with 10-year running medians shown in blue. Calculations were performed on daily flow data within each calendar month, and the time series of the monthly values across different years is shown here..... 5-29

Figure 5-9	Scatter plots of modelled monthly DSG X2 positions against the monthly interpolated X2 positions, grouped by month, river, and three different ranges of CVs for monthly flow	5-30
Figure 5-10	Scatter plots of DSG model residuals, grouped by month and river.	5-31
Figure 5-11	Scatter plots of DSG model residuals adjusted by the bias-correction model of Figure 5-10.	5-32
Figure 5-12	Time series of DSG model residuals adjusted by the bias-correction model of Figure 5-10.....	5-33
Figure 5-13	Scatter plots of modelled monthly Kimmerer-Monismith X2 positions against the monthly interpolated X2 positions, grouped by month, river, and three different ranges of CVs for monthly flow.	5-34
Figure 5-14	Scatter plots of K-M model residuals, grouped by month and river.....	5-35
Figure 5-15	Scatter plots of K-M model residuals adjusted by the bias-correction model of Figure 5-14.....	5-36
Figure 5-16	Time series of K-M model residuals adjusted by the bias-correction model of Figure 5-14.....	5-37
Figure 5-17	Scatter plots of modelled monthly Kimmerer-Monismith X2 positions against the monthly interpolated X2 positions, grouped by month, river, and three different ranges of CVs for monthly flow.	5-38
Figure 5-18	Scatter plots of K-M model residuals, grouped by month and river.....	5-39
Figure 5-19	Scatter plots of K-M model residuals adjusted by the bias-correction model of Figure 5-18.....	5-40
Figure 5-20	Time series of K-M model (with refitted coefficients) residuals adjusted by the bias-correction model of Figure 5-18	5-41
Figure 5-21	Trend decomposition of X2 time series data.....	5-42
Figure 5-22	Trend decomposition of Delta outflow and sea level time series data.....	5-43
Figure 5-23	Salinity structure in Bay and Delta stations using surface salinity values as a function of station distance normalized by X2 and grouped by X2 position.	5-44
Figure 5-24	Comparison of isohaline position S1 through S6 to X2.....	5-45

ACKNOWLEDGEMENTS

We thank the California Department of Water Resources, Bay-Delta Office, Delta Modeling Section, specifically Tara Smith, Eli Ateljevich and Joey Zhou for performing various analyses in support of this study. In particular, this includes an independent data cleaning procedure for the California Data Exchange Center (CDEC) data on salinity in the Delta, and the implementation of a Delta Simulation Model (DSM-2) run for 1921 to 1976 to allow computation of ratios between higher high tide salinity and daily average salinity.

EXECUTIVE SUMMARY

The location of the low salinity zone in San Francisco Bay is thought to be related to the health of several estuarine species. Specifically, the location where the bottom salinity is 2 parts per thousand (ppt) (termed as X2 and reported as the distance in kilometers from Golden Gate), has been used as the basis for outflow management in the estuary. There is great interest in understanding how the low salinity zone in general, and the X2 position in particular, has changed over time under different conditions of hydrology, exports, and development. The present work supports such an effort through the collection of data over a nine-decade period, with additional screening and cleaning to better characterize salinity trends in the Delta.

Data incorporated in this work include historical grab sample data and modern conductivity sensor data. The historical data are based on a compilation from documents from October 1921 to June 1971 from the California Department of Public Works (DPW) and its successor agency, the Department of Water Resources (DWR). Data from scanned paper copies of these bulletins were used to develop an electronic database of salinity throughout the Delta and portions of San Francisco Bay. In addition, modern databases were queried for data in Suisun Bay and the western Delta, including: 1) California Data Exchange Center (CDEC); 2) the Interagency Ecological Program (IEP) water quality data; and 3) USEPA's STORET dataset. The modern data were further supplemented by U.S. Geological Survey data for stations in San Francisco Bay to account for situations where the low salinity zone extends into the Bay, typically under high flows. The combined data gathering effort resulted in a master database containing salinity data from October 1921–September 2012, i.e. water years 1922–2012.

The data collected from these sources contained errors associated with variations in sampling and analytical methodology. For example, the historical data were grab samples collected every few days. Because salinity is a quantity that can vary significantly over the course of a day at a fixed location depending on when during the tidal cycle a grab sample is collected, this is a potential source of error. The modern data, collected every few minutes by automated conductivity sensors, do not have this challenge, but may also have errors associated with sensor malfunction or fouling. Recognizing these features of the data, a significant effort was expended to “clean” the data to remove values that appeared to be clearly inconsistent with other values.

The cleaned data were then used to develop daily estimates of salinity at each station. These daily estimates were used to calculate the daily and monthly X2 position along the Sacramento and San Joaquin Rivers. Other isohalines, corresponding to salinities from 1 to 6 ppt were also computed. Various statistical analyses were performed on the X2 and other isohalines to characterize behavior over time and in response to different hydrologic conditions.

Using the X2 time series calculations for the Sacramento and San Joaquin Rivers, we could fit the data using an auto-regressive equation structure as used by Kimmerer and Monismith (1992). The process resulted in a set of equations with coefficients that were similar to the original work. An important finding from the fitting of the longer data set using the K-M approach is that the general structure of the model holds even though there have been significant changes in the Delta and Bay over this period (changes in channel depth, Delta exports, regulatory changes, upstream land use changes, and some mean sea level rise). While it is possible that the changes in the coefficients for different time periods of fitting encapsulate this information, it is not straightforward to infer the mechanistic linkage between a coefficient and one or more of these changes. The linkage between the differing K-M coefficients and underlying causes was not explored in detail in this work.

Two different forms of the Kimmerer and Monismith model (original published coefficients and re-fit coefficients) and the Delta Salinity Gradient (DSG) model (Hutton, 2013) were used for additional evaluation using the interpolated X2 values developed in this work. The models captured major features of the interpolated X2 but there were differences in the nature of the fit and bias. In general, the largest systematic disagreements between modeled and interpolated X2s occur for interpolated X2s at the extreme ends of its range. For all three models, the change in long-term behavior of the model residuals was small compared to the disagreements between model and interpolated X2 positions under extreme salinity conditions. For future application, we have reported the linear function representing bias (function of X2 and month) for each of the models. These linear equations can be used to correct K-M or DSG-predicted X2 values. This evaluation of the bias between interpolated and modeled X2 provides insight into the future use of these models, especially where inferences are to be drawn between small differences in X2 or for conditions where X2 values fall in extreme high or low ranges.

Aside from comparison with models, the interpolated X2 values were subject to a variety of statistical tests. When the interpolated X2 values were grouped by water year type and compared across the pre- and post-project periods (1921–1967 and 1968–2012), a difference in the X2 position was noted in the wet months of drier years: X2 was higher in the more recent period during the wet months. Similarly in the dry months of dry years, X2 was lower in the post-project period. These visual observations were supported by a trend analysis that showed statistically significant increases in X2 from November through May (excluding March) over the entire period, and a statistically significant decrease in X2 in August and September. These findings were broadly true for X2 computed along both the Sacramento and San Joaquin Rivers.

This report is supported by electronic and text appendices detailing the data compilation, cleaning methodology, and statistical evaluation, and can serve as the basis for future studies of salinity in Suisun Bay and the western Delta.

1. INTRODUCTION

Freshwater inflows into estuaries have a direct influence on the salinity structure and thus the habitat available for estuarine species. In San Francisco Bay, the salinity distribution has been related to the health of estuarine species in the Suisun Bay and western Delta. In particular, the location of the low salinity zone, defined as the distance from Golden Gate where the bottom salinity is 2 parts per thousand (ppt) (termed as X2), has been identified as a metric that is thought to be related to the health of several species (Jassby et al., 1995). Using data collected over specific time frames, this zone has been associated with the greatest abundance of pelagic organisms of the upper estuary, including the threatened Delta smelt (*Hypomesus transpacificus*), the state-listed longfin smelt (*Spirinchus thaleichthys*) and juvenile striped bass (*Morone saxatilis*) (Jassby et al., 1995). The X2 position is also associated with the abundance of undesirable species such as the invasive Asian clam (*Corbula amurensis*). The relationship between the low salinity zone and the responses of individual species are a topic of continued research interest (Feyrer et al., 2007, 2011; Kimmerer et al., 2009), and broader science underlying the driving mechanisms between water quality, habitat quality, and species abundance continues to evolve.

The position of the X2 isohaline during the months of February through June is used as the basis of inflow management in the estuary (Water Right Decision 1641, State Water Resources Control Board, 1999). The outflow standard was intended to represent the relationship between springtime precipitation and the extent of estuarine habitat as had occurred in the late 1960s and early 1970s (US EPA, 2012). The standard does not define X2 requirements at other times of the year. The recent biological opinion on Delta smelt (USFWS, 2008) includes an X2 requirement in fall months following wet and above normal water years. Much of the published literature on X2 as well as its relationship to various biological indicators is based on data collected over limited periods, typically over the last 4 decades. Given the importance of the low salinity zone for estuarine species, and of X2 in the management of water flows in the estuary, the present analysis builds on past work by extending the salinity data set used for the original Jassby et al. (1995) analysis, using historical data (pre-1967) as well as more recent data (post-1991). It also extends other salinity trend evaluations in the Bay-Delta, which focused on more limited time periods or on salinity at specific stations and not on the isohaline position (Fox et al., 1991; Shellenbarger and Schoellhamer, 2011; Enright and Culberson, 2009; Moyle et al., 2010). Although the starting point of the data used here do not represent pre-development conditions such as those obtained through analysis of paleoclimatic signals (Stahle et al., 2001), they do represent a wide range of hydrologic conditions and watershed development activities, including construction of reservoirs, water exports, and changing land use (Fox et al., 1990; Contra Costa Water District, 2010).

As in all retrospective analysis of salinity, this work is focused on surface salinity measurements which are the form in which most historical data are available. The historical data are based on a compilation from documents from October 1921 to June 1971 from the

California Department of Public Works (DPW) and its successor agency, the Department of Water Resources (DWR). The specific numbered documents include Bulletins 23, 27, 65, and 130. Citations of the DPW/DWR bulletins used for the database are provided in the References section. Data from scanned paper copies of these bulletins were used to develop an electronic database of salinity throughout the Delta and portions of San Francisco Bay. For brevity, scanned data from all the bulletins will henceforth be referred to as Bulletin 23 data, and the originating agency referred to as DWR. In addition to the Bulletin 23 data, modern databases were queried for data in Suisun Bay and the western Delta, including: 1) California Data Exchange Center (CDEC) daily, hourly and event (15 Min) data; 2) the Interagency Ecological Program (IEP) water quality data; and 3) USEPA's STORET dataset. The modern data were further supplemented by U.S. Geological Survey data for stations in San Francisco Bay to account for situations where the low salinity zone extends into the Bay, typically under high flows. For brevity, the combined CDEC, IEP, STORET, and USGS data will be referred to as CDEC data from now on. The combined data gathering effort resulted in a master database containing salinity data from October 1921–September 2012, i.e. water years 1922–2012.

The database developed here, although mostly reported by a single agency (DPW and its successor DWR), is known to not be noise- and error-free; this noise may arise from variations in sampling and analytical methodology. For example, Bulletin 23 data were grab samples collected every few days. Because salinity is a quantity that can vary significantly over the course of a day at a fixed location depending on when during the tidal cycle a grab sample is collected, this is a potential source of error. The modern data, collected every few minutes by automated conductivity sensors, do not have this challenge, but may also have errors associated with sensor malfunction or fouling. Recognizing these features of the data, a significant effort was expended to “clean” the data to remove values that appeared to be clearly inconsistent with other values. These data were then used to develop daily and monthly estimates of salinity at each station.

Cleaned data from fixed salinity stations in the database were then used to interpolate daily and monthly values of X2 over the 1921–2012 period, wherever the data were adequate for the computation. To understand changes in the isohaline positions over the period of observational record, we also computed isohalines corresponding to 1 through 6 ppt total dissolved solids (TDS) (labeled as S1 through S6). Together, these multiple isohalines help define the low salinity zone in Suisun Bay and the western Delta.

The monthly isohaline data computed over the entire study period were evaluated for patterns over time visually and through statistical trend analysis. The isohaline position data were also compared by type of water year (whether wet, above normal, below normal, dry, or critically dry). The data were also evaluated by plotting against an X2-normalized scale to assess where there was consistent structure in the horizontal salinity in the Bay-Delta. Longer term trends in the data were also compared against two key variables that drive salinity in the Suisun Bay and western Delta: net Delta outflows and mean sea level.

The remainder of this report describes the database development process and evaluation of trends in salinity in Suisun Bay and the western Delta. The principal chapters are organized as follows, and the report is supported by multiple text and electronic data appendices.

Previous studies pertaining to the empirical characterization of the salinity field in San Francisco Bay are briefly discussed in Chapter 2.

Chapter 3 presents an overview of the data collection effort and the sources used to obtain data in the Delta and Bay. This chapter is supported by Appendix A outlining specific steps associated with the compilation of data from past DWR paper reports, and summaries of the resulting database from the DWR Bulletins and from modern sources.

Chapter 4 presents the cleaning approach utilized to remove erroneous data from the database and to convert the data values into consistent units. The methods applied differ for the Bulletin 23 data and the CDEC data. The interpolation approach used to calculate X2 (and other isohaline positions) for each month is also presented. Because the slope of the surface salinity-distance relationship changes with flow and with distance along the estuary, the position of X2 is dependent on the interpolation approach and stations used. The present approach focuses on using log salinity versus distance interpolation across stations that bound a specific isohaline level, i.e., for the X2 or 2,640 $\mu\text{s}/\text{cm}$ isohaline, we look for stations just higher and lower than this value. This chapter is supported by Appendix B which provides details on each of these steps.

Chapter 5 presents an evaluation of the variation of computed X2 over time and across specific time intervals and water year types. Also computed are trends in these values for different time intervals. A subset of analyses is reported for the S1 through S6 in Appendix C. This chapter is also supported by Appendix D which summarizes the approach for determining the trend of time series data.

Chapter 6 presents a summary and discussion of the analysis, highlighting the benefits of the use of a long record, and also the limitations associated with data quality, when different sampling/analysis approaches are combined.

2. BACKGROUND

The characterization of salinity in Suisun Bay and the western Delta has been the focus of substantial previous work, with models developed to allow prediction of the low salinity zone as a function of outflow and other variables. Given the need for developing relatively rapid estimates of salinity for regulating Delta outflows, there has been a particular interest in empirical models, in addition to more detailed hydrodynamic models for special studies. A brief description of these empirical methodologies is presented in this chapter.

In the original analysis in support of the water quality standard, an approach for estimating the position of X2 developed by Kimmerer and Monismith (1992) was utilized. This approach assumed that the bottom salinity of 2 ppt corresponded to an average surface salinity value of 1.76 ppt. For regulatory purposes, this bottom salinity is assumed to be equivalent to a surface electrical conductance (standardized to 25 °C) of 2,640 $\mu\text{s}/\text{cm}$. There was a need to convert from bottom salinity to surface salinity because most prior observations in the Bay and Delta had focused on surface salinity. For a specific day, using surface salinity observations at fixed stations, the value of X2 was interpolated using log salinity and distance normalized by upstream estuary volume. This approach was used to estimate X2 between 1967 and 1991. Using continuous daily data on surface salinity Kimmerer and Monismith (1992) derived an autoregressive equation where X2 is a function of antecedent X2 position and Delta outflow. The daily X2 equation was used to fill the gaps in the data record, and the resulting data series was used to estimate a monthly equation using a similar structure. The monthly flow-X2 relationship (Kimmerer and Monismith, 1992) has been expressed as¹:

$$X2(t) = 122.2 + 0.328X2(t-1) - 17.6 \log(Q_{\text{out}}(t))$$

where Q_{out} is the mean monthly Delta outflow in terms of cubic feet per second (cfs) and $X2(t-1)$ is the previous month isohaline position expressed as km from Golden Gate. As a general tool for estimating X2 under different flow conditions, the above equation is used widely (referred to as the K-M equation). More recently this equation has been updated using an exponent form of the Q_{out} term, rather than the logarithm, albeit using the same surface salinity dataset as in the original analysis (Monismith et al., 2002). However, at any point in time, X2 can also be interpolated directly from observations of salinity at fixed stations.

An empirical model of salinity was also developed by Denton and Sullivan (1993) (updated Denton, 1994), utilizing boundary salinity values representative of the downstream ocean and upstream riverine environments, and a concept called antecedent outflow, representing flow time-history in the Delta. The equation can be represented as:

¹ A slightly different intercept for this equation has also been reported for flow in m^3/second :
 $X2(t) = 95 + 0.33X2(t-1) - 17.6 \log(Q_{\text{out}}(t))$ (Jassby et al., 1995)

$$S = (S_o - S_b) * \exp[-\alpha * G(t)] + S_b$$

where S is the salinity at a given location, S_o and S_b are the ocean and river boundary salinities, and $G(t)$ is the term representing the flow history, and α is an empirically-determined constant, computed for selected Delta locations based on field data. The G-model estimates salinity at individual locations, rather than the X2 position estimated using the K-M equation.

A hybrid of the K-M equation and G-model, proposed by Hutton (2013), is called the Delta Salinity Gradient (DSG) model. In this model, by assuming the modified form of the X2 equation (Monismith et. al. 2002) and steady-state conditions, X2 is related to antecedent outflow as follows:

$$X2(t) = \Phi_1 * G(t)^{\Phi_2}$$

where Φ_1 and Φ_2 are empirically determined coefficients. Salinity is then estimated at individual locations through the following relationship:

$$S = (S_o - S_b) * \exp[\tau * (X/X2) - 1/\Phi_2] + S_b$$

where S is the salinity at a given location in mS/cm, S_o and S_b are representative downstream ocean and upstream riverine boundary salinities, and $\tau = \ln[(2.64 - S_b)/(S_o - S_b)]$. This equation can be used to determine salinity at any longitudinal distance from Golden Gate (X) given $X2$ and Φ_2 and assuming reasonable values for S_o and S_b .

Finally, in a study parallel to that presented in this document, an Artificial Neural Network (ANN) model is being developed to estimate salinity as a function of flow history and sea level at different longitudinal distances from Golden Gate for the entire period of the salinity record, with the model being trained on the available field data. This work builds upon previously developed ANNs being employed by DWR for water operations planning studies within the CalSim model (Finch and Sandhu, 1995; Mierzwa, 2002; Seneviratne et al., 2008). This work is ongoing and will be documented in a separate report.

3. DATA SUMMARY

Data were obtained from two categories of sources: scanned from paper reports published by DWR, representing values from October 1921 to June 1971, and from electronic sources from different entities, spanning July 1964 to September 2012. As expected, the major effort in this step was associated with compilation of the paper report data. Supporting data on flow and sea level were also obtained. Key steps and resulting datasets are described below. A map displaying the stations from both datasets that were used for this analysis is shown in Figure 3-1.

3.1. COMPILATION OF HISTORICAL DATA SOURCES

Salinity data were scanned from the reports shown in Table 3-1. The salinity data in these reports are grab samples collected at fixed stations nominally every 4 days, typically an hour and a half following higher high tide, which corresponds to the highest salinity for the day. However, there were exceptions in that some dates were not sampled or the sample was collected at a different point in the tidal cycle. The latter situation was noted in footnotes in the original source documents. The units for most observations were in terms of chloride, although the volume differed (some were in parts per million, others in parts per 100,000). In this effort, pages containing salinity data from each bulletin were manually transcribed into Microsoft Excel tables, retaining the structure in the original table, including numeric values, units, and footnotes. The Excel data were then independently checked against the paper copies for all years. After the final Excel tables were checked and corrected, they were converted to a Microsoft Access database where each observation was assigned a row describing the station, date, value, units, and footnotes, if any.

Details of the creation of this historical database are presented in Appendix A, with all supporting information in electronic files for independent review and audit. A map displaying all stations with available data is shown in Figure 3-2. The specific stations, focused on Suisun Bay and the western Delta, and the number of data points used as the raw data set for this analysis, are listed in Table 3-2. Although many other stations were identified in the historical data compilation, not all could be used because of limited data availability or because of their position in the interior Delta. Future studies employing these data may evaluate patterns at locations beyond those considered in the present work.

3.2. COMPILATION OF ELECTRONIC DATA SOURCES

Modern salinity data in Suisun Bay and the western Delta are obtained from conductivity probes and reported as electrical conductivity (EC) standardized to 25 °C, as opposed to analytical determinations of chloride noted above. Three primary datasets for the western Delta included the following: 1) CDEC daily, hourly and event (15-Min) data (downloaded from <http://cdec.water.ca.gov/>); 2) the IEP water quality data (downloaded from <http://www.water.ca.gov/iep/products/data.cfm>); and 3) the STORET dataset. These datasets cover different time periods and were merged to form the longest records possible for each station. When data from different sources are overlapping for a certain time period, the

merging of data followed the general priority of: 1) CDEC data; 2) IEP data; and 3) STORET data. When data are inconsistent among the data sources, the IEP and STORET data are given higher priority, merging through the order of IEP/STORET, then CDEC. The station locations for these data are shown in Figure 3-3 along a line estimated to represent the centerline of the estuary.

The following describes the processes and steps used to compile the salinity dataset:

1. Download CDEC daily EC data from the CDEC website for all stations of interest. Merge all the daily dataset for the same station. CDEC daily data generally cover the time period from the mid- to late-1990s, and in some cases from the 2000s.
2. Download CDEC hourly EC data from the website. Use the hourly data to fill in data gaps and extend records of the CDEC daily data discussed above. The hourly data were first converted to daily before merging with the daily data. CDEC hourly data generally cover a longer period from the mid- to late-1980s or the mid-1990s to 2012.
3. Further extend the records to the 1960s through merging with the IEP water quality dataset. The IEP dataset covers the period from mid 1960s to late 1990s. The IEP dataset if not reported as a daily time step, was converted to daily first before merging with the CDEC data.
4. Further merge or fill the data gaps using the STORET dataset. The STORET dataset covers the period from 1960s to 1992. Note that most of the records from STORET are identical to the IEP dataset and therefore are redundant.

Data obtained from these sources are summarized (stations and periods of data availability) in Table 2-3.

In addition to the Suisun Bay and western Delta locations, additional data from the U.S. Geological Survey (USGS) in San Francisco Bay were also included (http://sfbay.wr.usgs.gov/sediment/cont_monitoring/index.html). These stations are needed for the subset of conditions where the Delta outflow rates are high and the position of the X2 isohaline is downstream of the Martinez station. USGS data were reported in practical salinity units and were converted to EC (Schemel, 2001). Two locations with a relatively long period of observations (Point San Pablo at the surface, and Carquinez at mid-depth) were used in the analysis. These stations are also shown in Figure 3-3.

3.3. SUPPORTING DATA

Daily net Delta outflow (NDO) data from October 1, 1929 through September 30, 2012 were obtained from DAYFLOW (<http://www.water.ca.gov/dayflow/output/Output.cfm>). We extended this dataset back to October 1, 1921. Average monthly Delta outflow values were provided by DWR (DWR, 1957). Daily outflows were estimated by Paul Hutton for this extended period from daily Sacramento and San Joaquin River inflow data (DPW 1931).

Sea level data at Golden Gate were obtained from the National Oceanic and Atmospheric Administration (NOAA).

Table 3-1
DPW or DWR Bulletin Site Information

Report	Years
DPW/DWR Bulletin 23	1929–1961
DPW Bulletin 27	1921–1931
DWR Bulletin 65	1962
DWR Bulletin 130	1963– 1971

**Table 3-2
Bulletin 23 Data Summary of Data Used**

Station	Code	Start	End	Number of Grab Sample Observations	Distance from Golden Gate (km)
<i>Suisun and San Pablo Bays</i>					
Point Orient	PTO	2/10/1926	8/30/1957	2,427	19.8
Point Davis	PTD	2/6/1926	8/14/1957	1,907	40.6
Crockett	CRK	9/26/1946	6/30/1971	1,729	44.6
Benicia	BEN	1/15/1943	6/30/1963	1,616	52.3
Martinez	MRZ	1/2/1946	6/30/1971	1,773	52.6
Bulls Head Point	BHP	2/2/1926	7/14/1941	1,325	54.7
West Suisun	WSN	9/2/1946	6/30/1963	1,924	59.5
Bay Point	BPT	2/2/1926	10/22/1944	922	64.2
Port Chicago	PCT	9/2/1946	6/10/1971	2,385	66
O and A Ferry	OAF	6/2/1920	3/30/1957	2,904	74.8
Pittsburg ²	PTS	1/6/1942	5/6/1971	1,541	77.2
<i>Lower Sacramento River</i>					
Collinsville	CLL	6/2/1920	9/30/1969	3,564	81.8
Emmaton	EMM	6/4/1920	6/30/1971	2,067	92.9
Threemile Slough Bridge	TSB	9/4/1926	8/30/1969	2,377	96.6
Rio Vista	RVB	8/4/1920	5/26/1971	3,068	102.2
Isleton Bridge	ITB	7/2/1924	6/26/1971	2,008	110.6
Walnut Grove	WNG	8/14/1920	10/30/1939	250	124.6
<i>Lower San Joaquin River</i>					
Antioch	ANH	6/14/1920	6/26/1971	4,532	88.4
Antioch Bridge	ANB	10/2/1956	5/22/1971	804	93.7
Jersey Island	JER	6/2/1920	6/18/1971	1,376	98.8
False River	FRV	4/10/1965	6/30/1971	277	101.2
Oulton Point	OPT	9/2/1952	6/26/1963	779	108.1
San Andreas Landing	SAL	9/2/1952	6/2/1971	1,339	113.1
Webb Pump	WBP	7/28/1920	10/18/1952	1,151	115.9
Medford Island Pump	MIP	7/18/1924	11/6/1925	51	128.6
Kings Island Pump	KIP	6/18/1931	10/26/1939	94	135.5
Stockton Country Club	SCC	8/18/1926	11/6/1934	184	146.1
Stockton	SCT	9/2/1948	7/30/1952	250	152.6

² Anomalies found during the tidal adjustment of Bulletin 23 Pittsburg data prevented it from being used in the calculation of isohaline positions

**Table 3-3
CDEC Summary of Data Used**

Station	DWR Distance from Golden Gate (km)	RKI	Agency	Source	Data Type and Units	Frequency	Period of Record
<i>Suisun & San Pablo Bays</i>							
Martinez	54/55 ³	RSAC054	DWR	CDEC	EC (uS/cm)	Hourly	06/1994 – 07/2012
			DWR	CDEC	EC (uS/cm)	Daily	01/2006- 01/2012
			USBR	USBR-CVO	EC (uS/cm)	Daily	01/1965 – 01/1996
			USBR	STORET	EC (uS/cm)	Daily	10/1967- 04/1992
Port Chicago	64	RSAC064	USBR	CDEC	EC (uS/cm)	Daily	01/1999 – 01/2012
			USBR	CDEC	EC (uS/cm)	Hourly	12/1996 – 07/2012
			USBR	USBR-CVO	EC (uS/cm)	Daily	01/1966 – 01/1998
			USBR	USBR-CVO	EC (uS/cm)	Hourly	04/1996 – 05/2005
			USBR	STORET	EC (uS/cm)	Daily	10/1967- 04/1992
Mallard Island	75	RSAC075	DWR	CDEC	EC (uS/cm)	Daily	01/1995 – 07/2012
			DWR	CDEC	EC (uS/cm)	Hourly	12/1983 – 07/2012
			DWR	DWR-ESO	EC (uS/cm)	Event	09/1982 – 10/1985
			DWR	DWR-ESO	EC (uS/cm)	Hourly	01/1984 – 09/2002
			DWR	STORET	EC (uS/cm)	Daily	1/1981 – 12/1987
Chipps Island	75	RSAC075	DWR	STORET	EC (uS/cm)	Daily	05/1976 – 09/1992

³ The stations named Martinez are in slightly different locations for the USBR and CDEC data sources. The CDEC station is located at RKI RSAC054. The USBR station is at the Shell refinery pier, about 900 meters upstream of the CDEC station (Eli Ateljevich, personal communication). We treat the data as coming from one station for calculations not explicitly involving distance from Golden Gate (e.g., data cleaning and filling), but calculation of isohaline positions uses the distance corresponding to the relevant station location.

Table 3-3 (continued)
CDEC Summary of Data Used

Station	DWR Distance from Golden Gate (km)	RKI	Agency	Source	Data Type and Units	Frequency	Period of Record
<i>Lower Sacramento River</i>							
Collinsville	81	RSAC081	USBR	CDEC	EC (uS/cm)	Daily	01/1999 – 07/2012
			USBR	CDEC	EC (uS/cm)	Hourly	03/1988 – 07/2012
			USBR	USBR-CVO	EC (uS/cm)	Daily	01/1966 – 01/1998
			USBR	USBR-CVO	EC (uS/cm)	Hourly	04/1996 – 05/2005
			USBR	STORET	EC (uS/cm)	Daily	10/1967 – 11/1992
Emmaton	92	RSAC092	USBR	CDEC	EC (uS/cm)	Hourly	01/1988 – 07/2012
			DWR	DWR-BDO	EC (uS/cm)	15MIN	07/1988 – 02/2000
			USBR	USBR-CVO	EC (uS/cm)	Daily	01/1964 – 01/1996
			USBR	USBR-CVO	EC (uS/cm)	Hourly	04/1996 – 05/2005
			USBR	STORET	EC (uS/cm)	Daily	10/1967 – 11/1992
Rio Vista	101	RSAC101	USBR	CDEC	EC (uS/cm)	Daily	08/1999 – 07/2012
			DWR	CDEC	EC (uS/cm)	Daily	12/1995 – 10/2003
			DWR	CDEC	EC (uS/cm)	Hourly	01/1984 – 07/2012
			DWR	DWR-ESO	EC (uS/cm)	Hourly	05/1983- 09/2002
			USBR	USBR-CVO	EC (uS/cm)	Daily	01/1966 – 01/1998
			USBR	USBR-CVO	EC (uS/cm)	Hourly	04/1996 – 05/2005
			USBR	STORET	EC (uS/cm)	Daily	10/1967 – 11/1992

Table 3-3 (continued)
CDEC Summary of Data Used

Station	DWR Distance from Golden Gate (km)	RKI	Agency	Source	Data Type and Units	Frequency	Period of Record
<i>Lower San Joaquin River</i>							
Pittsburg	77	RSAC077	USBR	CDEC	EC (uS/cm)	Daily	01/1999 – 07/2012
			USBR	CDEC	EC (uS/cm)	Hourly	03/1988 – 07/2012
			USBR	USBR-CVO	EC (uS/cm)	Hourly	04/1996 – 05/2005
			USBR	USBR-CVO	EC (uS/cm)	Daily	01/1965 – 01/1998
			USBR	STORET	EC (uS/cm)	Daily	10/1967 – 11/1992
Antioch	85.75	RSAN007	USBR	CDEC	EC (uS/cm)	Daily	08/1999 – 07/2012
			DWR	CDEC	EC (uS/cm)	Daily	01/1995 – 07/2012
			DWR	CDEC	EC (uS/cm)	Hourly	02/1984 – 07/2012
			DWR	DWR-ESO	EC (uS/cm)	Hourly	05/1983- 09/2002
			USBR	STORET	EC (uS/cm)	Daily	10/1967 – 11/1992
Blind Point	92.85	RSAN014	DWR	CDEC	EC (uS/cm)	Daily	12/1995 – 08/1999
			DWR	CDEC	EC (uS/cm)	Daily	03/2010 – 07/2012
			DWR	CDEC	EC (uS/cm)	Hourly	01/1984 – 09/1999
			DWR	DWR-CD	EC (uS/cm)	Event	09/1982 – 09/1997
			DWR	STORET	EC (uS/cm)	Daily	08/1971 – 10/1979
Jersey Point	95.75	RSAN018	USBR	CDEC	EC (uS/cm)	Daily	08/1999 – 07/2012
			USBR	CDEC	EC (uS/cm)	Hourly	03/1988 – 07/2012
			USBR	USBR-CVO	EC (uS/cm)	Daily	01/1964 – 01/1998
			USBR	USBR-CVO	EC (uS/cm)	Hourly	04/1996 – 05/2005
			USBR	STORET	EC (uS/cm)	Daily	10/1967 – 11/1992
Three Mile Slough at San Joaquin River	100.4	SLTRM004	USGS	CDEC	EC (uS/cm)	Daily	06/2008 – 07/2012
			DWR	DWR-CD	EC (uS/cm)	15MIN	10/1987 – 02/1998
San Andreas Landing	109.2	RSAN032	USBR	CDEC	EC (uS/cm)	Daily	08/1999 – 07/2012
			USBR	CDEC	EC (uS/cm)	Hourly	03/1988 – 07/2012
			USBR	USBR-CVO	EC (uS/cm)	Daily	01/1964 – 01/1998
			USBR	USBR-CVO	EC (uS/cm)	Hourly	04/1996 – 05/2005
			USBR	STORET	EC (uS/cm)	Daily	10/1967 – 05/1988



Figure 3-1 CDEC and Bulletin 23 stations providing salinity data for this analysis. Gray lines are county boundaries.

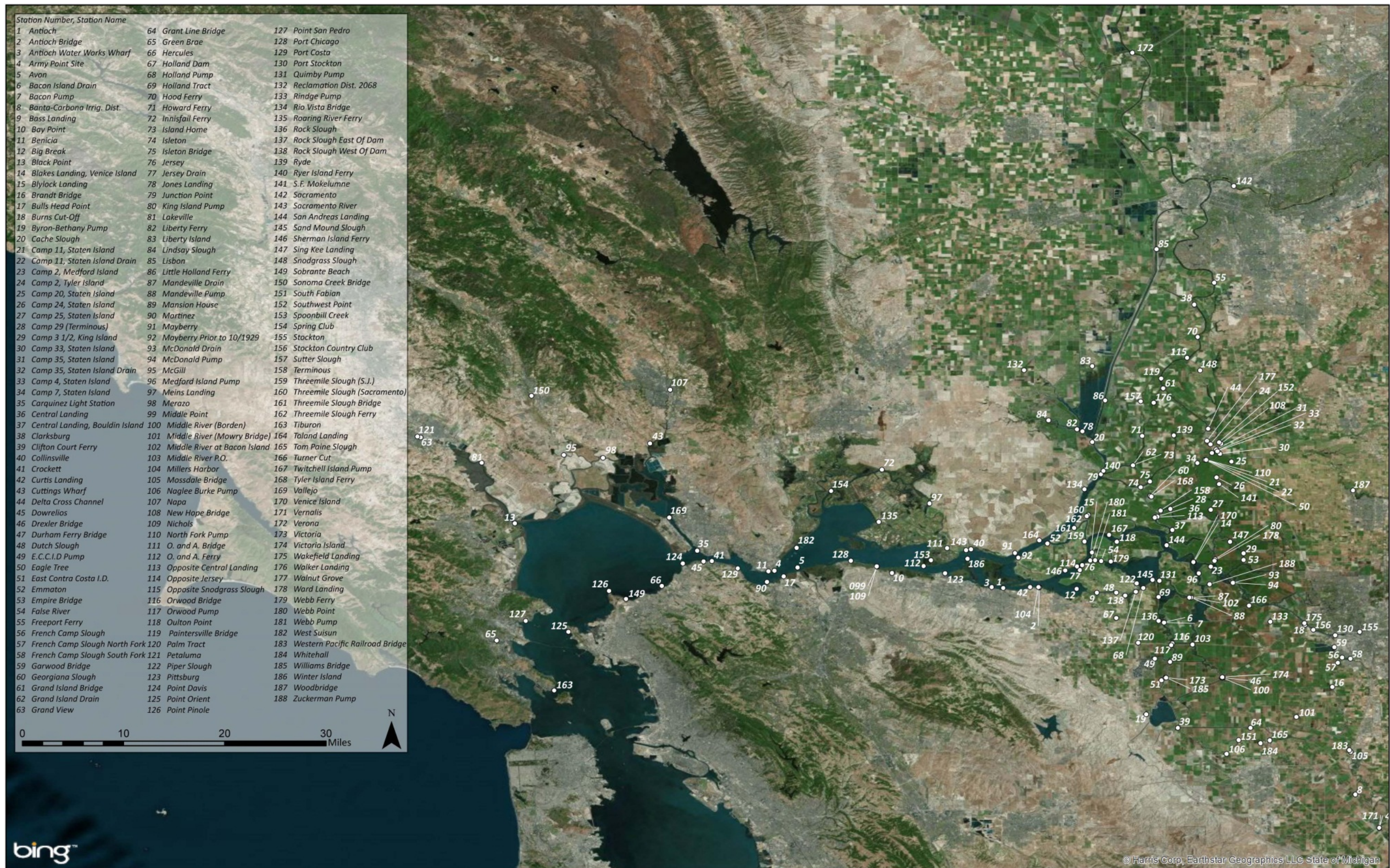


Figure 3-2 All Bulletin 23 stations with grab sample salinity data. A subset of these stations, largely based on availability of sufficient data, were used for the salinity trend analysis.

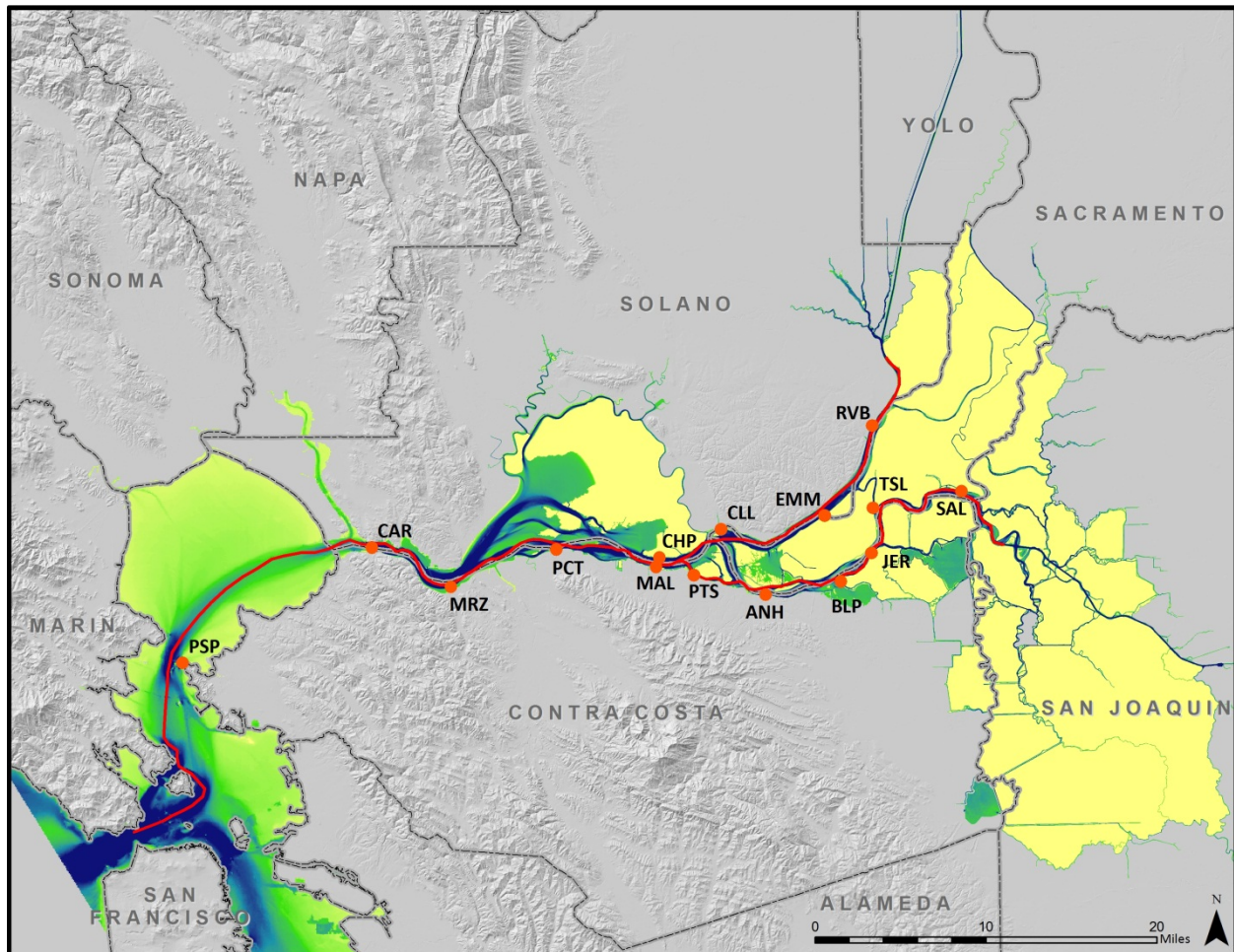


Figure 3-3 Stations in the CDEC dataset. The CAR and PSP stations data were obtained from the USGS, and the others primarily from CDEC or IEP. The color shading in the estuary corresponds to the most recent baywide bathymetry data. The solid line corresponds to the mid-depth along the approximate center of the estuary.

4. PROCEDURES FOR CLEANING DATA AND ISOHALINE COMPUTATION

The process of integrating the different observed data sets involved converting numerical values of salinity to a common set of units, accounting for tidal effects on grab sample measurements, performing conversions to represent the values as a daily average salinity, filling data gaps, and identifying appropriate locations to compute the position of specific isohalines. The goal of this chapter is to present a brief summary of these steps. Details are provided in the Appendix B and related sub-sections and in supporting electronic files.

4.1. UNIT CONVERSIONS

The CDEC data report salinity as EC standardized to 25 °C. The Bulletin 23 grab sample data report salinity as chlorides. All data were converted to EC using the following relationships developed from co-located chloride and EC data (Denton, 2013).

$$\text{EC} = f(x) = \begin{cases} -8.5 \times 10^{-5} \cdot x^2 + 3.5 \cdot x + 175, & x > 30 \text{ ppm Cl} \\ 6.67 \cdot x + 80, & x \leq 30 \text{ ppm Cl (San Joaquin River sites) ,} \\ 12.74 \cdot x + 76.8, & x \leq 30 \text{ ppm Cl (All other sites)} \end{cases}$$

where x is the input chloride concentration in ppm and the resulting EC is in $\mu\text{S/cm}$.

Two alternatives were explored for the unit conversion, but were rejected in favor of the above. The first alternative included computation of EC using chloride and temperature and using published relationships between these quantities (Hill et al., 1986 or Schemel, 2001). However, this alternative was rejected because this approach breaks down at lower salinities where watershed inputs of salts are quantitatively significant, and chloride is not the only anion at meaningful concentrations. The second alternative involved performing a direct correlation between grab sample salinity and observed EC for that day, where obtained through CDEC. This method was used by Enright and Culberson (2009) in an analysis of salinity data at two Delta locations over a similar time period. This method was rejected because it did not directly account for the tidal effect on salinity, described below.

4.2. ACCOUNTING FOR TIDAL EFFECTS

Over a tidal cycle, salinity at a fixed station varies, depending on the flow rate and location. The goal of the data integration was to convert all data to a daily average basis. The DWR Bulletin 23 grab sample data were usually obtained at higher high tide (HHT) or low high tide (LHT). Most stations' grab sample values were converted using the output of a Delta Salinity Model 2 (DSM2) simulation that was performed by DWR in support of this study. Statistical methods of tidal correction—estimated from datasets with representations of both high tide EC and daily average EC—were considered as alternatives to the DSM2 simulation. The DSM2 approach was selected because it appears to give superior results

when validated against the period of overlap (1964 to 1971) between the CDEC (daily average) and Bulletin 23 (high tide) datasets. Using the DSM2-based approach also simplified the correction of the numerous Bulletin 23 stations without corresponding daily average observations; using the statistical approaches to tidal corrections for these stations would have required using estimates from nearby stations for which direct estimates were possible. While the simulation was not refined to give a completely accurate characterization of the interior delta, it was considered to be adequate for Suisun Bay and the western Delta.

The daily averages were computed over 24 hours rather than a 25-hour tidal average. This may introduce some errors over a 14-day cycle. However, in examining the same issue over a period where both hourly and daily data were available, Monismith et al. (2002) reported that the error associated with this approximation was slight. The 24-hour averaging was therefore used for all of the data averaging in this work.

The simulation output consisted of daily maximum and average salinities at one kilometer intervals east of Martinez from October 1921 to September 1976. Data were also produced with specific output settings for a named set of important stations. For each station and date, the grab sample value was multiplied by the ratio of average salinity to maximum salinity for the corresponding station and date in the DSM2 output. If a station was located at one of the named DSM2 output settings, its ratio was used. Otherwise, the ratio from the nearest point on the one-kilometer grid was used.

Three stations (PTO, PTD, and CRK) are west of the downstream DSM2 boundary. For these stations, tidal correction was achieved using statistical relationships between daily maximum and average salinities estimated from continuous salinity datasets. Daily average values were predicted from daily maximum values using the predictions of a log-log linear regression. The relationship used to adjust the data at PTO was estimated from USGS station PSP. The relationship used at PTD and CRK was estimated from IEP station WIC (Shellenbarger and Schoellhamer, 2011). Both the PSP and WIC data were reported in practical salinity units and were converted to EC (Schemel, 2001) prior to regression.

For all stations, low high tide grab sample values were assumed to be equal to daily average value because the alternative statistical methods of tidal correction, which were described previously, indicated that LHT EC values were generally comparable to daily average EC values. Specific technical details of this method of accounting for tidal effects as well as the other methods considered can be found in Appendix B.

A comparison of salinity from Bulletin 23 source data (tidally corrected and expressed as EC) with CDEC data from the same day, where overlapping data were available (1964-1971), is shown in Figure 4-1. Although there is noise in the data, the method works well for several stations at higher salinities. There is also noise at the lower salinity stations (Rio Vista and San Andreas Landing) although this is explained by the more complex relationship between chloride and EC at low salinities in natural waters, specifically the contribution of watershed versus oceanic sources of salinity. However, the data from the Pittsburg station stand out and appear to be systematically lower than the corresponding CDEC station. For this reason, all Bulletin 23 Pittsburg data were excluded from the subsequent analysis.

4.3. SCREENING EC DATA WITH ERRONEOUS VALUES

The modern EC data (CDEC/IEP/STORET) were found to contain a variety of data validation issues. The following tests were performed to address the most obvious data concerns:

- Check for unit consistency. There are cases where values changed by large magnitude over long record periods in the same dataset. This was probably due to a shift in the EC units between mS/cm and μ S/cm. These values were converted to the same units (μ S/cm).
- Screen for extreme outliers. There are cases where extreme high values existed in the dataset for a certain station that are several times of the peak values observed. These values were very likely outliers because they are far outside the normal range of the salinity observed for that station. To more systematically identify these, we used a criterion of 5 times of the data range (defined here as difference between 99th and 1st percentile) observed for that station. These values were taken out of the data record.
- Check for data errors. Cross-referencing using nearby stations and multiple data sources for the same station were performed to check for potential data errors. For example, cases where values are shown as zero but show continuous data in the nearby stations, are indicative of data errors and were deleted from the merged dataset.
- Scan the data for long runs of repeated values. When the exact same numeric value appears repeatedly, it is indicative of sensor malfunction or related error. These values are very likely invalid, so they were removed or replaced with data from secondary sources.

Salinity data from the bay stations (Point San Pablo and Carquinez Strait) from USGS were previously validated to remove the types of errors noted above and did not need to be similarly cleaned.

4.4. PAIRWISE STATION CROSS-CHECKING

Once the Bulletin 23 data had been converted to daily average EC and the CDEC data were cleaned as described above, a more sophisticated cleaning exercise was performed by comparing daily average EC values at pairs of stations. The underlying conceptual model is that for moderately high salinities, perhaps exceeding 500 to 1,000 μ S/cm, where the ocean signal is dominant, there should be a clear west to east gradient of decreasing salinity. Thus, as one moves east from Golden Gate, daily average observed salinity should decrease. If, however, the data at a pair of stations are not consistent with this pattern, i.e., an eastern station has a higher salinity than a western station, the challenge is to determine which of the two salinity values is erroneous, and there is no *a priori* way of making this determination. To perform this cleaning step, we statistically estimated piecewise-polynomial fits of nearby stations' EC data using least-squares regressions. The values that differed greatly (by more than four standard errors) or too often (by more than two standard errors multiple times) from regression predictions were removed from the dataset. Specific technical details of the cleaning process can be found in Appendix B.

The conclusion of this process resulted in what we term a “cleaned” daily salinity data set. The cleaning procedure as described in this section is somewhat subjective, and it is possible that other methods of cleaning will result in slightly different data sets. A more stringent exclusion procedure may result in data that more closely adhere to the conceptual model of distance versus salinity, at the risk of rejecting a much larger number of possibly correct observations. The role of cleaning is discussed in subsequent chapters of this report.

4.5. DATA FILLING

The irregular salinity data availability and the method of isohaline calculation (see next section) require that some data filling be done to have a reasonably complete isohaline record. First, we filled missing values based on the salinity data of nearby stations. The same procedure of running regressions between the EC values of pairs of stations that was used for data cleaning in the previous section was repeated on the cleaned dataset. We attempted to fill each missing value with the prediction of one of these regressions; the specific prediction used varied daily, depending on data availability and relative station position. In particular, the filling of downstream stations from upstream stations on days with very low upstream salinities was often restricted because of low predictive power in that situation—downstream salinity can vary across orders of magnitude for the same small upstream salinity.

After this “neighbor station filling” was completed, we linearly interpolated any remaining short gaps (up to 8 days, inclusive) in each station’s salinity record. Specific technical details of the cleaning process can be found in Appendix B.

Time series plots of the final converted (Bulletin 23) or observed (CDEC) EC data after cleaning and filling are shown in Figure 4-5 and Figure 4-6.

4.6. ISOHALINE CALCULATIONS

Different interpolation approaches may be used to calculate X2 (and other isohaline positions) for each day. Because the slope of the surface salinity-distance relationship changes with flow and with distance along the estuary, the position of X2 is somewhat dependent on the interpolation approach and stations used. The approach used here focuses on using log salinity versus distance interpolation across two stations that bound a specific isohaline level, i.e., for the X2 or 2,640 $\mu\text{s}/\text{cm}$ isohaline, we look for the station just higher and lower than this value. If the two bounding stations are further than 25 km apart, we left the isohaline position uncalculated due to uncertainty about interpolation accuracy when using stations with very large spatial separations (this occurs in about 10% of cases in the calculation of X2 at the daily time step). The monthly isohaline positions are defined as the mean value of all non-missing daily isohaline positions for months where at least 14 daily isohalines values were computed.

Calculating a unique isohaline position at each day with this bounding method is based on the notion of a monotonic west to east salinity gradient in the Delta. The data generally follow this conceptual model: when there are sufficient data to perform the calculation of daily X2, 92% of cases have a unique pair of stations that bound X2 as in Figure 4-2. Some robustness in the calculation procedure is desired for the remaining cases, however. This is

particularly important in the calculations of daily isohalines and relatively more important in the Bulletin 23 dataset than in the CDEC dataset.

If the bookending pair is not near the western boundary of the dataset but all stations west of the bookending pair indicate salinities below the target isohaline value, we left the isohaline position uncalculated because the lone station above the target isohaline value is more likely to be erroneous than all of the western stations. This situation occurs in about 0.5% of all days in calculation of X2 at the daily time step. See Figure 4-3 for one example.

If more than one pair of stations bounds the isohaline level, we calculate the isohaline position as a (nonlinear) weighted average of the westernmost and easternmost of the positions determined by the bounding pairs, where the weighting is determined by the salinities of the intermediate stations. This tiebreaking process is necessary in less than 8% of X2 calculations at the daily time step. See Figure 4-4 for an example where the westernmost and easternmost positions are far apart and the weighting predicts an isohaline position close to the western bounding pair due to many intermediate stations with salinities below 2,640 $\mu\text{S}/\text{cm}$.

The whole calculation process is repeated for each combination of dataset (CDEC or Bulletin 23), river (Sacramento or San Joaquin), and time step (daily or monthly). For the period in the mid-1960s to early-1970s where salinity data from both datasets are available, the isohaline position calculated from the CDEC dataset is used preferentially when combining the CDEC and Bulletin 23 datasets. Specific technical details of the isohaline calculations can be found in Appendix B.

4.6.1 Station Distances

In the original work describing the development of the X2 calculation, station distances in the estuary are shown diagrammatically and are stated to be based on the distance along the deepest part of the estuary along the main shipping channel (Jassby et al., 1995). However, there is no official line that can be used to compute distances for any station not listed in Jassby et al. (1995). Because the analysis presented here considered fixed stations that were both east and west of the stations in the original analysis, we used the officially accepted distances in DWR's databases that are listed in Table 3-3 for the CDEC dataset. For the Bulletin 23 dataset, we used the station distances listed on the scanned bulletins, which are shown converted to kilometers in Table 3-2.

4.6.2 Other Isohalines

The presentation in the main section of this report is focused principally on the X2 isohaline. However, the positions of the isohalines corresponding to 1, 2, 3, 4, 5, and 6 ppt TDS at the surface were used computed for the corresponding EC values (Suits, 2002). Together these isohalines are used to define the low salinity zone in the estuary. These use the letter S to distinguish from X2:

S1: 1,700 $\mu\text{S}/\text{cm}$

S2: 3,400 $\mu\text{S}/\text{cm}$

S3: 5,100 $\mu\text{S}/\text{cm}$

S4: 6,800 $\mu\text{S}/\text{cm}$

S5: 8,400 $\mu\text{S}/\text{cm}$

S6: 10,000 $\mu\text{S}/\text{cm}$

The series of these 7 daily and monthly isohaline values are provided in the accompanying Excel spreadsheet “Table9-isohaline-positions.xlsx”.

4.6.3 Review of Interpolated Isohaline Positions

A visual review of the final dataset identified several periods where some isohaline positions appeared to vary only a small amount over long periods of time:

- Sacramento River S1 and X2, August to November 1927
- San Joaquin River S1, May to June 1928
- San Joaquin River S5 and S6, October 1957 to January 1958
- San Joaquin River S6 September 1958 to January 1959

A closer examination of these time periods revealed this behavior was consistent with the prevailing salinity conditions. As an additional check, we computed the isohaline positions in the same manner as above using only the cleaned data (no within- or between-station filling), and these unfilled isohaline positions show similar behavior as the final cleaned and filled isohaline positions during the above periods.

There were also times when the EC values at Port Chicago (1925–1946) and Emmaton (1940-1955) were periodically higher than those of their western neighbors under low-salinity conditions. This appears to be related to the filling from upstream stations (mainly OAF for PCT and TSB for EMM) and the weaker interstation relationship with low tidal signals. In light of these potential inaccuracies, the isohaline calculation procedure used was designed to be resistant to isolated errors, as shown in Figure 4-4. When a single value along the salinity gradient demonstrated unusual behavior, the interpolation procedure considered additional stations in estimating isohaline positions. In this instance, the computed X2 positions were minimally affected if the filled values at Port Chicago and Emmaton were excluded from the interpolation process.

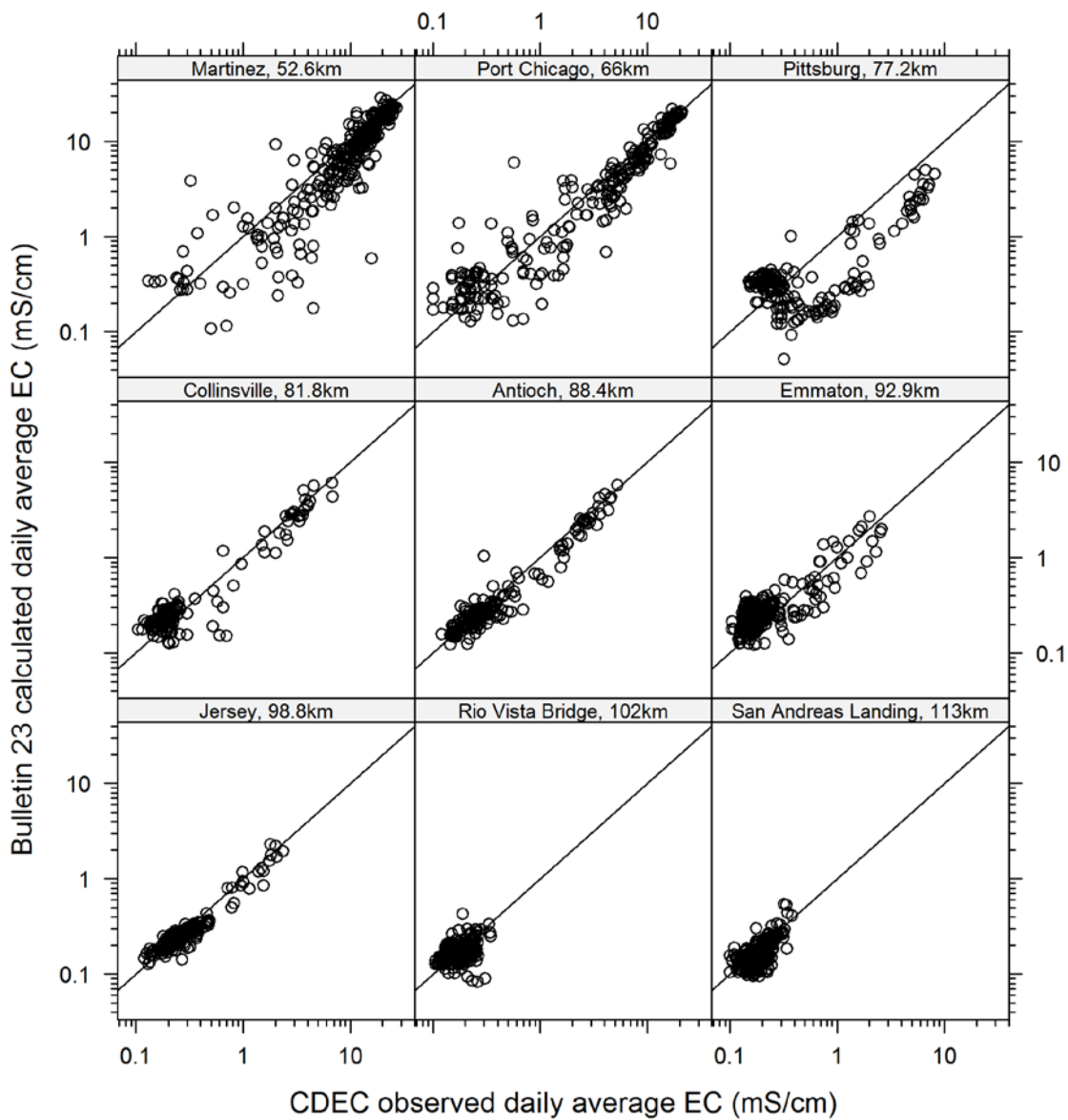


Figure 4-1 Comparison of salinity from Bulletin 23 source data (tidally corrected and expressed as EC) with CDEC data from the same day, where overlapping data were available. Distances shown are distances from scanned bulletins.

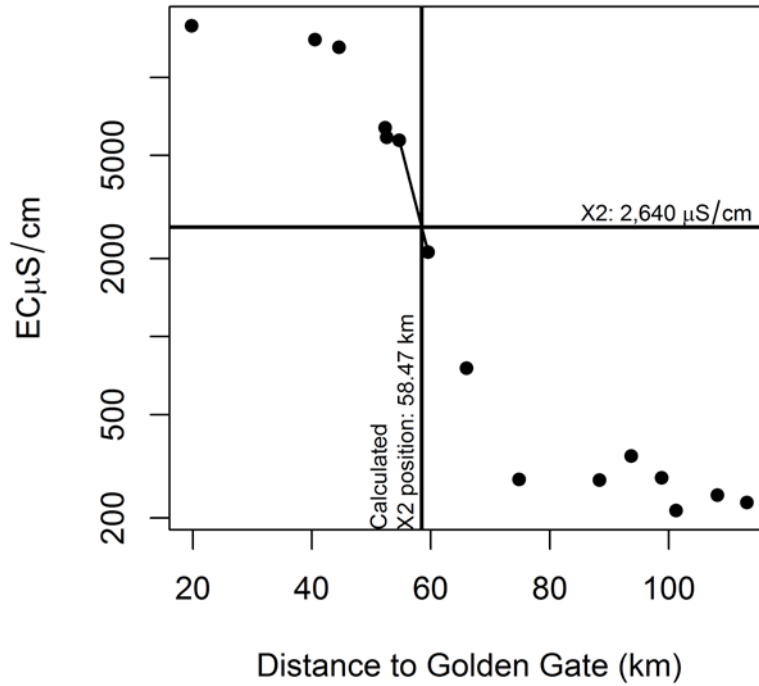


Figure 4-2 Example of usual isohaline calculation: X_2 salinity (horizontal) with exactly one pair of bounding stations, April 1, 1957, along the San Joaquin River.

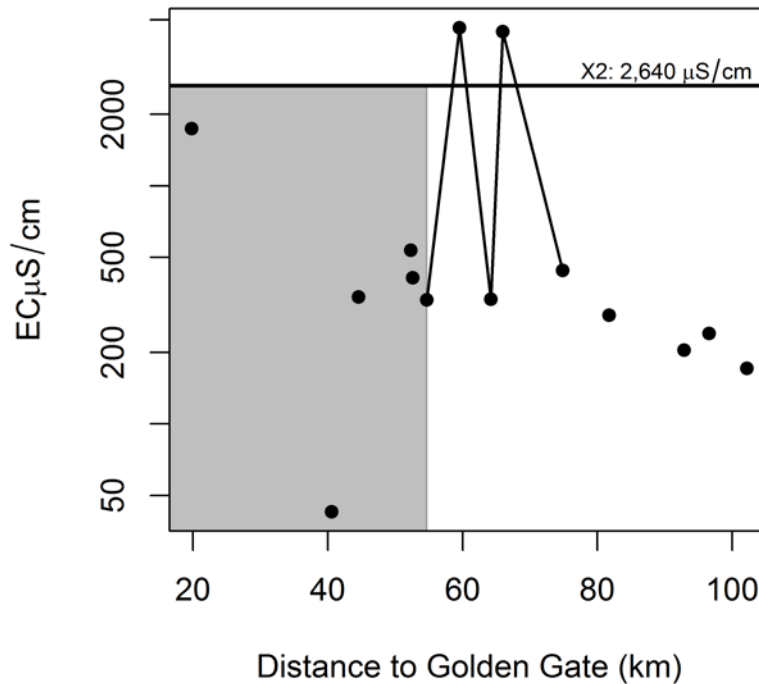


Figure 4-3 Example of leaving isohaline uncalculated: X_2 salinity (horizontal) with lower salinity western stations and high salinity outliers, February 14 1938, along the Sacramento River.

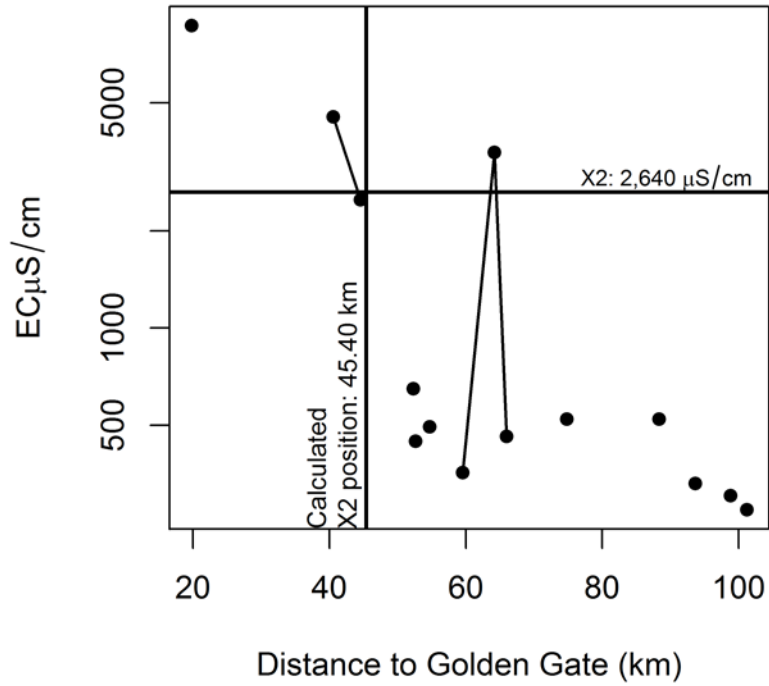


Figure 4-4 Example of heavy weighting toward western isohaline bounding pair: predicted X2 position (vertical) and X2 salinity (horizontal) with monthly station salinities, March 25, 1952, along the San Joaquin River.

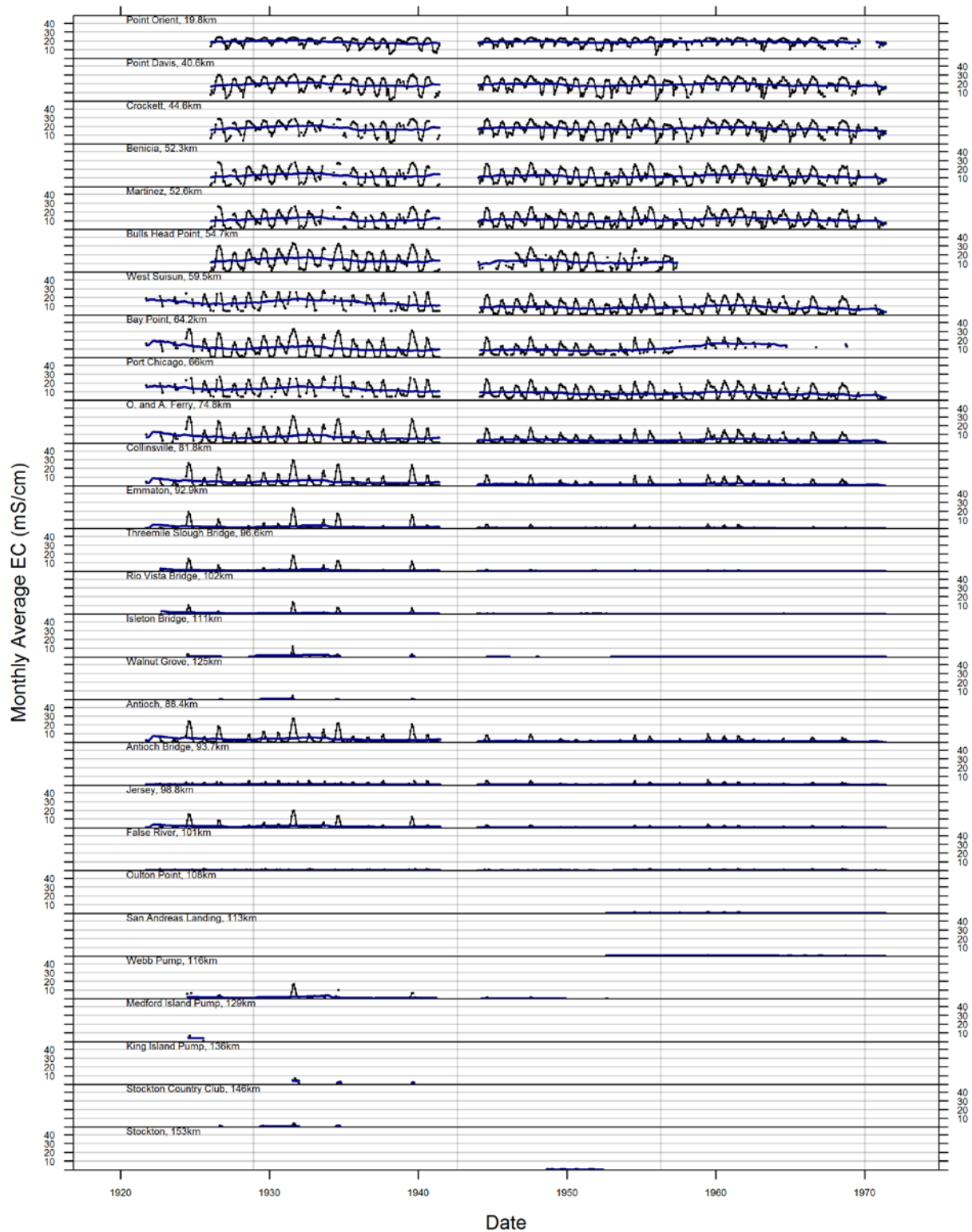


Figure 4-5 Bulletin 23 derived monthly average EC values after cleaning and filling with 5-year moving average.

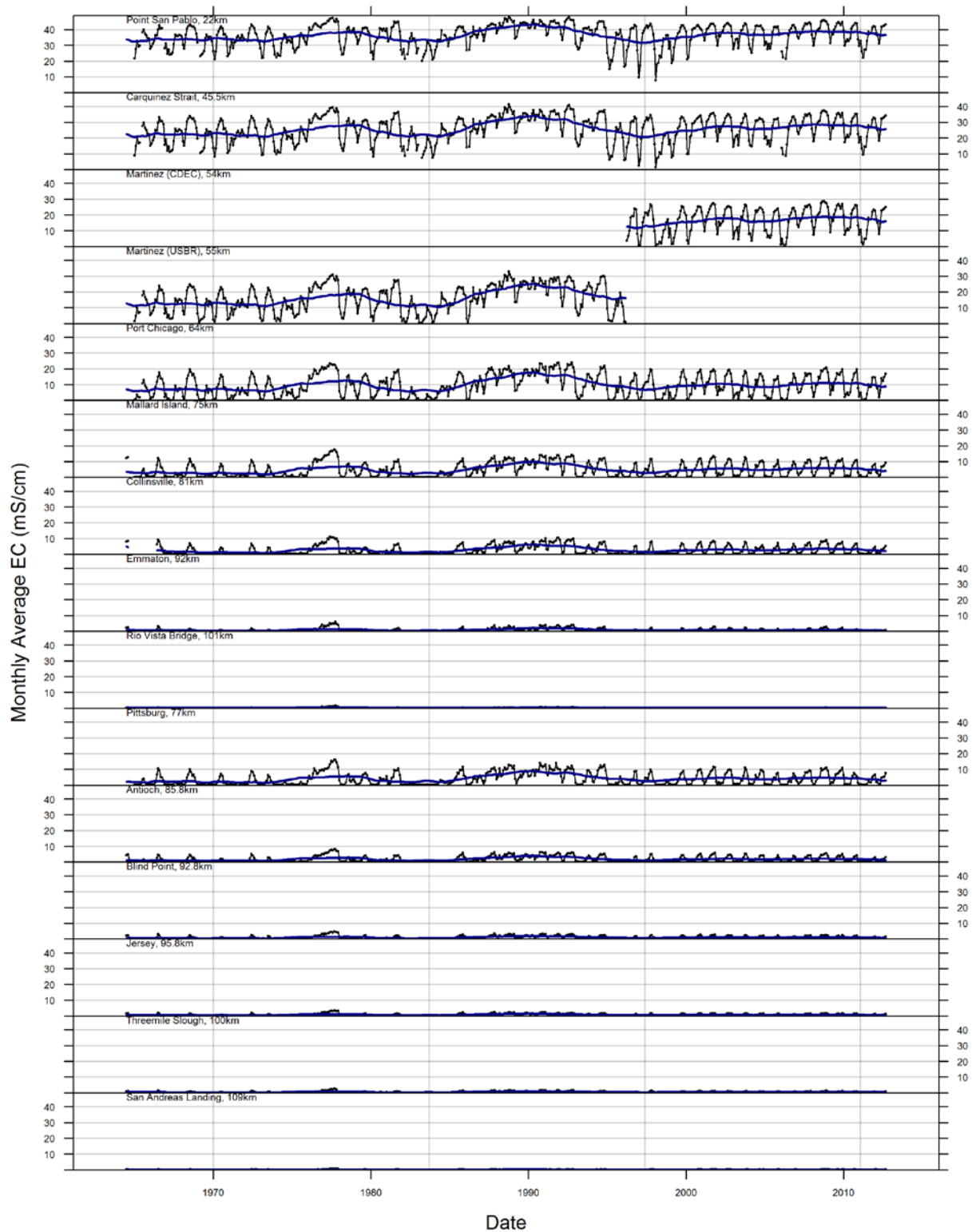


Figure 4-6 CDEC monthly average EC values after cleaning and filling with 5-year moving average.

5. PATTERNS AND TRENDS IN ISOHALINES

This chapter presents our exploration of the changes in the isohalines over the period for which the data have been compiled and organized in the preceding sections. Different types of analyses are performed: time series of monthly isohaline position over the period of record, box plots of monthly isohalines grouped into three periods, plots showing isohaline position by month as a function of the water year type (whether wet, above normal, below normal, dry, or critically dry), and statistical evaluation of trends in isohaline position. We present plots comparing trends in X2 versus driving variables such as Delta outflow and mean sea level. Finally, we also consider the horizontal structure of salinity in the bay and Delta, where salinity at different locations is shown as a function of distance normalized to X2. Similar plots and tables for key analyses for isohalines other than X2 (S1, S2, S3, S4, S5, and S6) are presented in appendices as noted below.

5.1. TIME SERIES OF X2

The monthly values of X2 for the period of the data record are shown in Figure 5-1 and Figure 5-2. For the Sacramento River, the position of the X2 isohaline could be computed for 1,016 months over this period (out of a total of 1,090 possible months over October 1921 to September 2012). For the San Joaquin River, the position of the X2 isohaline could be computed for 1,001 months over the same period. Gaps are significant in the early part of the record, where the value of X2 could not be computed because of insufficient data.

These data, coupled with net Delta outflow data from DAYFLOW (Q_{out}) were used to fit a set of autoregressive equations, for different time periods and different rivers, in the form of Kimmerer and Monismith (1992) and Jassby et al. (1995). The fitted equation from Kimmerer and Monismith, 1992, was:

$$X2(t) = 122.2 + 0.328X2(t-1) - 17.6 \log(Q_{out}(t)).$$

We recalibrated the same model,

$$X2(t) = A + B X2(t-1) - C \log(Q_{out}(t)),$$

for each river for several different time periods:

- the entire record, October 1921 to September 2012;
- the period with only Bulletin 23 data, October 1921 to June 1964;
- the period with only CDEC data, July 1971 to September 2012; and

- the period for which the above estimate of Kimmerer and Monismith was computed, October 1967 to November 1991.

Results are shown in Table 5-1. Note that the logarithmic term in the K-M equation precludes its use for negative outflows that occurred during some periods of the historical record.

The following observations can be made from this fitting exercise over different time periods:

- In all cases, equations that are broadly similar to the original K-M equation provide reasonable fits, with coefficients that are approximately in the same range for the flow term. For example, the coefficient for the flow term ranges between -16.2 and -18.8, compared to the original coefficient of -17.6. The coefficient for the previous month's X2 shows greater variation and ranges between 0.392 and 0.439, compared to the original coefficient of 0.328. Even though there have been significant changes in the Delta and Bay over this period (changes in channel depth, Delta exports, regulatory changes, upstream land use changes, and some mean sea level rise), it appears that the model formulation adequately captures these changes. While it is possible that the changes in the coefficients for different time periods of fitting encapsulate this information, it is not straightforward to infer the mechanistic linkage between a coefficient and one or more of these changes. This linkage between coefficients and other Delta and Bay changes was not explored in detail in this work.
- In general the fit is slightly better when a smaller time period is used, likely reflecting lower variability over this period. Fits were slightly poorer for the entire period of record (1921–2012) and for the more recent period (1971–2012) with better quality continuous EC data, and were likely related to the wider range of environmental driving conditions. Fits were also poorer for the grab sample data-derived X2 (1921–1964), possibly reflecting the greater underlying noise in this data set.
- Importantly, however, the fitted coefficients are not identical to those reported by Kimmerer and Monismith, even when the same 1967-1991 fitting period is used. There are several possible reasons for this difference: (i) the raw data used for the original analysis was not available, and the present work used an independent data set that, albeit developed from the same sources, may contain small differences for flow as well as salinity; (ii) Kimmerer and Monismith computed one X2 value per day, not separate values for the two river branches; and (iii) there may be subtle differences in methodology, i.e., the gaps in the daily X2 in Kimmerer and Monismith's work were filled by an autoregressive equation before the monthly X2 was calculated (Jassby et al., 1995), whereas in this work, we filled salinity values and then computed the X2.
- The best information on the original Kimmerer and Monismith analysis that we had access to was the X2 values used for developing the equation (Ed Gross, personal communication, 2013). No corresponding salinity data were available. Additional

characterization of the original X2 values and the X2 values developed in this work is presented below in Section 5.4.

5.2. MONTHLY BEHAVIOR OF X2 POSITION

Box plots of the X2 isohaline value for different months, with water years in seven groups (1922–1944 (pre-Shasta), 1945–1967, 1968–1999, 2000–2012 (POD era), 1922–1967, 1968–2012, and 1922–2012) are shown in Figure 5-3. Although changes in the upstream watershed have occurred over the entire period, water years 1967 and 1968 are used as an important boundary in these plots reflecting the full implementation of the State and Federal Water Projects by this time. Presented in this manner, the data show broadly similar behavior, although the pre-Project data show a greater month-to-month variation in X2 position than the post-Project years. A similar set of plots for the other isohalines S1 through S6 is presented in Appendix C.

The variation in the X2 values as a time series by month is also shown in Figure 5-4, indicating a small decrease in the range of X2 (difference between 10th and 90th percentile) over time, suggesting greater control on this quantity through the management of outflows. In some periods, such as the late 1980s/early 1990s, the range of X2 is considerably compressed compared to values earlier in the record, and may be associated with the prevalence of multiple critically dry years as well as flow management during this period: between 1988 and 1992, four of the five years were classified as critically dry by the DWR.

5.3. X2 POSITION AS A FUNCTION OF WATER YEAR TYPE

The State of California uses unimpaired watershed runoff to characterize water years in the Sacramento and San Joaquin River Basins. Depending on the volume of unimpaired runoff, water years are characterized as wet, above normal, below normal, dry, or critically dry, with specific runoff thresholds for each basin. The Sacramento Valley Index represents a much larger volume of water than the San Joaquin Valley Index, and therefore we consider only the Sacramento Valley Index in the following analysis. Note, however, that we are associating the October and November values with the preceding water year, as the hydrology in the preceding months is the major driver for isohaline position in these months.

Line and scatter plots of X2 by month are shown by water year type in Figure 5-5 for the Sacramento and San Joaquin Rivers. The lines join the median values of the X2 value for each month. Because the separation of the data into five water year categories significantly reduces the number of points in each plot, we chose to display all data as points rather than as box and whisker plots. These data show that the X2 behavior in the 1968–2012 period differs from the 1922–1967 period in drier years (dry or critically dry), and the behavior in wet years is similar. In the wet months of these drier years, the 1968–2012 salinities are much higher than the corresponding 1922–1967 salinities. In the dry months of the drier years, the 1968–2012 salinities are much lower than the corresponding 1922–1967 salinities. Similar plots for other isohalines are shown in Appendix C.

5.4. COMPARISON OF INTERPOLATED X2 TO DAILY KM X2

To get a sense of how the overall data processing methodology compares to previous approaches, we compared the X2 values as used in the original Kimmerer and Monismith

(1992) work⁴ and the interpolated X2 values in the present work, both data sets reflecting the identical 1967–1991 period. Note that the original K-M X2 values were not distinguished by river, and the single value for each day was matched to both Sacramento and San Joaquin X2 from the present work.

In Figure 5-6 a set of scatter plots show the two X2 datasets by month and river. The best fit lines fall along the 1:1 line for most months and r^2 values range from 0.92-0.97. Although the fits are very good, they are not an exact match, and may be related to the causes identified in Section 5.1. In the absence of the raw data used in the original K-M analysis, it is not possible to specifically identify the causes underlying the differences.

5.5. COMPARISON OF INTERPOLATED AND MODELED X2

The X2 positions interpolated from the salinity data were compared with X2 positions calculated from two models based on delta outflow: the Kimmerer-Monismith (K-M) equation and the DSG model (Hutton, 2013). These models are used for planning studies with the goal of calculating X2 under different export and hydrologic scenarios. By comparing with the interpolated X2 data, the goal of this analysis is to provide insight into the potential bias in these existing models, and provide an approach for correcting this bias.

The K-M equation was initially seeded with the first interpolated monthly value of X2. One of the limitations of the K-M model is the inclusion of a logarithmic outflow component: whenever Delta outflow is non-positive (461 days for daily flows and 12 months for monthly flows over the period of record), the predicted X2 is undefined. Whenever this occurred, we reseeded the model with the corresponding interpolated X2. We ran the K-M model with both the original coefficients of Kimmerer and Monismith (1992) and with the coefficients refit on the entire interpolated X2 dataset. The DSG model (Hutton, 2013) has a single antecedent outflow initial condition but is otherwise dependent only on the outflow time series. The parameters in the DSG model were originally estimated using daily data. In this evaluation, these same parameters were used for a monthly version of the model, i.e., the model was not recalibrated for the monthly data.

Note that for the original K-M model, no difference between rivers was made for the predicted X2 positions. In this comparison, the single daily K-M position was associated with both the Sacramento and San Joaquin X2 position for the corresponding day. The K-M model with refit coefficients and the DSG model both make separate predictions for each river.

Each model being examined uses monthly average outflows to predict X2 positions, and flow conditions in months with widely varying hydrology may not be able to be accurately represented by a single monthly average. In this context, we computed the absolute value of the coefficient of variation (CV)—the standard deviation divided by the mean—for each month of the Delta outflow data. The CVs for each month across all years are shown as boxplots in Figure 5-7 and as time series in Figure 5-8. Generally, the summer months display lower flow variability than the winter months.

⁴ These data were provided by Dr. Ed Gross. Note that the values referred to here are the X2 values used in the development of the K-M equation, not values produced from the K-M equation.

In Figure 5-9 through Figure 5-20 we show various comparisons of model and interpolated X2 for each of the models mentioned above using a common template. First, scatter plots conditioned on river, month, and CV of outflow within the month show the corresponding values on the scale of the X2 positions. Second, plots of the residuals (interpolated X2 subtracted from model X2) against interpolated X2 show the agreement between modeled and interpolated values for various salinity conditions. We used these residuals to fit a linear bias-correction model,

$$\hat{y} = a_{m,r} + b_{m,r} \cdot X2_{\text{interp}},$$

where \hat{y} is the model residual, $a_{m,r}$ and $b_{m,r}$, are fitted coefficients for each river and month, and $X2_{\text{interp}}$ is the interpolated X2 position. The red lines display the fitted values of this model, and Table 5-18 to Table 5-20 show the coefficients. Bias-corrected residuals were determined by subtracting the estimated biases from the raw residuals, and scatter plots of these values are third in the series of model diagnostic plots. Finally, time series of the bias-corrected residuals by month are shown for the period of record; moving averages are displayed on all panels, and linear trend lines are shown when the estimated slope was found to be significant. Important observations related to the residuals and bias for each model are discussed below:

DSG Model

- The modeled values agree closely with the interpolated values in months with low flow variability (low CV) on both rivers. With increasing flow variability, there is increasing disagreement between modeled and interpolated values. Additionally, this disagreement in high flow CV months appears to be seasonal: the modeled values are consistently below the interpolated values in winter months but higher than the interpolated values in summer months. The overall correlation between modeled and interpolated values is 0.94.
- The model residual (DSG model X2 minus interpolated X2) versus X2 shows a small seasonal bias, positive in the summer and negative in the winter. Residuals are otherwise approximately random where X2 is between about 50–100 km. At lower X2, residual is positive for both rivers, i.e., the DSG X2 is more east of the interpolated X2. At higher X2, the residual is positive for the Sacramento River and negative for the San Joaquin River.
- The bias-corrected residuals show a downward time trend in June and July for both rivers and an upward trend in the fall (September and October for San Joaquin, only September for Sacramento). Both rivers show a downward trend in January but not for any other winter month.

K-M model, original coefficients

- The level of agreement between modeled and observed X2 positions is less strongly associated with flow CV than was the case for the DSG model. There is a similar seasonal disagreement in high flow CV months: the modeled values are consistently

below the interpolated values in winter months but higher than the interpolated values in summer months. The overall correlation between modeled and interpolated values is 0.95.

- The model residual (K-M model X2 minus interpolated X2) versus X2 shows that residuals are approximately random where X2 are between about 50-90 km. At lower X2, the residual is positive for both rivers, i.e., the K-M X2 is more east of the interpolated X2. At higher X2, the residual is significantly negative for the San Joaquin River. The bias appears to be less seasonal than for the DSG model.
- The bias-corrected residuals show a downward time trend in June and July for both rivers and an upward trend in the fall (September and October for San Joaquin, only September for Sacramento).

K-M model, refit coefficients

- The level of agreement between modeled and observed X2 positions is less strongly associated with flow CV than was the case for the DSG model. There is a similar seasonal disagreement in high flow CV months: the modelled values are consistently below the interpolated values in winter months but higher than the interpolated values in summer months. The overall correlation between modeled and interpolated values is 0.96.
- The model residual (K-M model X2 minus interpolated X2) versus X2 shows that residuals are approximately random where X2 are between about 50-90 km. At lower X2, residual is positive for both rivers, i.e., the K-M X2 is more east of the interpolated X2. At higher X2, the residual is significantly negative for the San Joaquin River. The bias appears to be less seasonal than for the DSG model. The results are quite similar to the K-M model with original coefficients.
- The bias-corrected residuals show a downward time trend in June and July for both rivers. There is also a downward trend in November (both rivers) and December (San Joaquin only). Compared to the K-M model with original coefficients, the upward fall trend is limited to only September for both rivers.

Summary of Model Comparisons

In general, the largest systematic disagreements between modeled and interpolated X2s occur for interpolated X2s at the extreme ends of its range. For all three models, the change in long-term behavior of the model residuals was small compared to the disagreements between model and interpolated X2 positions under extreme salinity conditions. For future application, we have reported the linear function representing bias (function of X2 and month) for each of the models. These linear equations can be used to correct K-M or DSG-predicted X2 values.

The bias between the modeled and interpolated monthly X2 is likely linked to the within-month Delta outflow variability, and also inaccuracies in the estimation of the Delta outflow.

For the K-M model, an additional source of bias may be related to the accumulation of error in the autoregressive formulation, where the preceding month's *calculated* X2 is used for the current month's X2 calculation, repeated every month over a 90+ year period. To correct for this, we performed an additional analysis (details not shown) where each month we re-seeded the K-M model with the X2 interpolated from the data. Making this change did not affect the quality of the fit or the nature of the bias. Based on this, we suggest that the bias is likely attributable to flow variability and inaccuracy rather than the model structure.

5.6. TREND EVALUATION OF X2

Sen's non-parametric estimate of slope was used to perform a trend analysis of the calculated monthly X2 positions over seven time periods (1922–1944, 1945–1967, 1968–1999, 2000–2012, 1922–1967, 1968–2012, and 1921–2012). The Mann-Kendall (MK) test is performed on the Sen slope at the 95% confidence level, with results listed as either an upward trend (↑), no trend (↔), or a downward trend (↓). The trend slope listed in the tables is computed using the median value of the Sen slope. Non-zero values of this slope may or may not be found to be statistically significant using the Mann-Kendall test. Details of the implementation of the trend evaluation are presented in Appendix D.

Results from the trend analysis are shown in Table 5-2 through Table 5-15 with the analysis for the two rivers shown separately. Similar trend analysis results for other isohalines are presented in Appendix E. Key results are summarized below:

- The monthly trend evaluation for the entire period of record (1922–2012) (Table 5-8 and Table 5-15), shows that months with the greatest incidence of statistically significant increase in X2 occur in November through May. Decreases in X2 occur in July through September in the Sacramento River and only in August and September for the San Joaquin River.
- Over the pre-Project period of the record (1922–1967) (Table 5-6 and Table 5-13), there is no significant change from January through July, although there is a statistically significant decrease in X2 from August to December. The directions of the trends are identical for the two rivers.
- Over the post-Project period (1968–2012) (Table 5-7 and Table 5-14), there is a nearly inverse response in trends, with a statistically significant increase in X2 from September to December, and with identical trend directions in both rivers.
- Within the four shorter periods investigated (1922–1944, 1945–1967, 1968–1999, and 2000–2012) (Table 5-2 through Table 5-5 and Table 5-9 through Table 5-12), the tests generally do not indicate any widespread pattern of significant change over 1922-1944 and over 1945-1967 for both rivers. For the slightly longer sub-period 1968–1999, there is an increase for October and November for both rivers. For 2000–2012, there is a decrease in October/November X2 for the San Joaquin River but not for the Sacramento River.

5.7. COMPARISON OF ISOHALINE POSITIONS IN WATER YEAR TYPES

The non-parametric Wilcoxon Rank Sum test was used for the comparison of isohaline values for a specific water year type (wet, above normal, below normal, dry, or critically dry). This formal test was used in addition to the visual comparison shown in Figure 5-5 for the Sacramento and San Joaquin Rivers. The values of the isohaline for the pre-Project period (1921–1967) were compared to the values for the post-Project period (1968–2012). There are three possible results of each test of the two groups of data, identified as A and B: A is equal to B; A is larger than B; A is smaller than B. The 95% confidence level was used for the test. Details of the procedure are summarized in Appendix D.

The results of the Wilcoxon Rank Sum test are summarized for the Sacramento and San Joaquin River X2 isohaline positions in Table 5-16 and Table 5-17, and for other isohalines in Appendix E. In general, for the Sacramento River, dry and critically dry years show that post-Project X2 values were statistically significantly higher in November through May, and lower in August and September, confirming the visual patterns shown earlier. The results are similar for the San Joaquin River. At the other extreme of flows, in wet years, the test shows that post-Project X2 values were higher in May and June and lower in August and September. The statistical test adds more detail to the visual patterns which show somewhat more change during lower flow years.

5.8. RELATIONSHIP OF X2 TO LONG TERM TRENDS IN DELTA OUTFLOW AND MEAN SEA LEVEL

A seasonal-trend decomposition procedure based on loess (local regression) (Cleveland et al., 1990) was applied to the monthly time series data of X2, net Delta outflow, and mean sea level to examine the inter-relationships between these variables (Figure 5-21 and Figure 5-22). These figures show each monthly data set decomposed into seasonal and underlying trends (for the Sacramento and San Joaquin River X2 values). The seasonal and trend values, plus the noise term (not shown) can be added to return the original time series. The seasonal component of the flow shows a signal typical of Northern California and Mediterranean climates, with clusters of wet years and dry years on approximately decadal scales (similar results were shown by Enright and Culberson, 2009). The X2 data do not show a similar decadal pattern as the flows, but do show a decrease in the variability over the period of record. This is especially pronounced in the drought periods of the late 1980s and early 1990s. When the seasonal signal is removed, the X2 data indicate an inverse correspondence with flow, and over the period of record, an increase over time. In the most recent 2 to 3 decades of the record, there is a trend toward decreasing flows and increasing X2. Similar patterns are noted for the Sacramento and San Joaquin Rivers data series. Mean sea level over this period shows a continual increase with time. This may potentially contribute to the explanation of X2 behavior, although over the most recent period, the sea level effect and flow effectively tend support one another (leading to higher X2), and it is difficult to parse out their relative impacts on X2.

5.9. STRUCTURE OF SALINITY GRADIENT IN THE ESTUARY

An interesting feature of the salinity data that was reported by Jassby et al. (1995) pertained to what was termed the self-similar structure of the data, i.e., when depth averaged salinity data (not surface salinity data, as used throughout this report) were plotted against distance from Golden Gate (X) normalized by X2, the data collapsed around a central line (Figure 2

in the original paper). This was shown for data from January 1990 through February 1992, although not for the entire period that was used was computing the autoregressive equation for X2. Revisiting the issue, Monismith et al. (2002) showed a similar behavior for depth-averaged daily salinity over a slightly longer data record from 1988–1992. In general, this form of the equation is useful to show data across a large range of salinities including data from stations in the Bay, and demonstrates that when X/X_2 is lower than about 0.5, the depth-averaged salinities exceed 20 psu. Importantly, however, Monismith et al. (2002) also showed that the self-similar structure broke down at higher flows (using February–April 1986 data), with low salinity values even when X/X_2 was well below 0.5.

The concept of the self-similar horizontal structure of salinity was explored using a longer data record than the aforementioned studies, and also by using primarily near-surface data from a set of stations in the bay and western Delta (Figure 5-23). An exception is the set of data from the CAR station which was only available for mid-depth values. The data used for these plots were from CDEC and from the USGS. An additional station, identified by the USGS as Marker 1 (USGS station code CM1) was also included to provide a more horizontal resolution of the data. The plots show how the structure varies as a function of X2 value, with greater scatter at low values of X2 (high flows), and reduced scatter and higher salinity values at higher values of X2 (lower flows). The CAR station does not stand out in these plots despite not being a surface station. The discrepancy at higher flows is not surprising given the likelihood of greater stratification and lower surface salinity values. This feature is independently explored through three-dimensional hydrodynamic modeling performed by Gross et al. (2007, 2010), who show how stratification and surface salinity change in the bay locations as outflow increases. The understanding from the hydrodynamic modeling suggests that the assumption of a fixed horizontal salinity structure (normalized to X2) is a useful concept for low flow conditions, but is not generally applicable.

Another aspect of the salinity structure that can be explored is the relative position of the different surface salinity isohalines compared to the X2 position (Figure 5-24). Three dimensional modeling under a range of flow conditions (Gross et al., 2007; MacWilliams et al., undated) suggests that the relative positions of surface salinity isohalines relevant to the S1 through S6 range are expected to be approximately uniform except at high flows. The scatterplots of all six isohalines show reasonable consistency across the X2 range, following a linear behavior. The relationships show minimal scatter for salinity levels close to X2 (S1 and S2), and become noisier at higher salinities, where different stations may have been used for the isohaline interpolation. As with the self-similar structure (station distance normalized to X2), there appears to be a reasonable pattern except during high flows.

5.10. SUMMARY OF EVALUATION

A variety of visual and statistical techniques were used to explore the behavior of the X2 interpolated values (and other surface salinity isohalines) over the period that we studied. The interpolated X2 values, which for this work may be considered an “observed” value, were also compared with the DSG model and the K-M model to examine the differences between the models and the X2 observations. The following findings from this exploration are important to highlight:

- X2 values could be computed for a large fraction of months over the October 1921–September 2012 study period. Missing data for the interpolation largely occurred in the first two decades of the data record. In this work, X2 values were calculated separately for positions along the Sacramento and San Joaquin Rivers. Although numeric values of the isohalines may differ along the rivers, the broad trends summarized below apply to both X2 values.
- Over the period for which X2 was calculated there was a reasonably wide range in the computed values, typically 50–100 km from Golden Gate. A somewhat greater range in the X2 values, as represented by the difference in the 10th and 90th percentile values, was observed in the pre-Project period compared to the last two decades.
- The constants in the K-M equation were recalibrated for the data period of this study (1922–2012), and for consistency, for the data period used in the original work (Oct 1967–Nov 1991). The equation was calibrated separately for the Sacramento and San Joaquin Rivers. The equation was also calibrated to the Bulletin 23 data (1922–1964). Although the original constants could not be replicated exactly—and the data used for that work are not readily available—an equation using the same autoregressive structure was found to describe the data well for these different cases, with similar coefficients. The fit was better for the shorter record, reflecting the limited variability in this period. Fits were slightly poorer for the entire period of record (1921–2012) and for the more recent period (1971–2012) with better quality continuous EC data, and were likely related to the wider range of environmental driving conditions. The fits to the 1921–1964 data, although resulting in similar coefficients to the modern data, were also poorer than fits to the CDEC data over different time periods. It was nonetheless surprising that the model formulation was able to adequately represent X2 over a nine-decade period during which there have been significant changes in the Delta and Bay: changes in channel depth, Delta exports, regulatory changes, upstream land use changes, and some mean sea level rise. While it is possible that the coefficients for different time periods of fitting encapsulate these changes, the mechanistic linkage between a coefficient and one or more of these changes was not explored in this work.
- The largest systematic disagreements between modeled and interpolated X2s occur for interpolated X2s at the extreme ends of its range. For the three models evaluated (DSG model, and K-M model with original and refit coefficients), the change in long-term behavior of the model residuals was small compared to the disagreements between model and interpolated X2 positions under extreme salinity conditions. In general, the largest systematic disagreements between modeled and interpolated X2s occur for interpolated X2s at the extreme ends of its range. For future application, we have reported the linear function representing bias (function of X2 and month) for each of the models. These linear equations can be used to correct K-M or DSG-predicted X2 values.
- When the interpolated X2 values were evaluated as a function of water year, there was a pattern in the pre- and post-Project periods, with lower pre-Project X2 values in the winter months of dry and critically dry years but higher pre-Project X2 values

in the summer months. These values were confirmed through a non-parametric Wilcoxon Rank Sum test that compared the pre- and post-Project values of X2.

- An evaluation of the statistical significance of trend showed that over the entire period of record, there were statistically significant increases in X2 from November through May (excluding March), and statistically significant decreases in X2 in August and September.
- By decomposing the interpolated X2, Delta outflow, and mean sea level values into seasonal and underlying trends, we see an inverse relationship between Delta outflow and X2. The influence of sea level rise is harder to discern through this approach because over the last 2–3 decades the increase in sea level has co-occurred with a decreasing underlying trend in Delta outflows.
- The concept of a uniform horizontal salinity structure, when expressed in terms of surface salinity only (as opposed to depth averaged salinity), was found to work best for low flows, and to break down at higher flows. The concept does not appear to be generally applicable across all conditions and for surface salinity.
- The position of the X2 line was compared with the other isohalines that were similarly computed. The scatterplots of both isohalines show reasonable consistency across the X2 range, with increasing noise at higher flows.

Table 5-1
Recalibration of KM-equation with Monthly Interpolated X2s.
Coefficient Columns are Displayed as Estimate +/- One Standard Error.

River	Period of Regression	r ²	Standard Error of Regression (km)	A	B	C
SAC	10/01/1921 to 09/01/2012	0.930	3.51	114. +/- 1.80	0.418 +/- 0.0106	-17.3 +/- 0.291
SAC	10/01/1921 to 06/01/1964	0.923	3.95	112. +/- 2.65	0.432 +/- 0.0158	-17.2 +/- 0.439
SAC	07/01/1971 to 09/01/2012	0.939	3.07	119. +/- 2.63	0.392 +/- 0.0153	-17.9 +/- 0.418
SAC	10/01/1967 to 11/01/1991 (K-M period)	0.948	2.79	110. +/- 3.36	0.419 +/- 0.0198	-16.2 +/- 0.517
SJR	10/01/1921 to 09/01/2012	0.923	3.92	119. +/- 1.92	0.425 +/- 0.0107	-18.5 +/- 0.321
SJR	10/01/1921 to 06/01/1964	0.912	4.57	119. +/- 2.91	0.433 +/- 0.0162	-18.8 +/- 0.506
SJR	07/01/1971 to 09/01/2012	0.935	3.31	120. +/- 2.75	0.410 +/- 0.0155	-18.4 +/- 0.445
SJR	10/01/1967 to 11/01/1991 (K-M period)	0.946	3.00	110. +/- 3.52	0.439 +/- 0.0201	-16.5 +/- 0.551

Table 5-2
Sacramento X2 Mann-Kendall Test Results, WY 1922–1944

Month	Sample Size	Sen's Trend Slope Median (km per year)	Test Decision of MK Test
Dec	17	0.33	↔
Jan	15	-0.08	↔
Feb	17	0.02	↔
Mar	17	-0.79	↔
Apr	17	-0.27	↔
May	17	-0.17	↔
Jun	18	-0.88	↔
Jul	20	-0.58	↔
Aug	18	0.09	↔
Sep	20	0.18	↔
Oct	20	0.07	↔
Nov	18	0.24	↔
All	214	-0.57	↓

**Table 5-3
Sacramento X2 Mann-Kendall Test Results, WY 1945–1967**

Month	Sample Size	Sen's Trend Slope Median (km per year)	Test Decision of MK Test
Dec	23	-0.19	↔
Jan	23	-0.11	↔
Feb	23	-0.23	↔
Mar	23	0.04	↔
Apr	22	0.16	↔
May	23	0.45	↔
Jun	22	0.40	↔
Jul	22	0.20	↔
Aug	23	0.10	↔
Sep	23	-0.15	↔
Oct	23	-0.28	↔
Nov	23	-0.13	↔
All	273	0.02	↔

**Table 5-4
Sacramento X2 Mann-Kendall Test Results, WY 1968–1999**

Month	Sample Size	Sen's Trend Slope Median (km per year)	Test Decision of MK Test
Dec	32	0.48	↔
Jan	32	0.36	↔
Feb	30	-0.06	↔
Mar	30	0.04	↔
Apr	31	0.01	↔
May	32	-0.06	↔
Jun	32	-0.03	↔
Jul	32	-0.05	↔
Aug	32	0.05	↔
Sep	32	0.29	↔
Oct	32	0.47	↑
Nov	32	0.62	↑
All	379	0.23	↑

**Table 5-5
Sacramento X2 Mann-Kendall Test Results, WY 2000-2012**

Month	Sample Size	Sen's Trend Slope Median (km per year)	Test Decision of MK Test
Dec	13	0.50	↔
Jan	12	0.59	↔
Feb	13	0.41	↔
Mar	13	0.52	↔
Apr	12	-0.60	↔
May	13	-0.28	↔
Jun	13	-0.28	↔
Jul	13	-0.21	↔
Aug	13	0.02	↔
Sep	13	-0.23	↔
Oct	13	-0.53	↔
Nov	13	-0.15	↔
All	154	-0.11	↔

**Table 5-6
Sacramento X2 Mann-Kendall Test Results, WY 1922-1967**

Month	Sample Size	Sen's Trend Slope Median (km per year)	Test Decision of MK Test
Dec	40	-0.21	↓
Jan	38	-0.11	↔
Feb	40	-0.08	↔
Mar	40	0.05	↔
Apr	39	0.13	↔
May	40	0.12	↔
Jun	40	0.02	↔
Jul	42	-0.04	↔
Aug	41	-0.20	↓
Sep	43	-0.43	↓
Oct	43	-0.32	↓
Nov	41	-0.21	↓
All	487	-0.16	↓

Table 5-7
Sacramento X2 Mann-Kendall Test Results, WY 1968–2012

Month	Sample Size	Sen's Trend Slope Median (km per year)	Test Decision of MK Test
Dec	45	0.37	↑
Jan	44	0.23	↔
Feb	43	0.10	↔
Mar	43	0.04	↔
Apr	43	0.01	↔
May	45	-0.18	↔
Jun	45	-0.08	↔
Jul	45	-0.06	↔
Aug	45	0.06	↔
Sep	45	0.20	↑
Oct	45	0.28	↑
Nov	45	0.37	↑
All	533	0.13	↑

Table 5-8
Sacramento X2 Mann-Kendall Test Results, WY 1922–2012

Month	Sample Size	Sen's Trend Slope Median (km per year)	Test Decision of MK Test
Dec	85	0.12	↑
Jan	82	0.12	↑
Feb	83	0.09	↑
Mar	83	0.09	↑
Apr	82	0.14	↑
May	85	0.14	↑
Jun	85	0.11	↑
Jul	87	-0.04	↔
Aug	86	-0.13	↓
Sep	88	-0.12	↓
Oct	88	0.00	↔
Nov	86	0.11	↑
All	1020	0.06	↑

**Table 5-9
San Joaquin X2 Mann-Kendall Test Results, WY 1922–1944**

Month	Sample Size	Sen's Trend Slope Median (km per year)	Test Decision of MK Test
Dec	17	0.24	↔
Jan	15	-0.08	↔
Feb	17	0.02	↔
Mar	17	-0.79	↔
Apr	17	-0.27	↔
May	17	-0.17	↔
Jun	18	-0.88	↔
Jul	17	-0.30	↔
Aug	14	0.60	↔
Sep	17	0.38	↔
Oct	18	0.30	↔
Nov	17	0.19	↔
All	201	-0.41	↓

**Table 5-10
San Joaquin X2 Mann-Kendall Test Results, WY 1945–1967**

Month	Sample Size	Sen's Trend Slope Median (km per year)	Test Decision of MK Test
Dec	23	-0.18	↔
Jan	23	-0.08	↔
Feb	23	-0.23	↔
Mar	23	0.04	↔
Apr	22	0.12	↔
May	22	0.28	↔
Jun	22	0.26	↔
Jul	22	0.13	↔
Aug	23	0.00	↔
Sep	22	-0.25	↔
Oct	23	-0.34	↔
Nov	23	-0.18	↔
All	271	-0.03	↔

Table 5-11
San Joaquin X2 Mann-Kendall Test Results, WY 1968–1999

Month	Sample Size	Sen's Trend Slope Median (km per year)	Test Decision of MK Test
Dec	32	0.53	↔
Jan	32	0.40	↔
Feb	30	-0.06	↔
Mar	30	0.06	↔
Apr	31	0.01	↔
May	32	-0.06	↔
Jun	32	-0.06	↔
Jul	32	-0.12	↔
Aug	32	-0.01	↔
Sep	32	0.25	↔
Oct	32	0.44	↑
Nov	32	0.67	↑
All	379	0.22	↑

Table 5-12
San Joaquin X2 Mann-Kendall Test Results, WY 2000–2012

Month	Sample Size	Sen's Trend Slope Median (km per year)	Test Decision of MK Test
Dec	13	0.42	↔
Jan	12	0.83	↔
Feb	13	0.41	↔
Mar	13	0.52	↔
Apr	12	-0.61	↔
May	13	-0.28	↔
Jun	13	-0.37	↔
Jul	13	-0.27	↔
Aug	13	-0.04	↔
Sep	13	-0.29	↔
Oct	13	-0.35	↓
Nov	13	-0.29	↓
All	154	-0.17	↔

Table 5-13
San Joaquin X2 Mann-Kendall Test Results, WY 1922–1967

Month	Sample Size	Sen's Trend Slope Median (km per year)	Test Decision of MK Test
Dec	40	-0.23	↓
Jan	38	-0.11	↔
Feb	40	-0.08	↔
Mar	40	0.05	↔
Apr	39	0.13	↔
May	39	0.07	↔
Jun	40	0.02	↔
Jul	39	0.07	↔
Aug	37	-0.19	↔
Sep	39	-0.51	↓
Oct	41	-0.37	↓
Nov	40	-0.27	↓
All	472	-0.13	↓

Table 5-14
San Joaquin X2 Mann-Kendall Test Results, WY 1968–2012

Month	Sample Size	Sen's Trend Slope Median (km per year)	Test Decision of MK Test
Dec	45	0.42	↑
Jan	44	0.25	↔
Feb	43	0.10	↔
Mar	43	0.04	↔
Apr	43	0.02	↔
May	45	-0.20	↔
Jun	45	-0.11	↔
Jul	45	-0.12	↔
Aug	45	0.05	↔
Sep	45	0.22	↑
Oct	45	0.25	↑
Nov	45	0.40	↑
All	533	0.12	↑

Table 5-15
San Joaquin X2 Mann-Kendall Test Results, WY 1922–2012

Month	Sample Size	Sen's Trend Slope Median (km per year)	Test Decision of MK Test
Dec	85	0.14	↑
Jan	82	0.13	↑
Feb	83	0.10	↑
Mar	83	0.09	↑
Apr	82	0.15	↑
May	84	0.14	↑
Jun	85	0.10	↔
Jul	84	-0.02	↔
Aug	82	-0.14	↓
Sep	84	-0.13	↓
Oct	86	-0.01	↔
Nov	85	0.11	↑
All	1005	0.07	↑

Table 5-16
Sacramento X2 Wilcoxon Rank Sum Test Results
(comparison of 1968–2012 values against 1922–1967 values)

Year Type	All	Dec	Jan	Feb	Mar	Apr	May	Jun	Jul	Aug	Sep	Oct	Nov
Critical	↑	↑	↔	↑	↑	↑	↑	↔	↔	↓	↓	↔	↑
Dry	↑	↑	↑	↑	↑	↑	↑	↔	↓	↓	↓	↔	↔
Below Normal	↑	↔	↔	↑	↔	↑	↑	↑	↑	↔	↔	↔	↔
Above Normal	↔	↑	↔	↔	↔	↔	↔	↔	↓	↓	↓	↔	↑
Wet	↑	↔	↔	↑	↔	↔	↑	↑	↔	↓	↓	↔	↔

Table 5-17
San Joaquin X2 Wilcoxon Rank Sum Test Results
(comparison of 1968–2012 values against 1922–1967 values)

Year Type	All	Dec	Jan	Feb	Mar	Apr	May	Jun	Jul	Aug	Sep	Oct	Nov
Critical	↑	↑	↔	↑	↑	↑	↔	↔	↔	N/A ⁵	↓	↔	↑
Dry	↑	↑	↑	↑	↑	↑	↑	↔	↓	↓	↓	↔	↑
Below Normal	↑	↔	↔	↑	↔	↑	↑	↑	↔	↔	↔	↔	↔
Above Normal	↔	↑	↔	↔	↔	↔	↔	↔	↓	↓	↓	↔	↔
Wet	↑	↔	↔	↑	↔	↔	↑	↑	↔	↓	↓	↔	↔

⁵ Insufficient data to perform test

Table 5-18
Fitted Slopes and Intercepts for Bias-correction of DSG Model
(p-value of less than 0.05 indicated by shading)

Month	SAC_intercept	SAC_slope	SJR_intercept	SJR_slope
Dec	0.670	-0.0721	9.52	-0.203
Jan	7.26	-0.163	6.65	-0.160
Feb	9.01	-0.170	7.67	-0.154
Mar	6.47	-0.0899	5.84	-0.0843
Apr	5.30	-0.0579	3.69	-0.0340
May	5.75	-0.0687	3.53	-0.0347
Jun	6.65	-0.0503	5.30	-0.0270
Jul	6.70	-0.0433	13.4	-0.128
Aug	-3.76	0.0825	13.7	-0.133
Sep	-7.53	0.115	21.1	-0.244
Oct	-5.11	0.0781	16.4	-0.192
Nov	-6.93	0.0568	7.41e-05	-0.0394

Table 5-19
Fitted Slopes and Intercepts for Bias-correction of K-M Model
(p-value of less than 0.05 indicated by shading)

Month	SAC_intercept	SAC_slope	SJR_intercept	SJR_slope
Dec	19.7	-0.291	22.4	-0.333
Jan	19.2	-0.290	21.7	-0.328
Feb	18.1	-0.268	19.2	-0.288
Mar	11.8	-0.152	13.6	-0.183
Apr	12.1	-0.162	13.2	-0.181
May	12.0	-0.167	12.8	-0.179
Jun	10.9	-0.130	11.6	-0.141
Jul	6.41	-0.0674	10.9	-0.135
Aug	-6.12	0.0887	7.31	-0.0934
Sep	18.1	-0.216	31.4	-0.393
Oct	22.8	-0.283	31.6	-0.400
Nov	20.3	-0.278	24.9	-0.347

Table 5-20
Fitted Slopes and Intercepts for Bias-correction of K-M Model (refit coefficients)
(p-value of less than 0.05 indicated by shading)

Month	SAC_intercept	SAC_slope	SJR_intercept	SJR_slope
Dec	15.7	-0.232	15.6	-0.226
Jan	15.6	-0.240	15.2	-0.229
Feb	13.6	-0.209	11.5	-0.175
Mar	5.58	-0.0726	3.48	-0.0404
Apr	5.26	-0.0835	2.33	-0.0384
May	4.45	-0.0805	1.03	-0.0286
Jun	2.67	-0.0377	-0.997	0.0195
Jul	-5.40	0.0656	-4.93	0.0612
Aug	-17.3	0.218	-7.34	0.0915
Sep	9.68	-0.109	21.9	-0.258
Oct	15.2	-0.182	22.7	-0.267
Nov	14.8	-0.201	16.5	-0.219

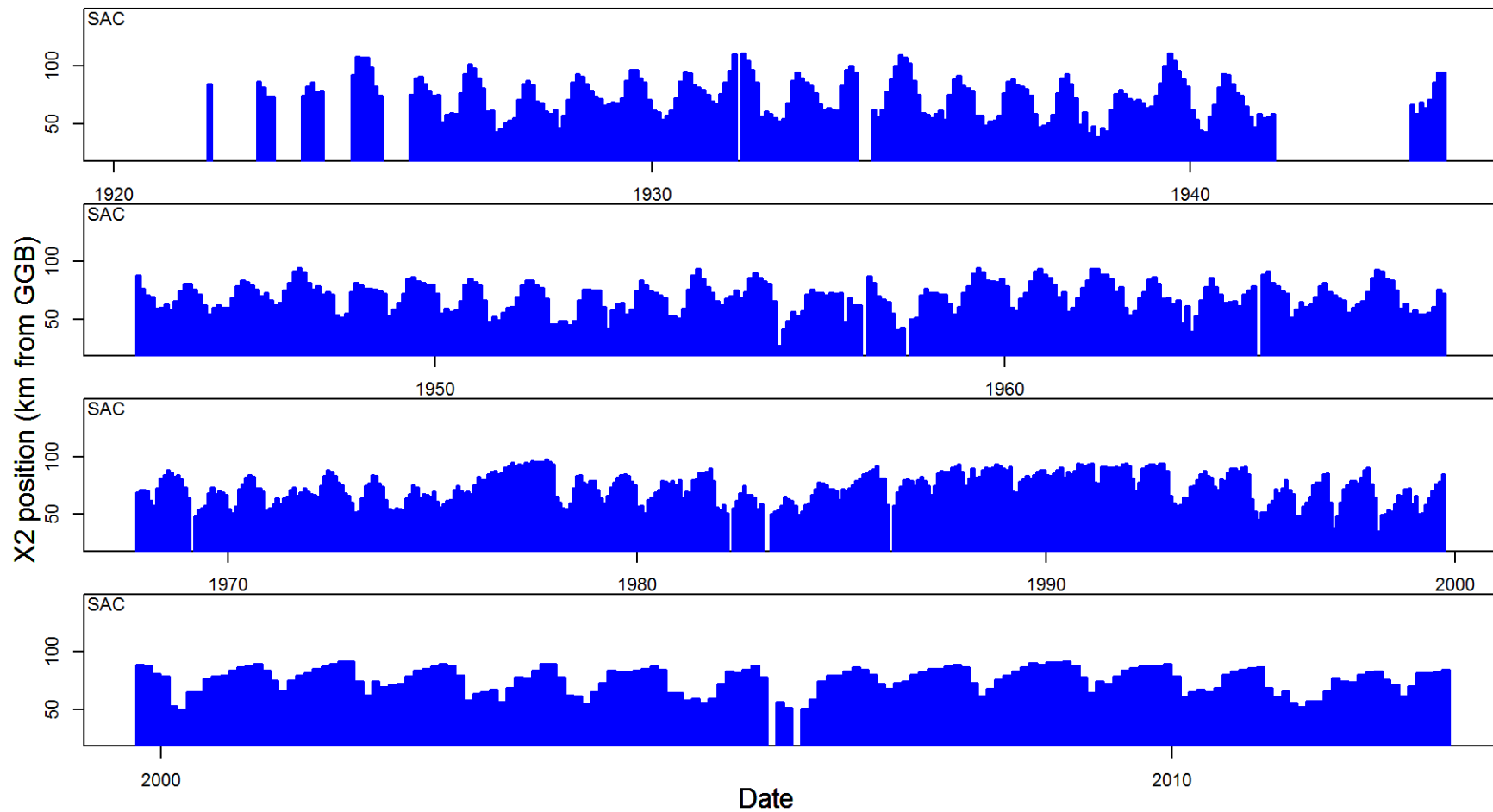


Figure 5-1 Time series of Sacramento X2 from October 1921– September 2012.

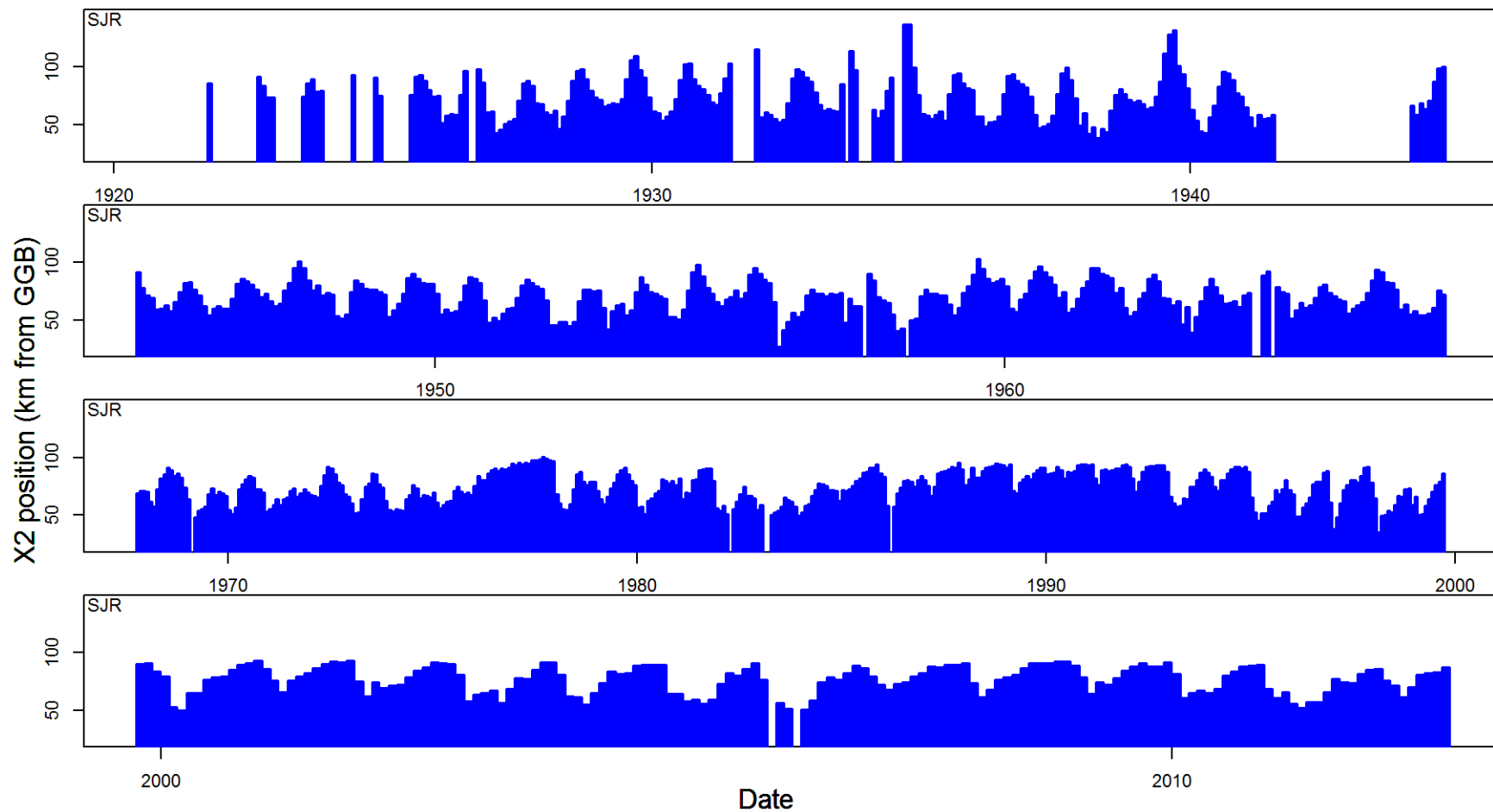


Figure 5-2 Time series of San Joaquin X2 from October 1921– September 2012.

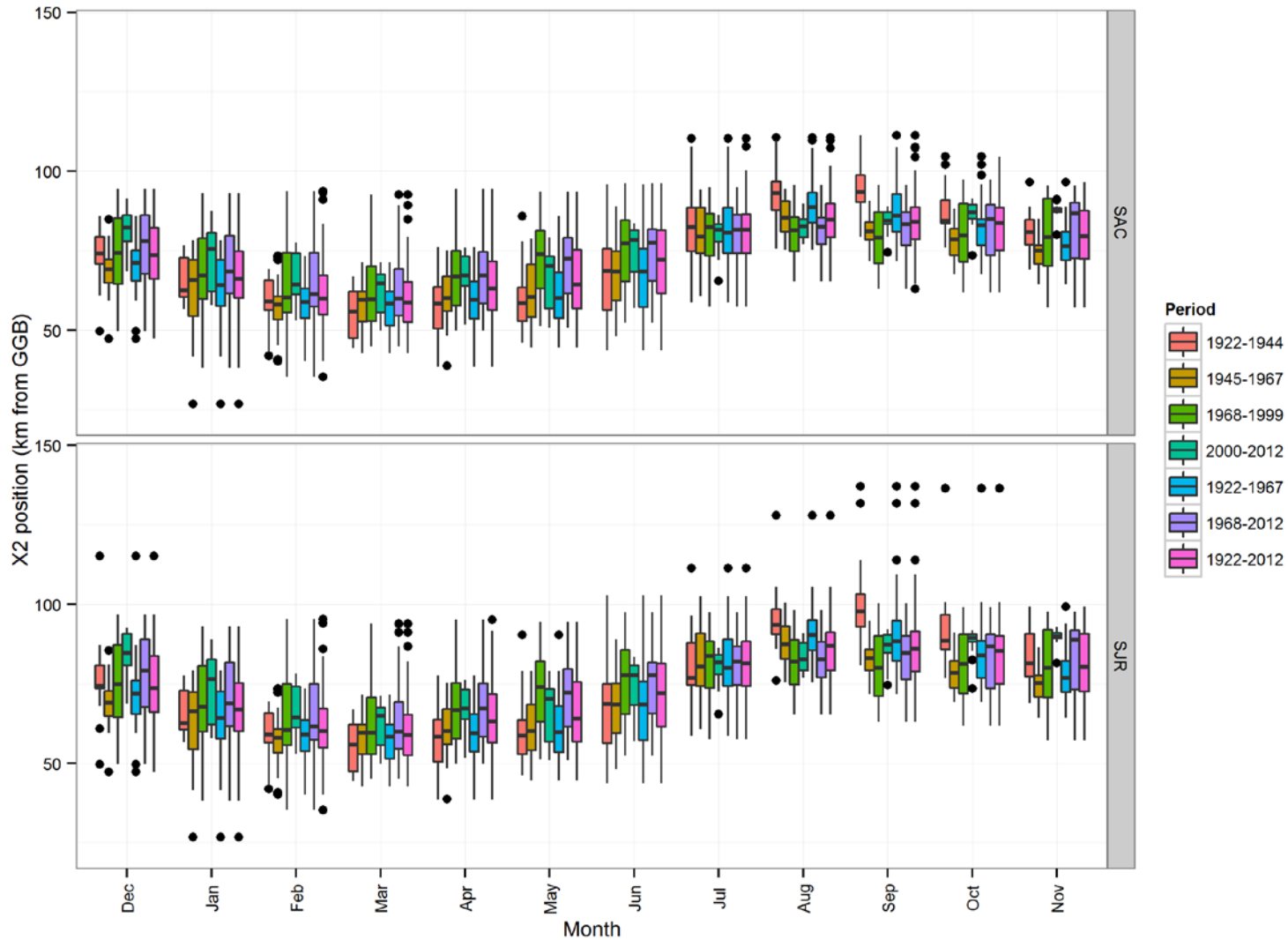


Figure 5-3

Box plots of X2 for various time intervals—four shorter intervals: 1922–1944, 1945–1967, 1968–1999, and 2000–2012; two longer intervals: 1922–1967 and 1968–2012; and the entire record 1921–2012. In the box plots, each box represents the 25th and 75th percentile of values, the line represents the median, and the whiskers extend to the most extreme data point no further than 1.5 times the interquartile range from the box. Outliers are shown as discrete symbols.

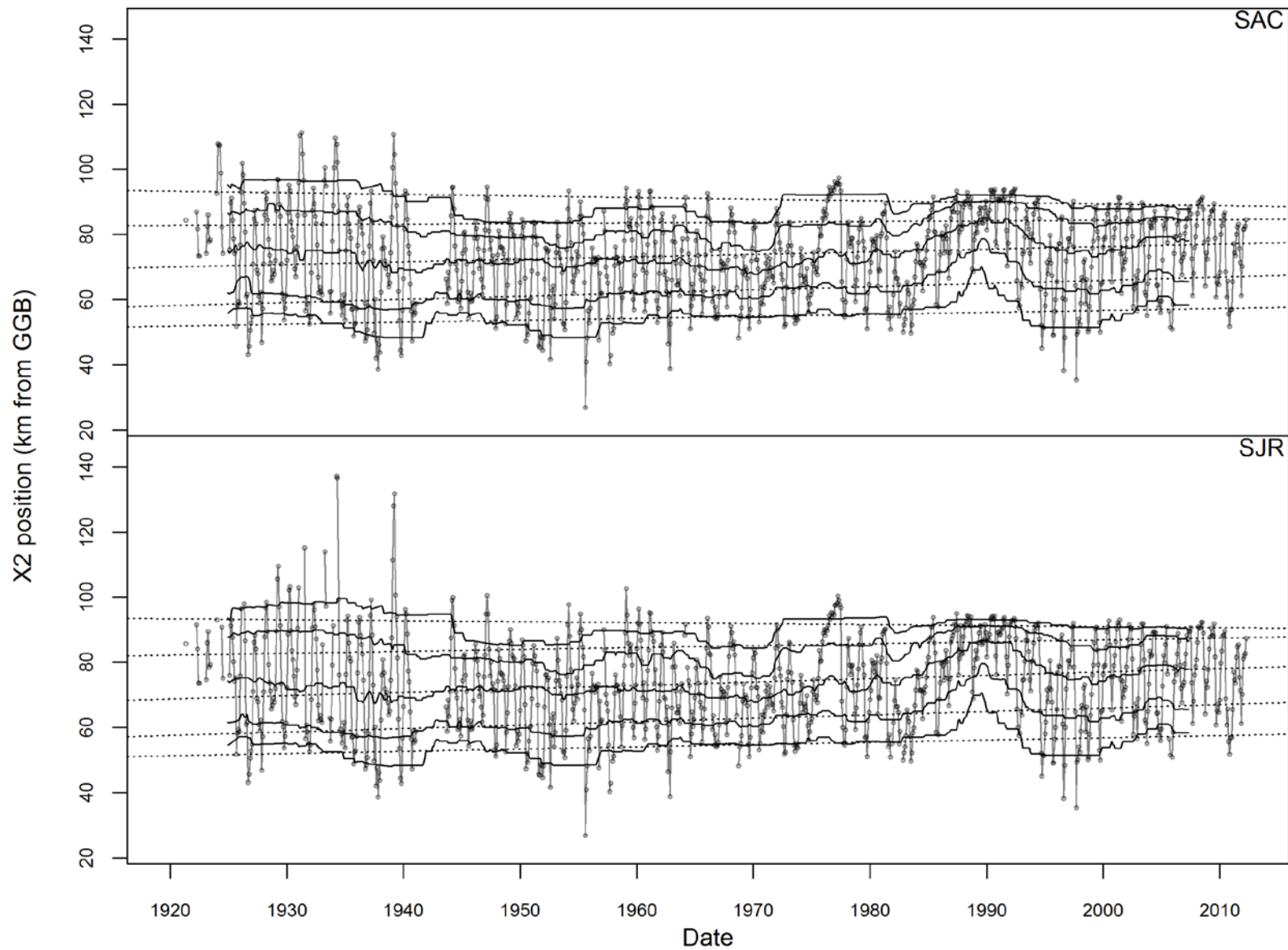


Figure 5-4 Variation in X2 over the period of record. The dark solid lines display 120 month moving windows for the 10th, 25th, 50th, 75th, and 90th percentiles. The corresponding dotted lines are linear trends for the same percentiles.

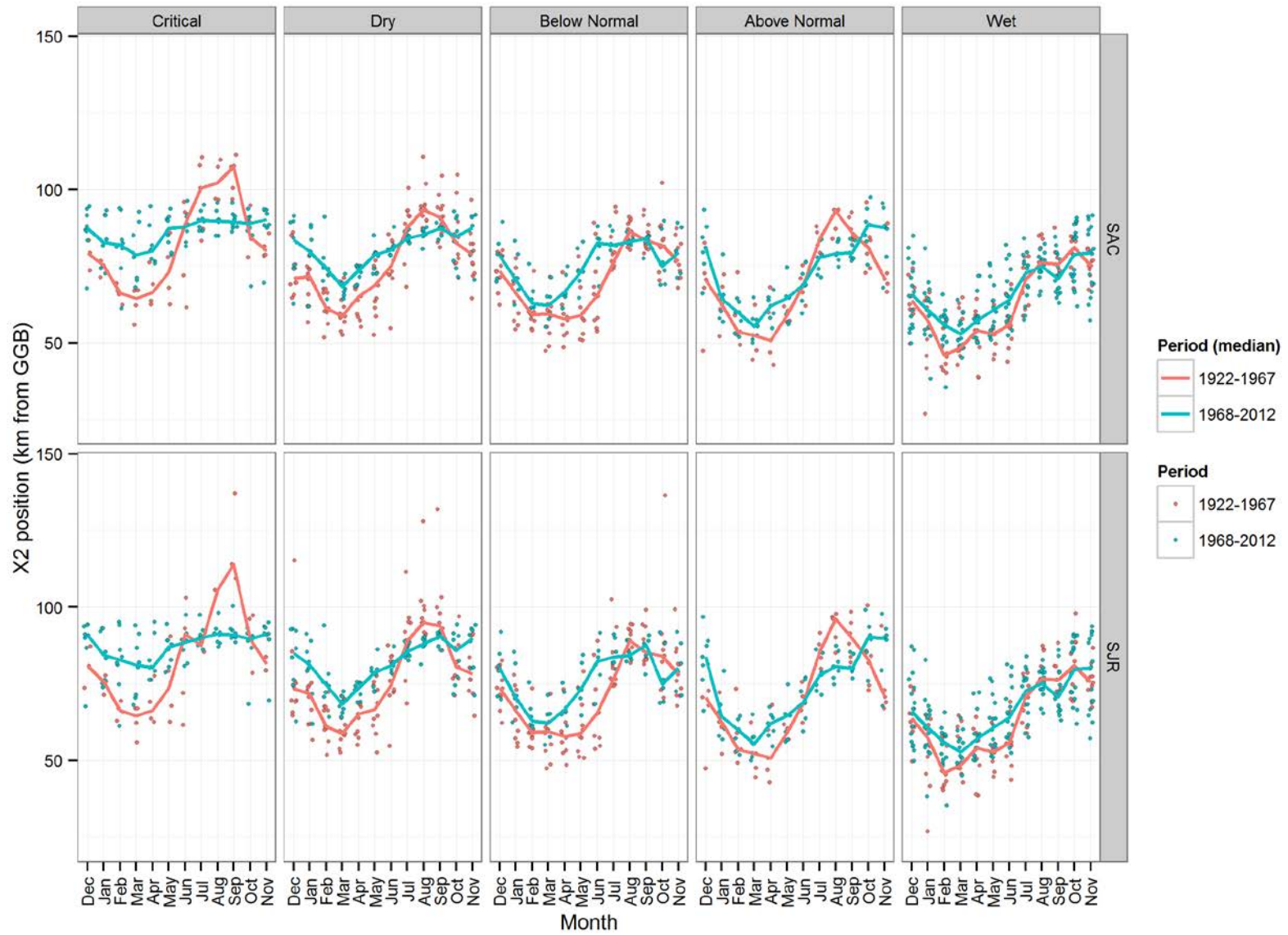


Figure 5-5 Line and scatter plots of X2 by month and by water year type.

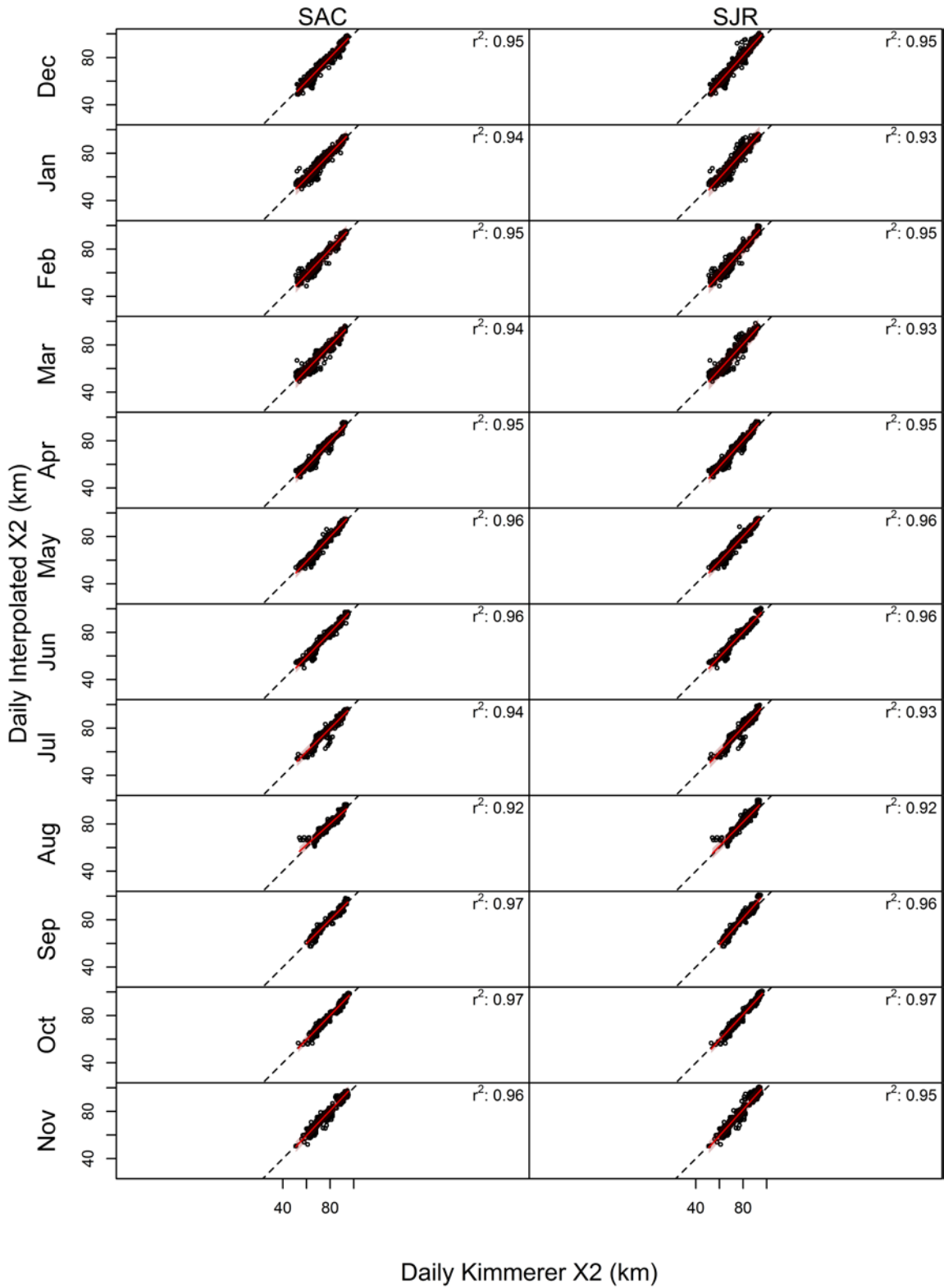


Figure 5-6 Comparison of daily interpolated X2 from this report and X2 from Kimmerer and Monismith (copy of electronic data provided through personal communication with Ed Gross 2013) at daily time resolution. Red line is linear best fit predictions with 95% confidence interval; dashed line is 1:1 slope.

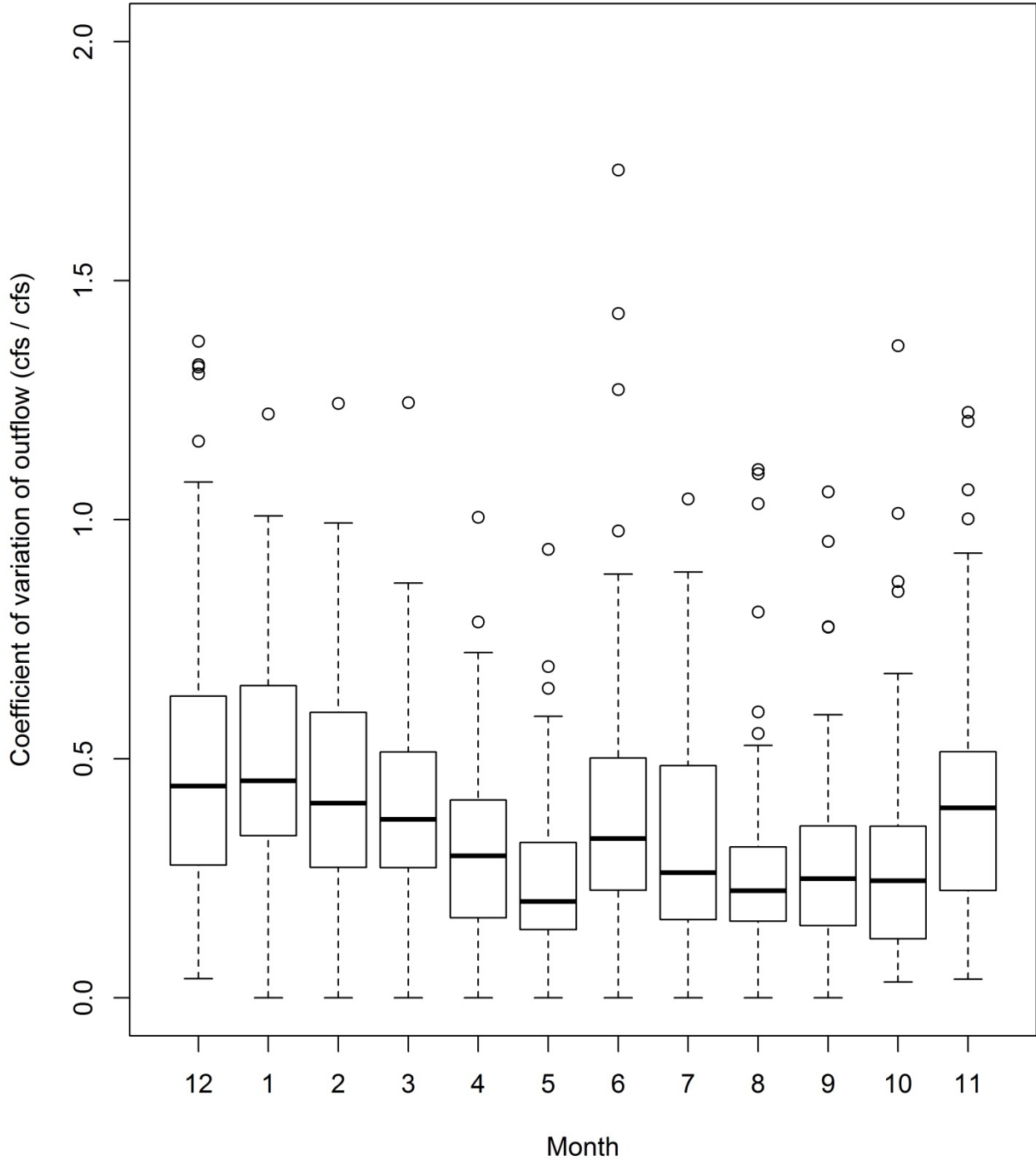


Figure 5-7 Boxplots of coefficient of variations of Delta outflow, with whiskers extending to the most extreme data points no further than 1.5 times the interquartile range from the box edges. Calculations were performed on daily flow data within each calendar month, and the distribution of the monthly values across different years is shown here. Five outliers are excluded from the plot due to choice of y-axis limits.

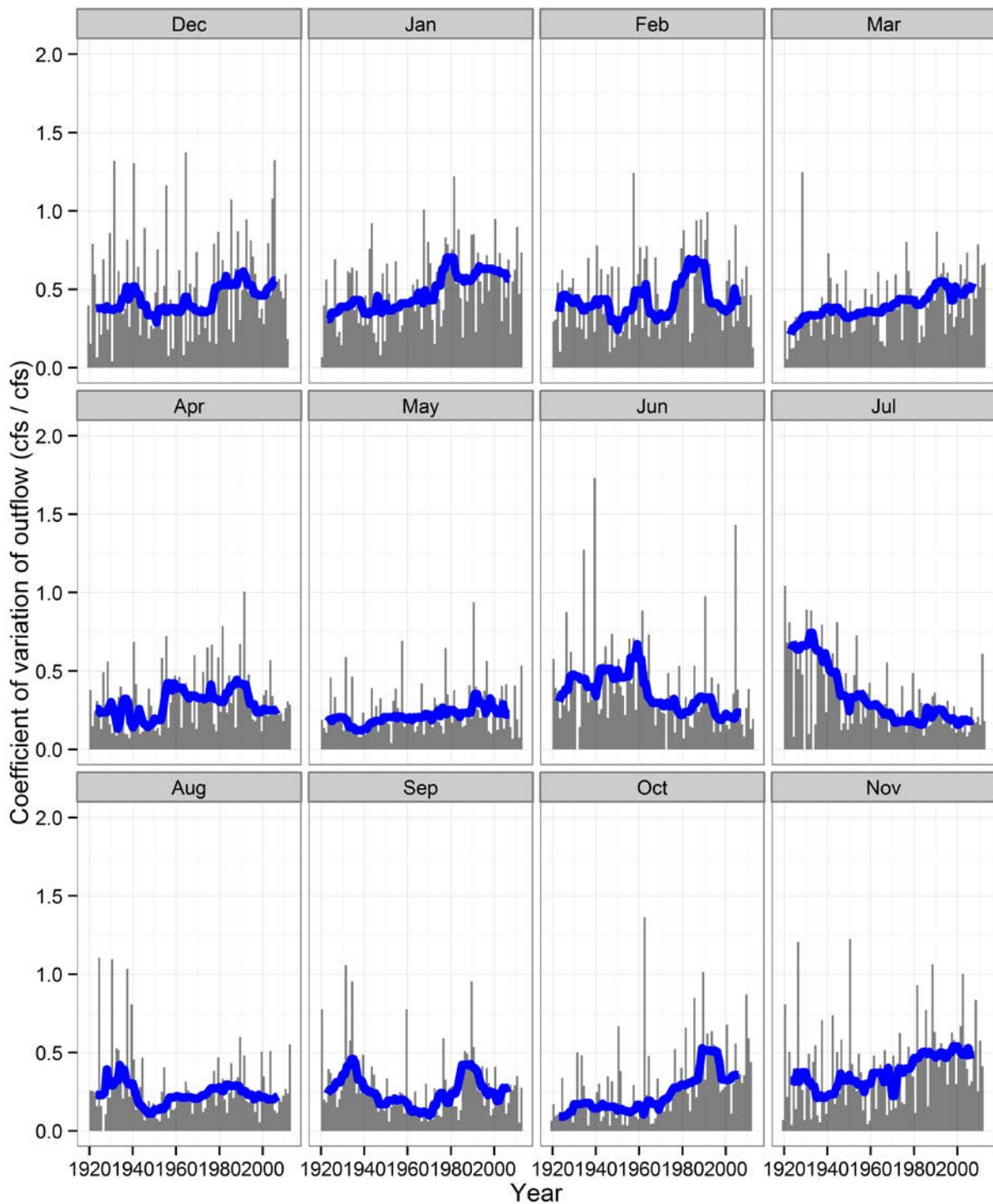


Figure 5-8 Time series of coefficient of variations of Delta outflow, with 10-year running medians shown in blue. Calculations were performed on daily flow data within each calendar month, and the time series of the monthly values across different years is shown here. Five outliers are excluded from the plot due to choice of y-axis limits.

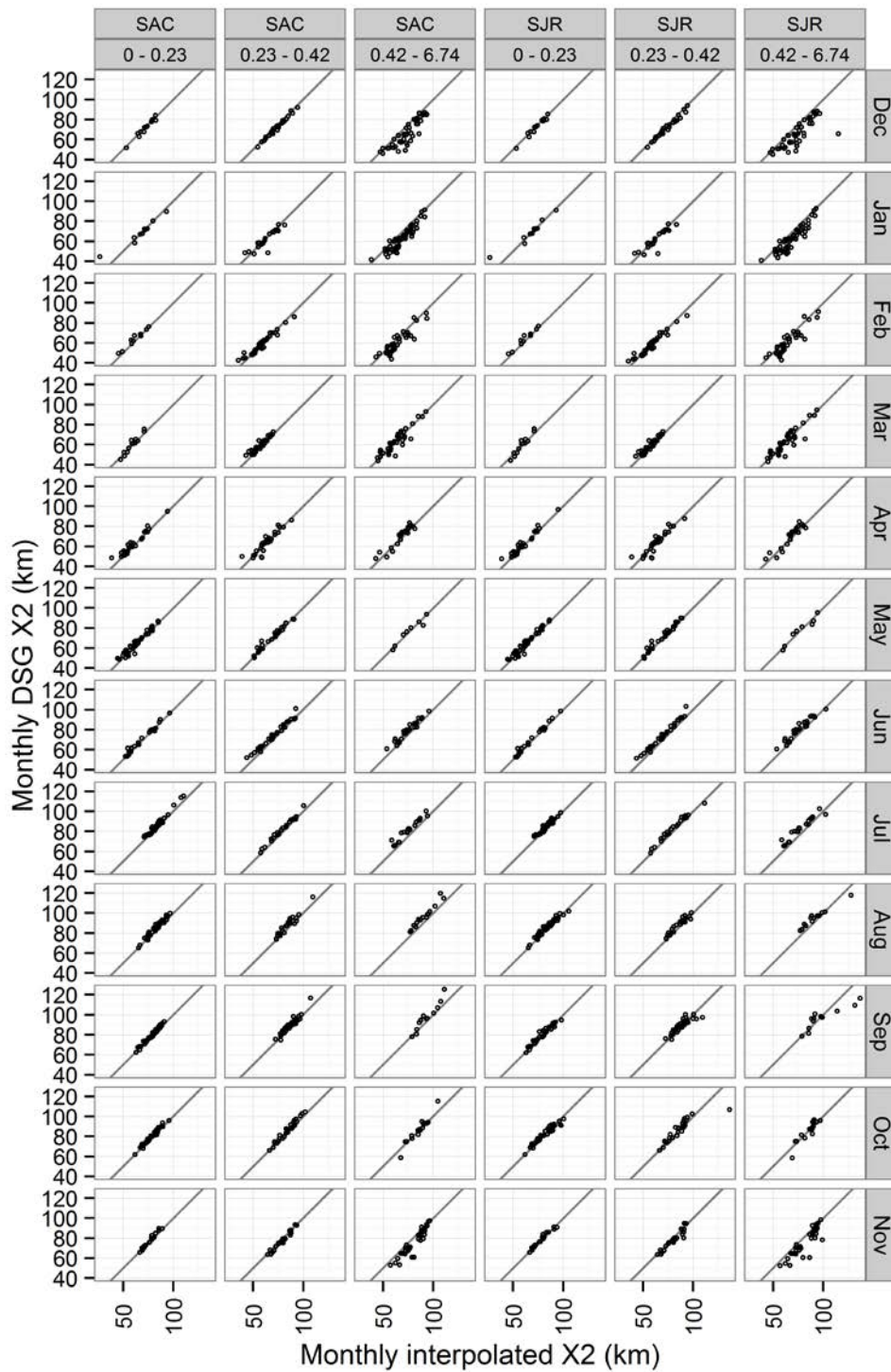


Figure 5-9 Scatter plots of modelled monthly DSG X2 positions against the monthly interpolated X2 positions, grouped by month, river, and three different ranges of CVs for monthly flow. The CV ranges are the lower, middle, and upper thirds of the flow CV data. The diagonal lines are 1:1 lines.

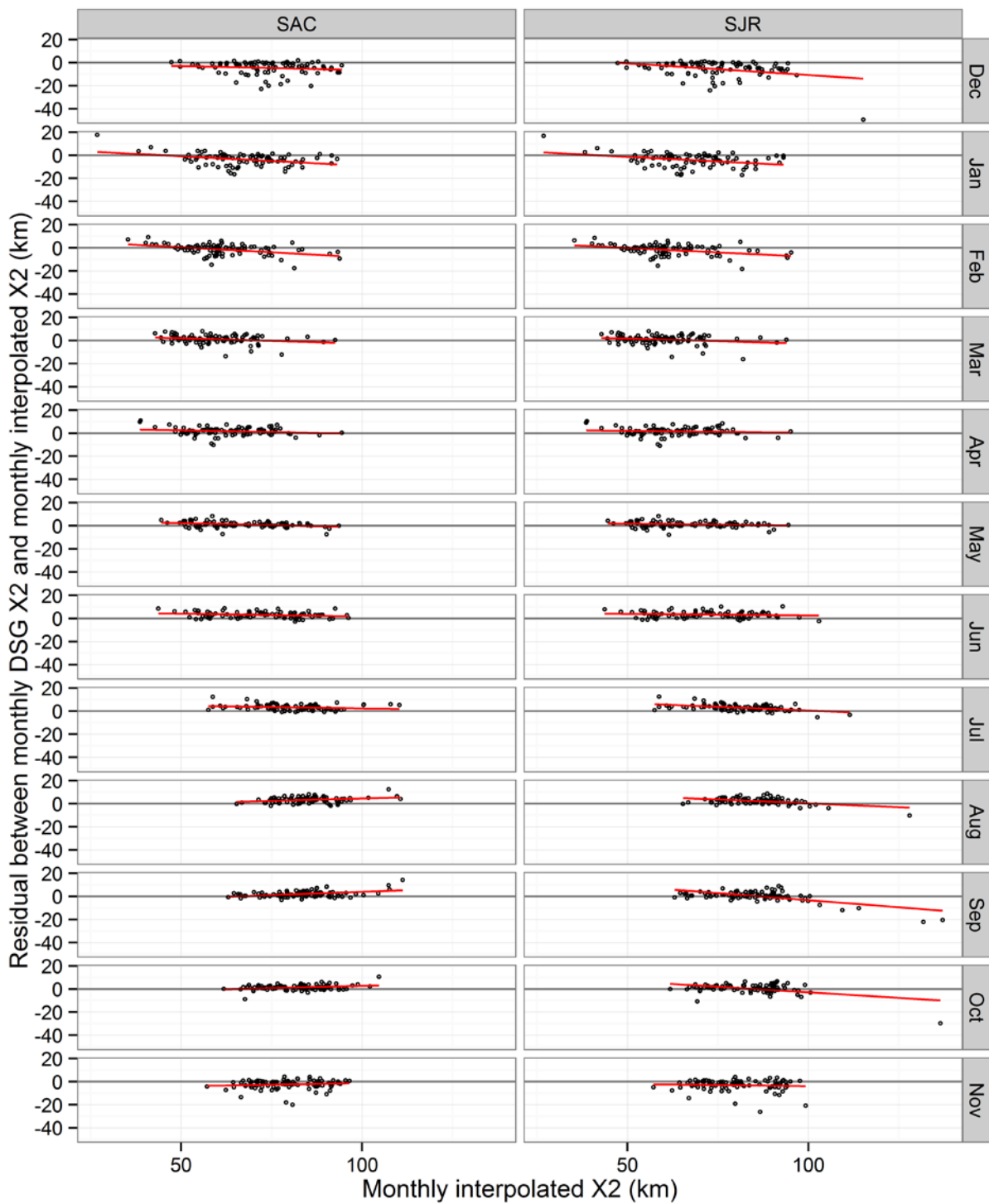


Figure 5-10 Scatter plots of DSG model residuals, grouped by month and river. Within each panel, a linear bias-correction model is displayed as a red line.

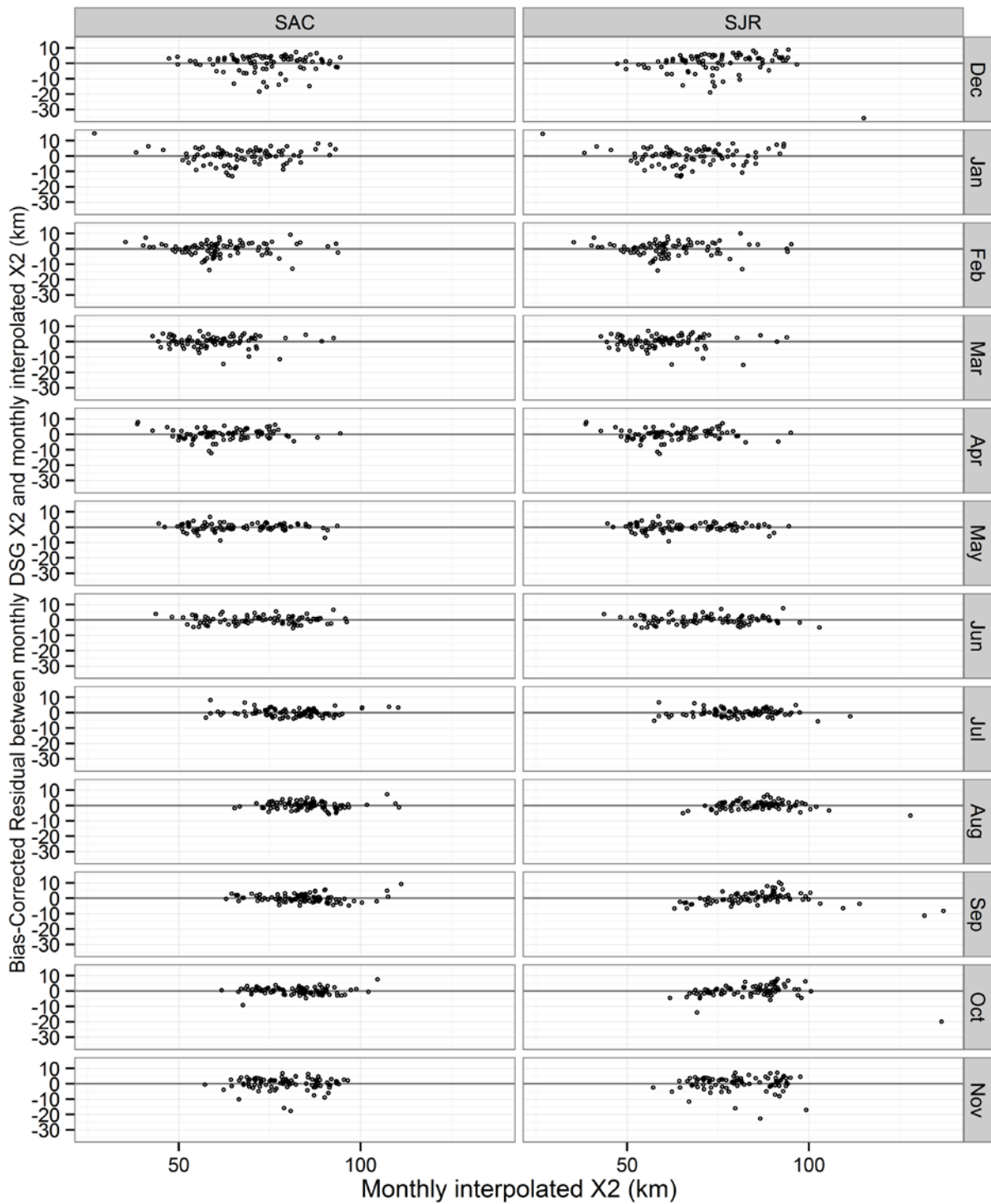


Figure 5-11 Scatter plots of DSG model residuals adjusted by the bias-correction model of Figure 5-10.

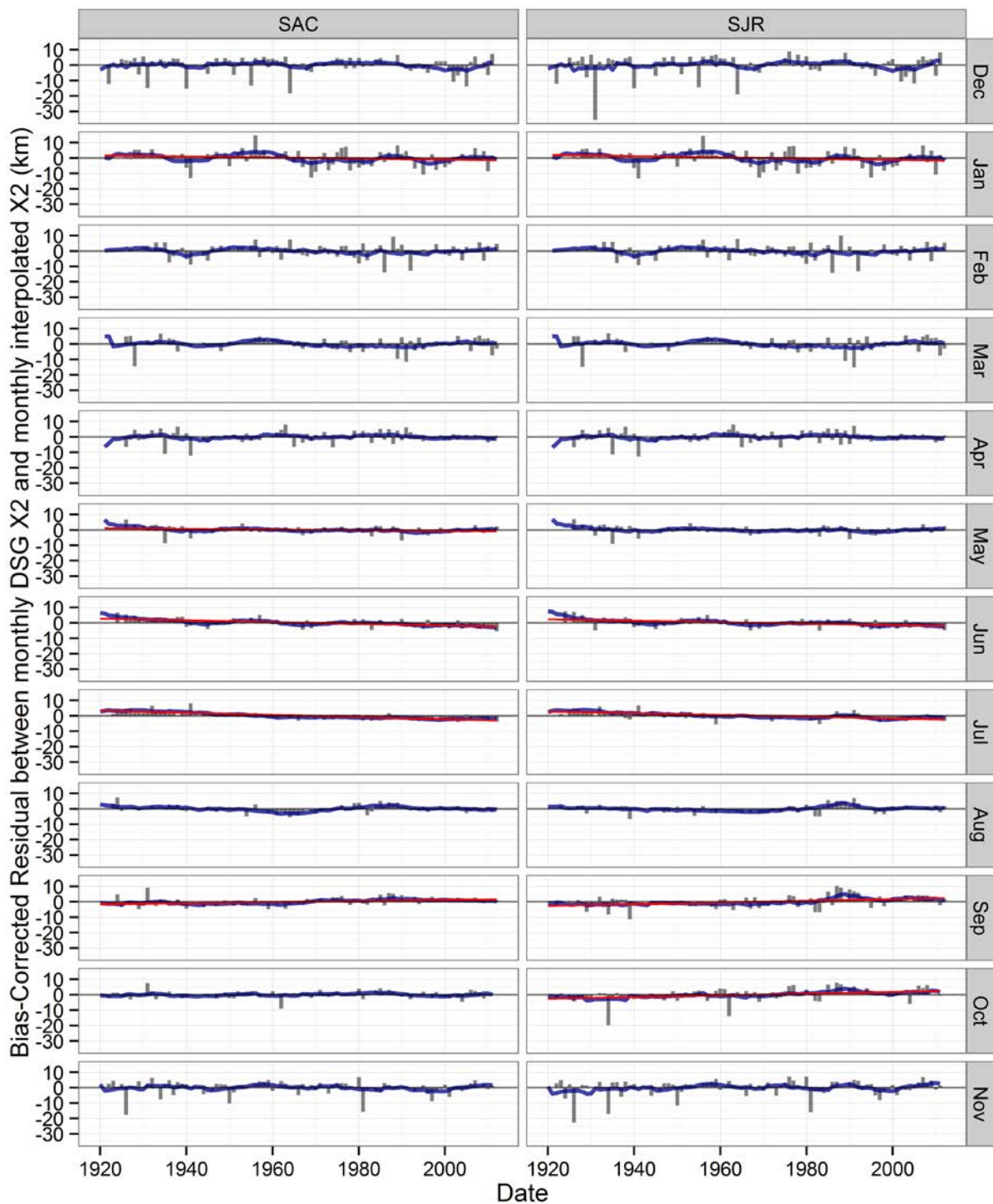


Figure 5-12 Time series of DSG model residuals adjusted by the bias-correction model of Figure 5-10. The blue line is a 10-year running average. The red line, when present, indicates a linear time trend with a slope significant at the 5% level.

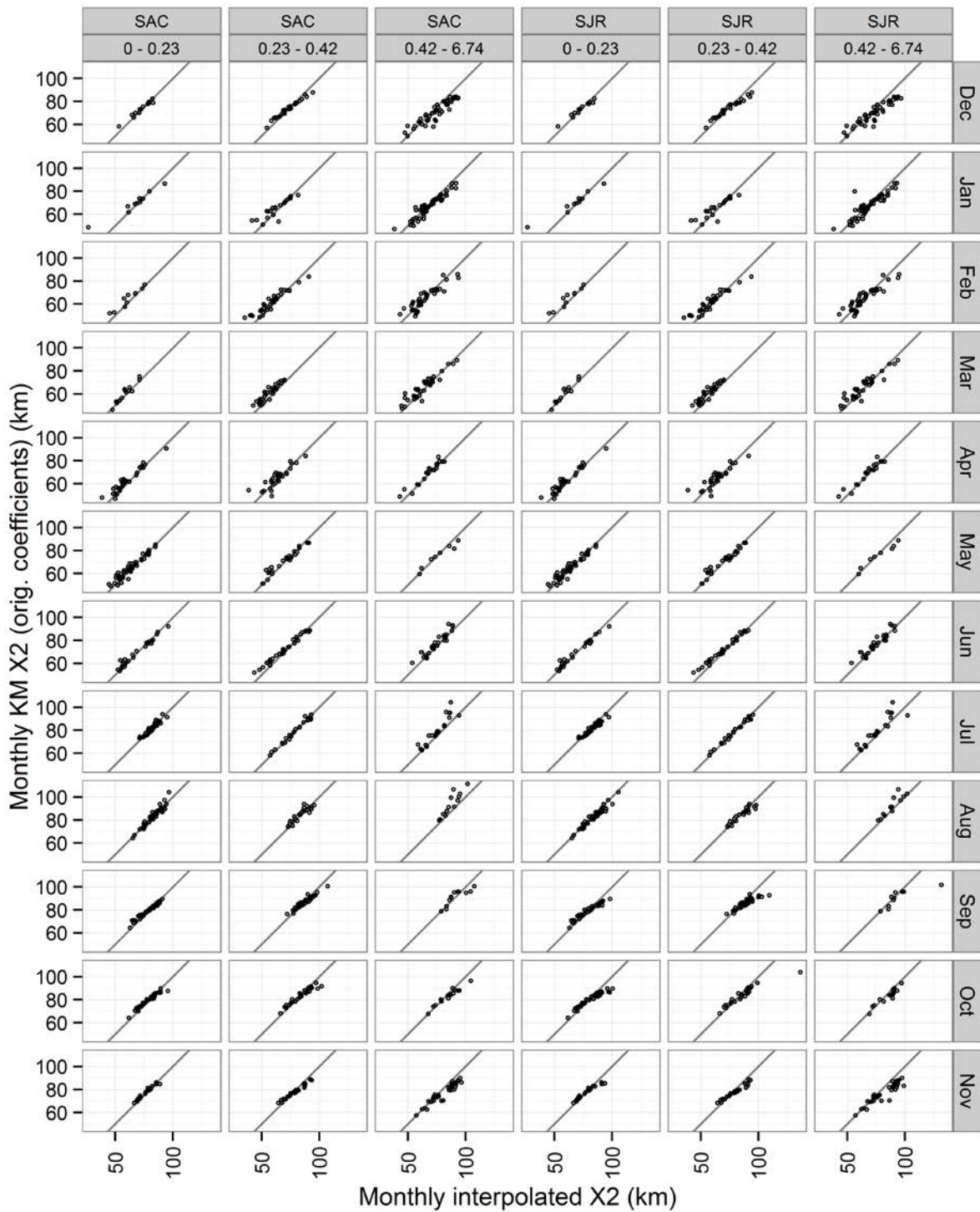


Figure 5-13 Scatter plots of modelled monthly Kimmerer-Monismith X2 positions against the monthly interpolated X2 positions, grouped by month, river, and three different ranges of CVs for monthly flow. The CV ranges are the lower, middle, and upper thirds of the flow CV data. The diagonal lines are 1:1 lines.

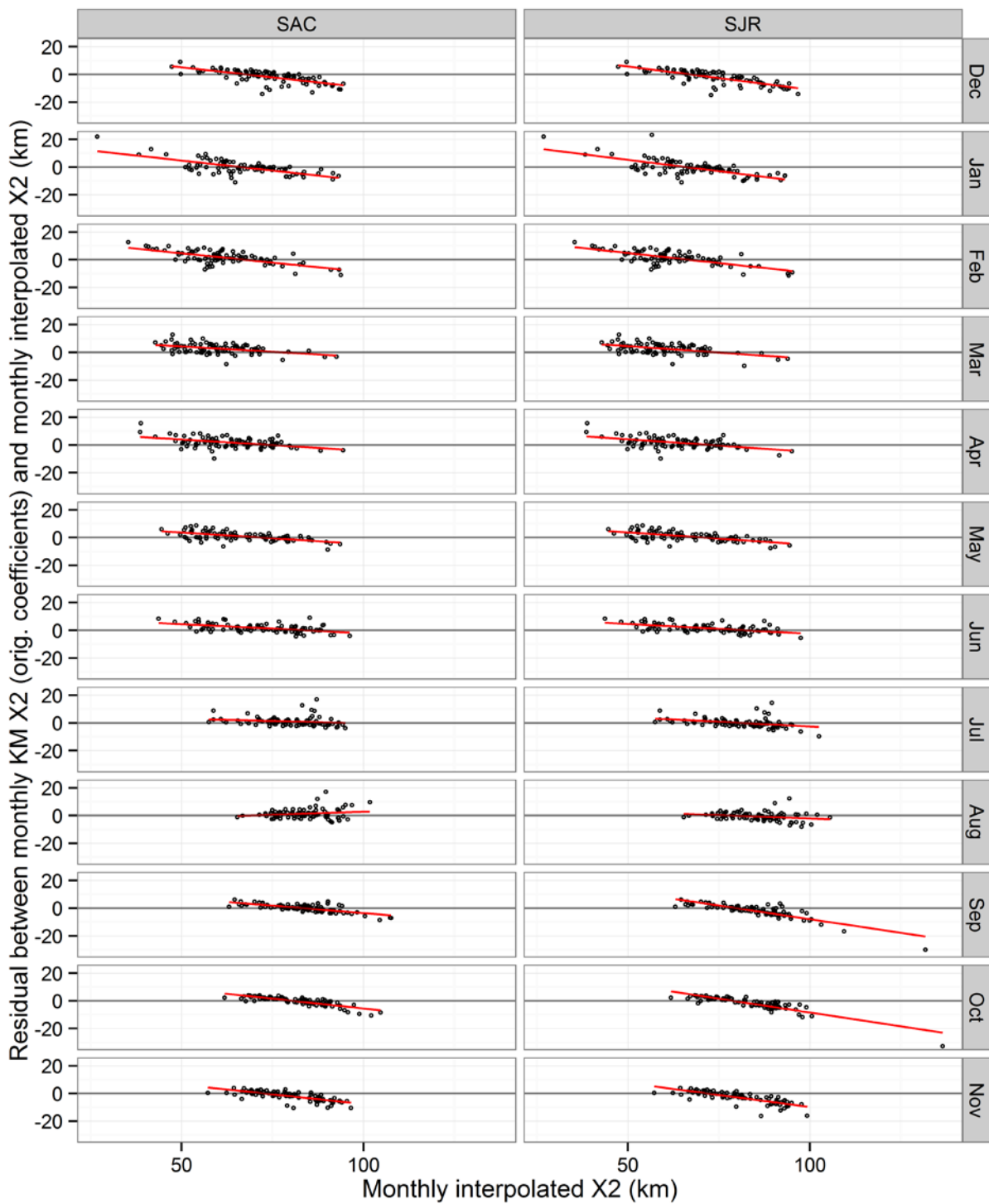


Figure 5-14 Scatter plots of K-M model residuals, grouped by month and river. Within each panel, a linear bias-correction model is displayed as a red line.

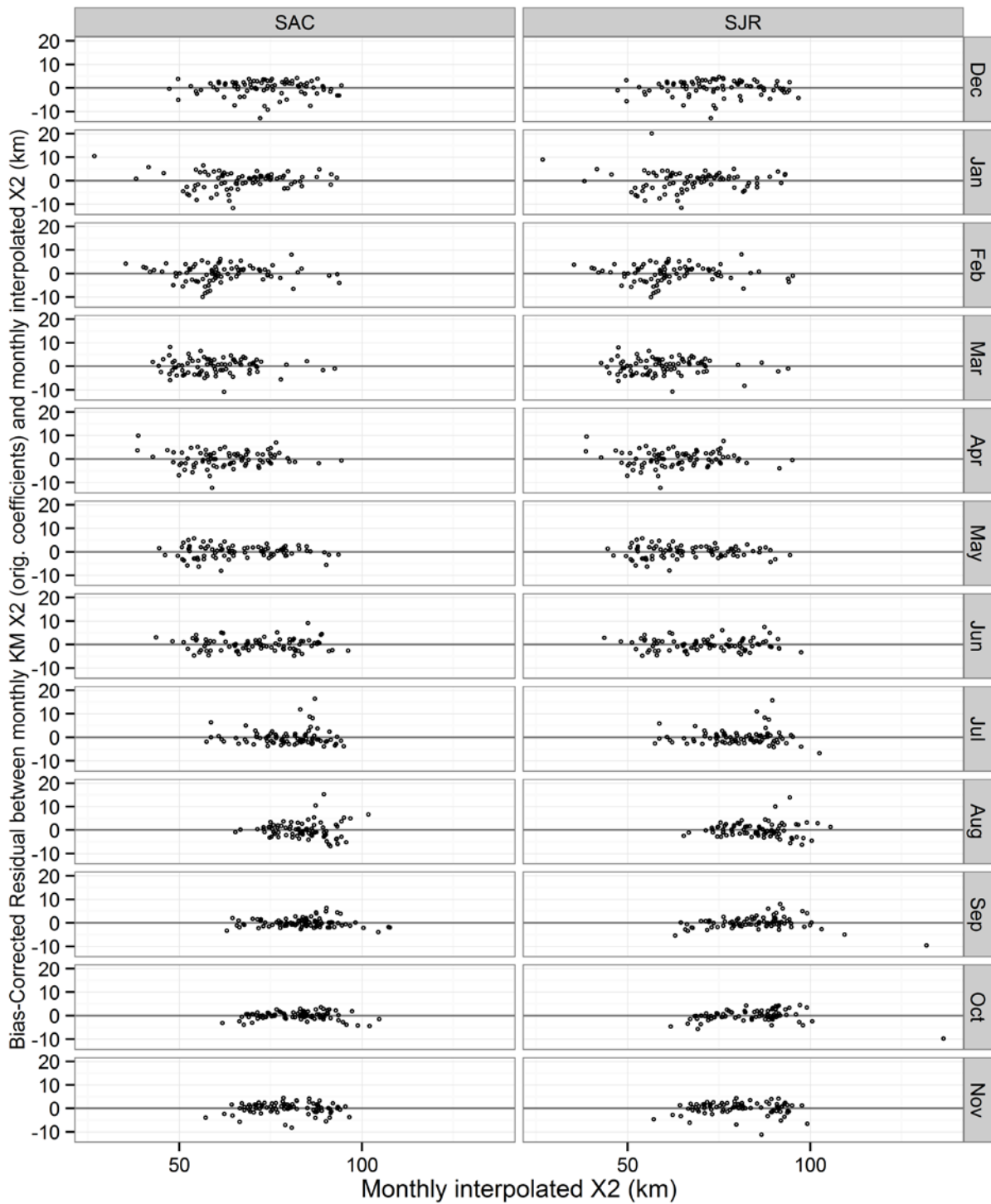


Figure 5-15 Scatter plots of K-M model residuals adjusted by the bias-correction model of Figure 5-14.

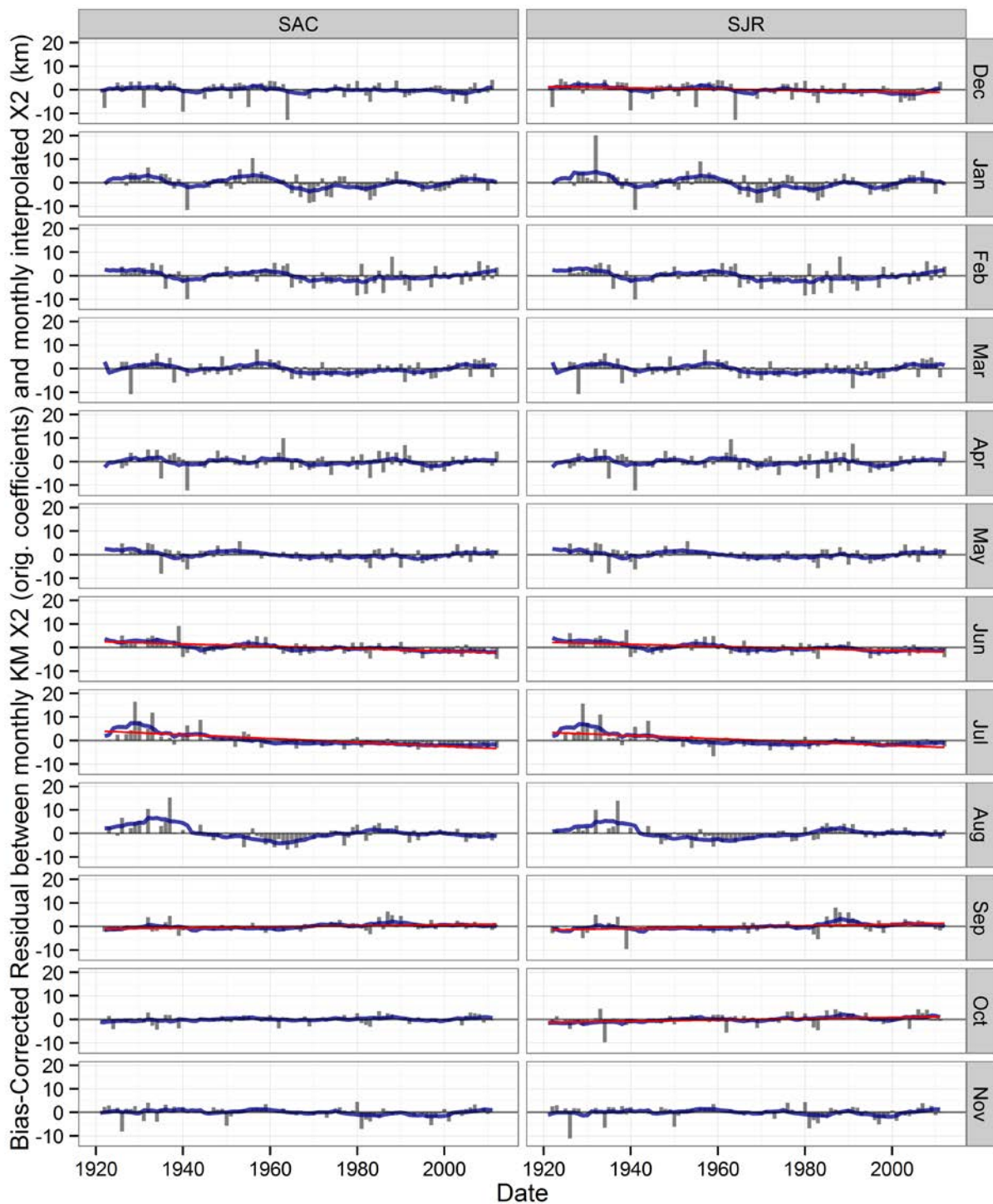


Figure 5-16 Time series of K-M model residuals adjusted by the bias-correction model of Figure 5-14. The blue line is a 10-year running average. The red line, when present, indicates a linear time trend with a slope significant at the 5% level.

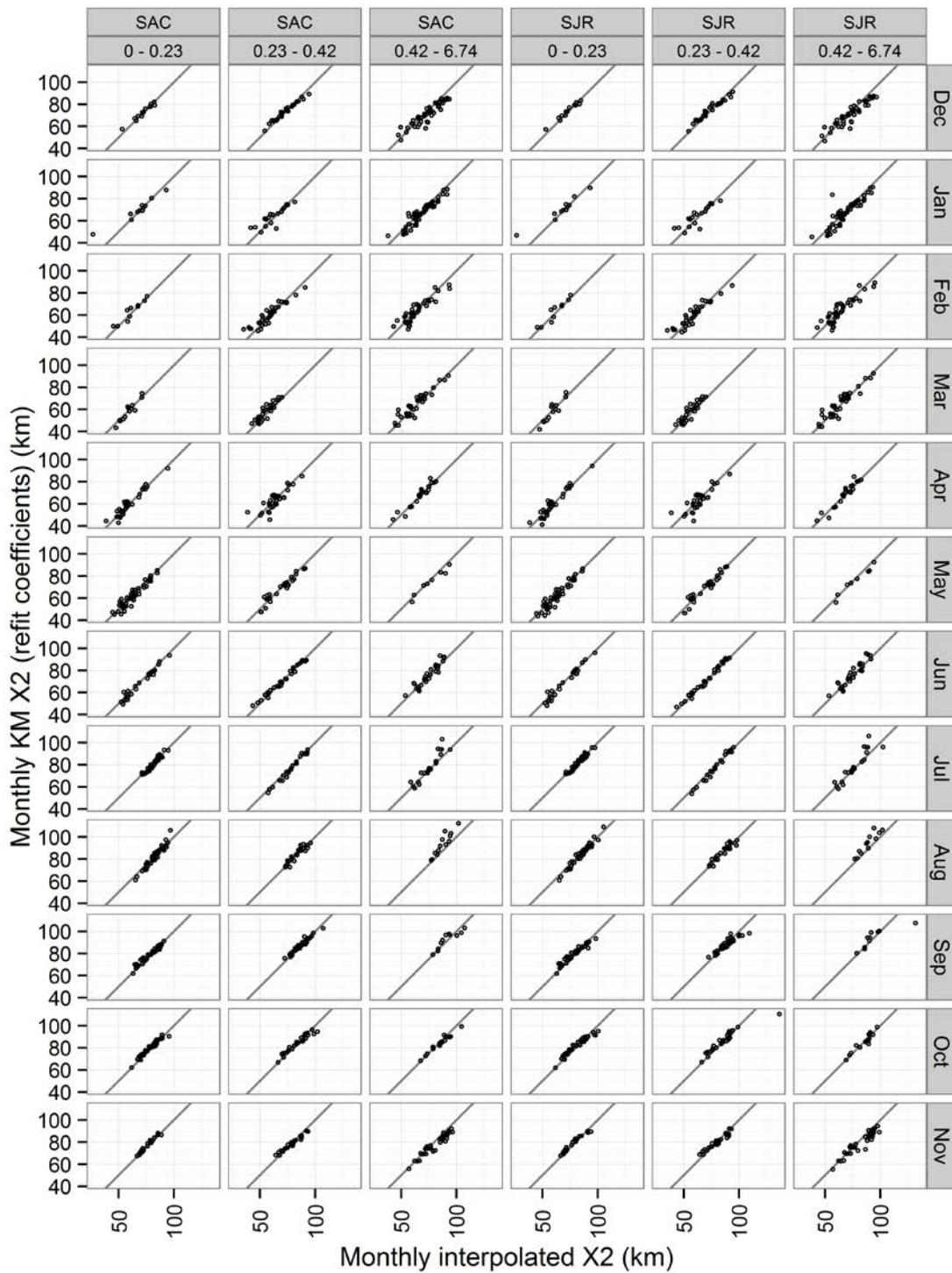


Figure 5-17 Scatter plots of modelled monthly Kimmerer-Monismith X2 (with refit coefficients) positions against the monthly interpolated X2 positions, grouped by month, river, and three different ranges of CVs for monthly flow. The CV ranges are the lower, middle, and upper thirds of the flow CV data. The diagonal lines are 1:1 lines.

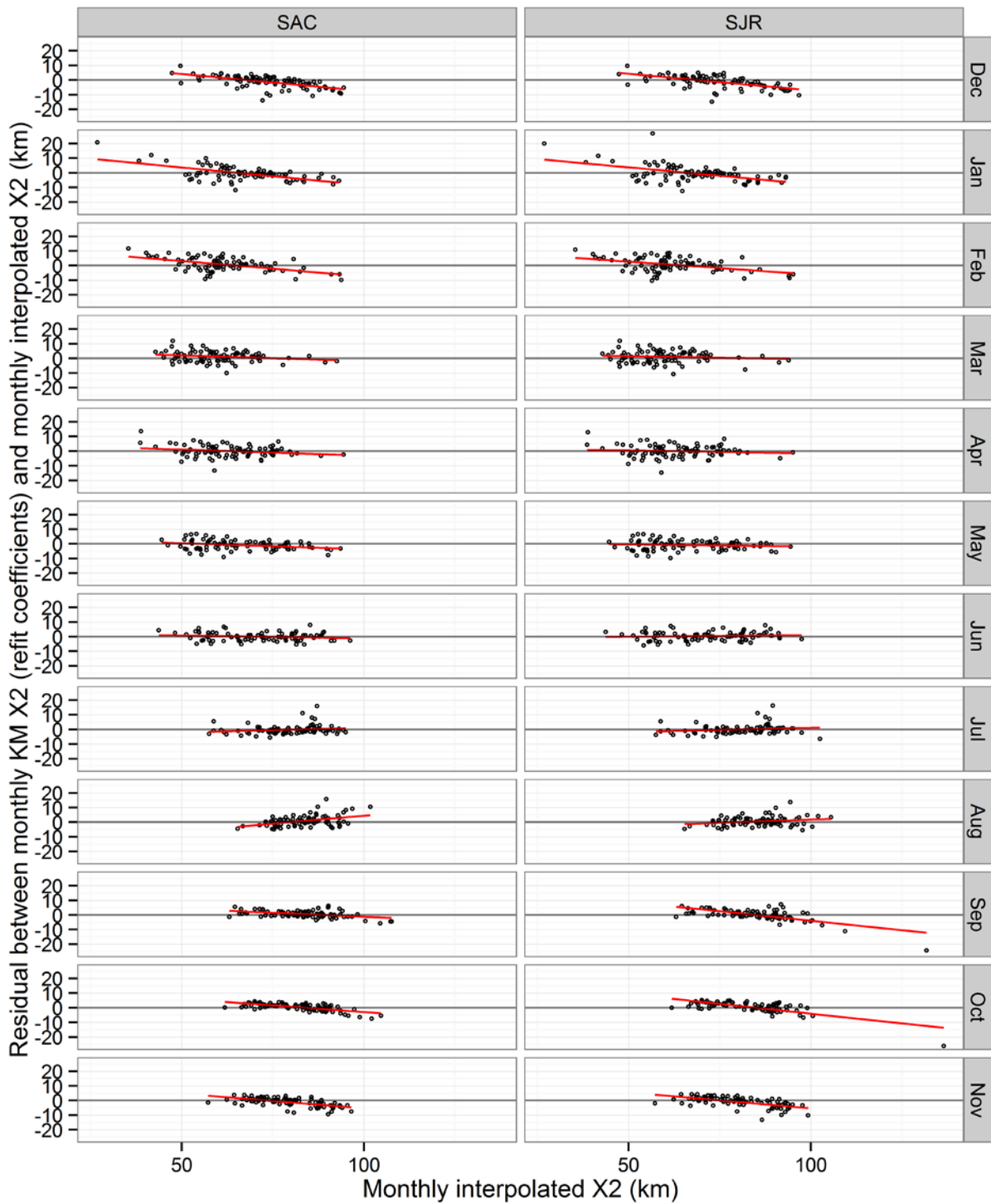


Figure 5-18 Scatter plots of K-M model (with refit coefficients) residuals, grouped by month and river. Within each panel, a linear bias-correction model is displayed as a red line.

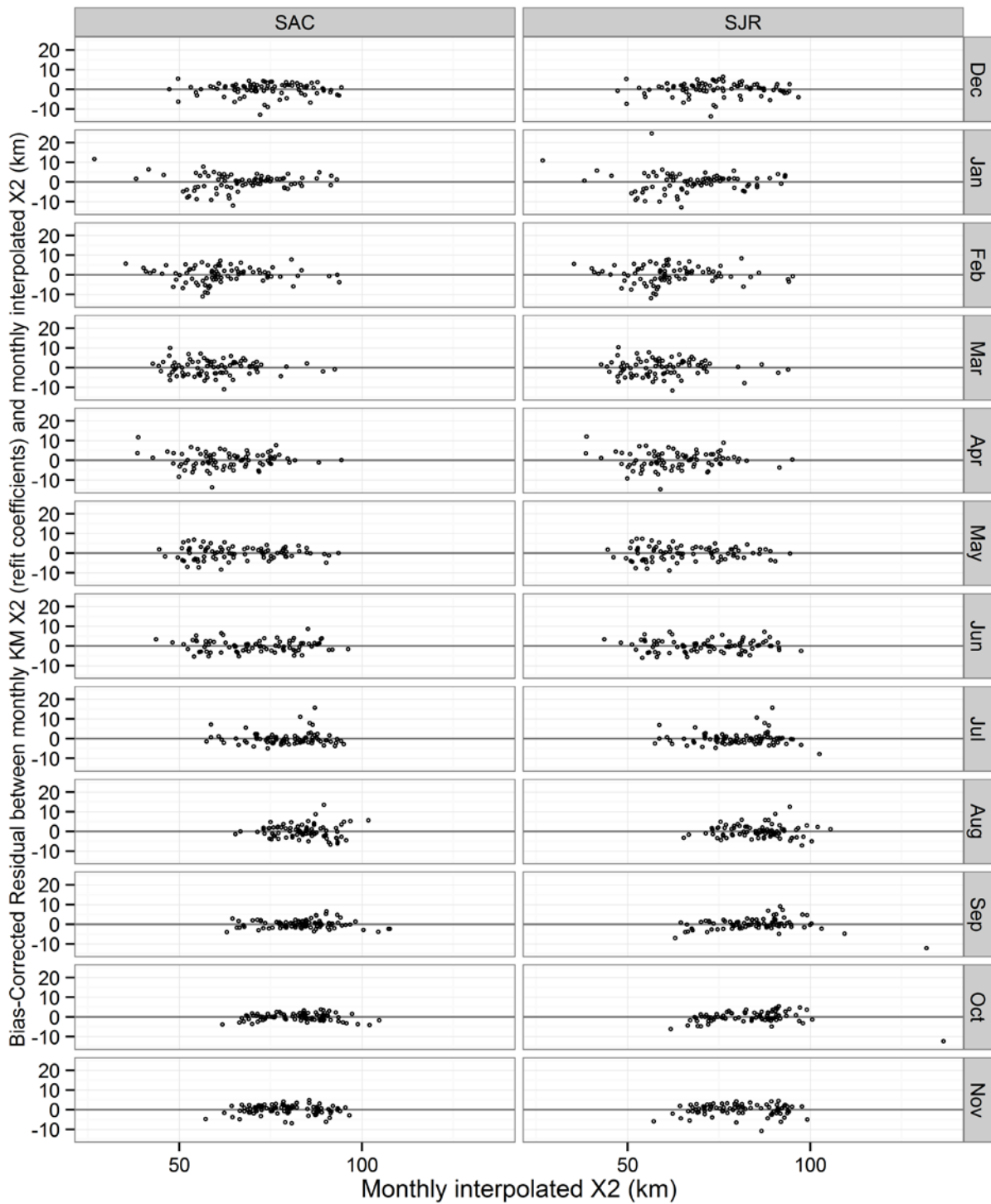


Figure 5-19 Scatter plots of K-M model (with refit coefficients) residuals adjusted by the bias-correction model of Figure 5-18.

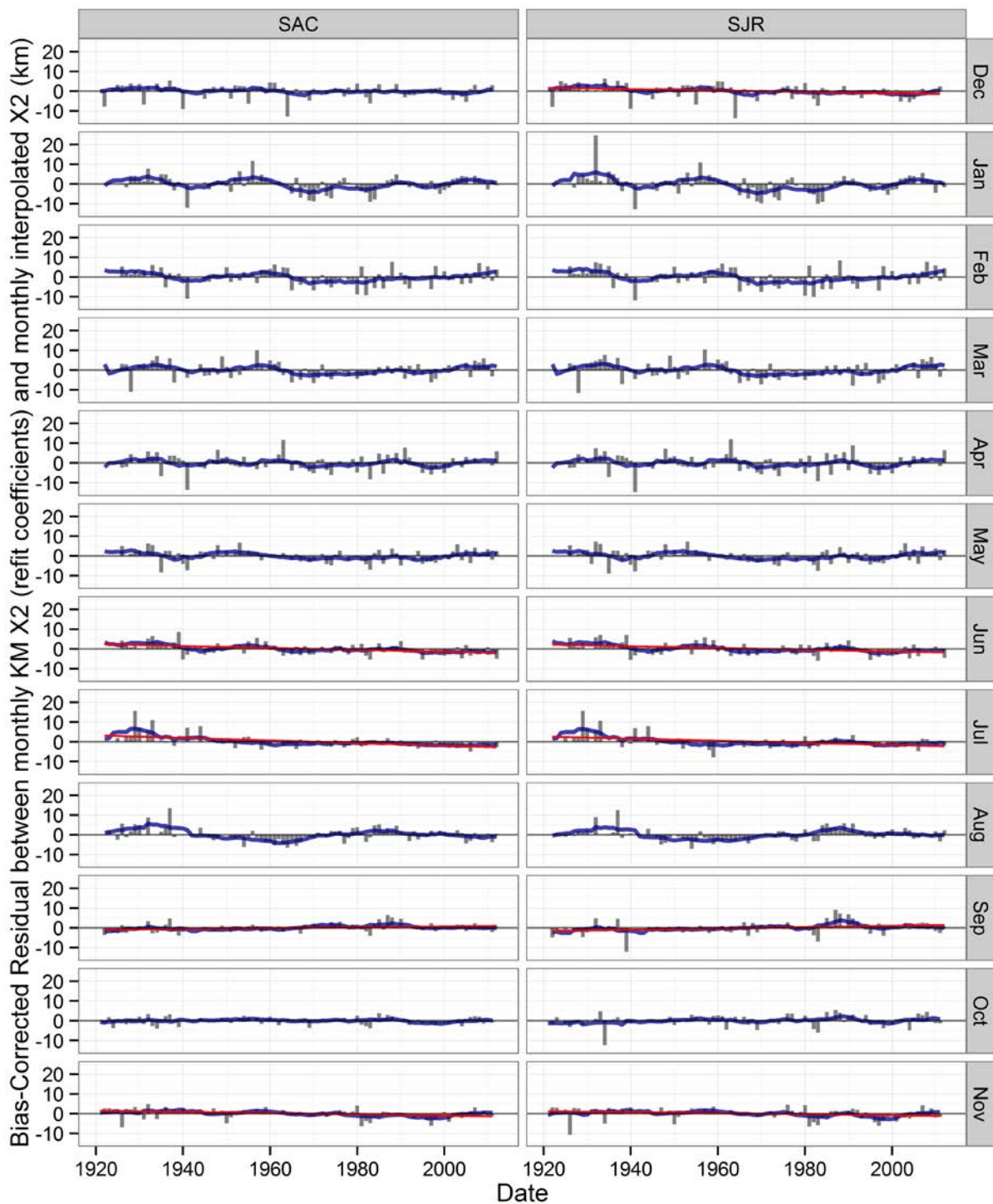


Figure 5-20 Time series of K-M model (with refitted coefficients) residuals adjusted by the bias-correction model of Figure 5-18. The blue line is a 10-year running average. The red line, when present, indicates a linear time trend with a slope significant at the 5% level.

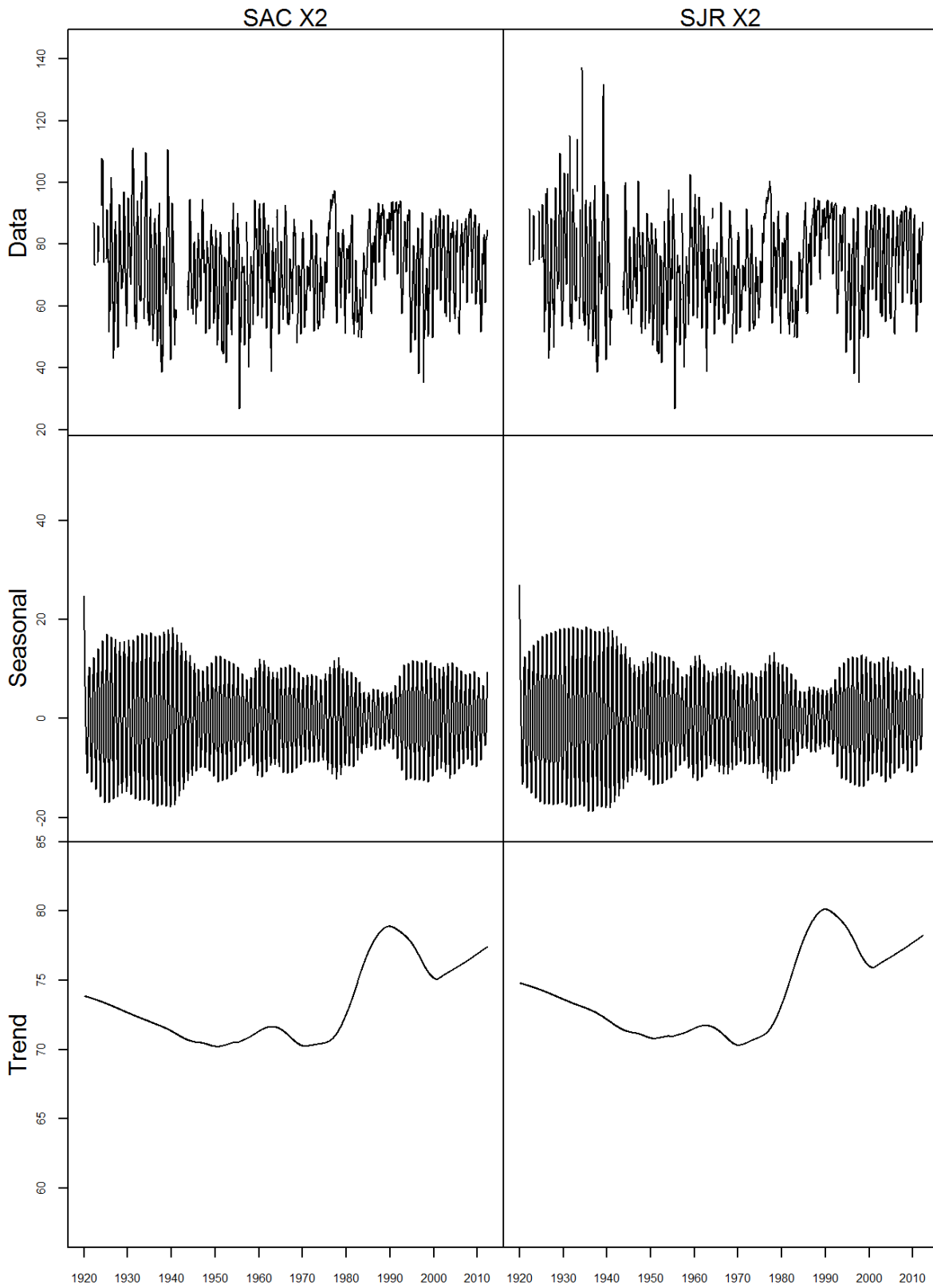


Figure 5-21 Trend decomposition of X2 time series data.

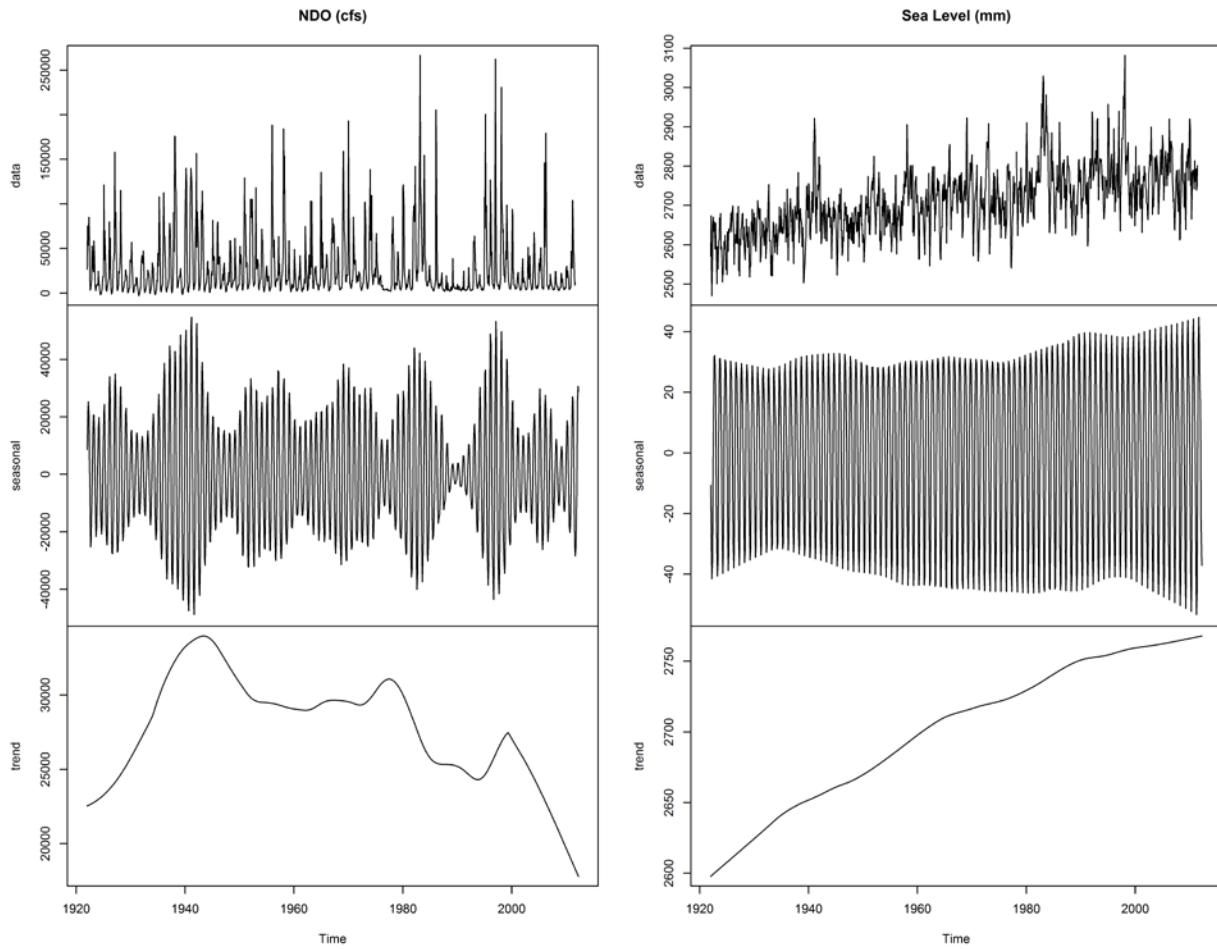


Figure 5-22 Trend decomposition of Delta outflow and sea level time series data.

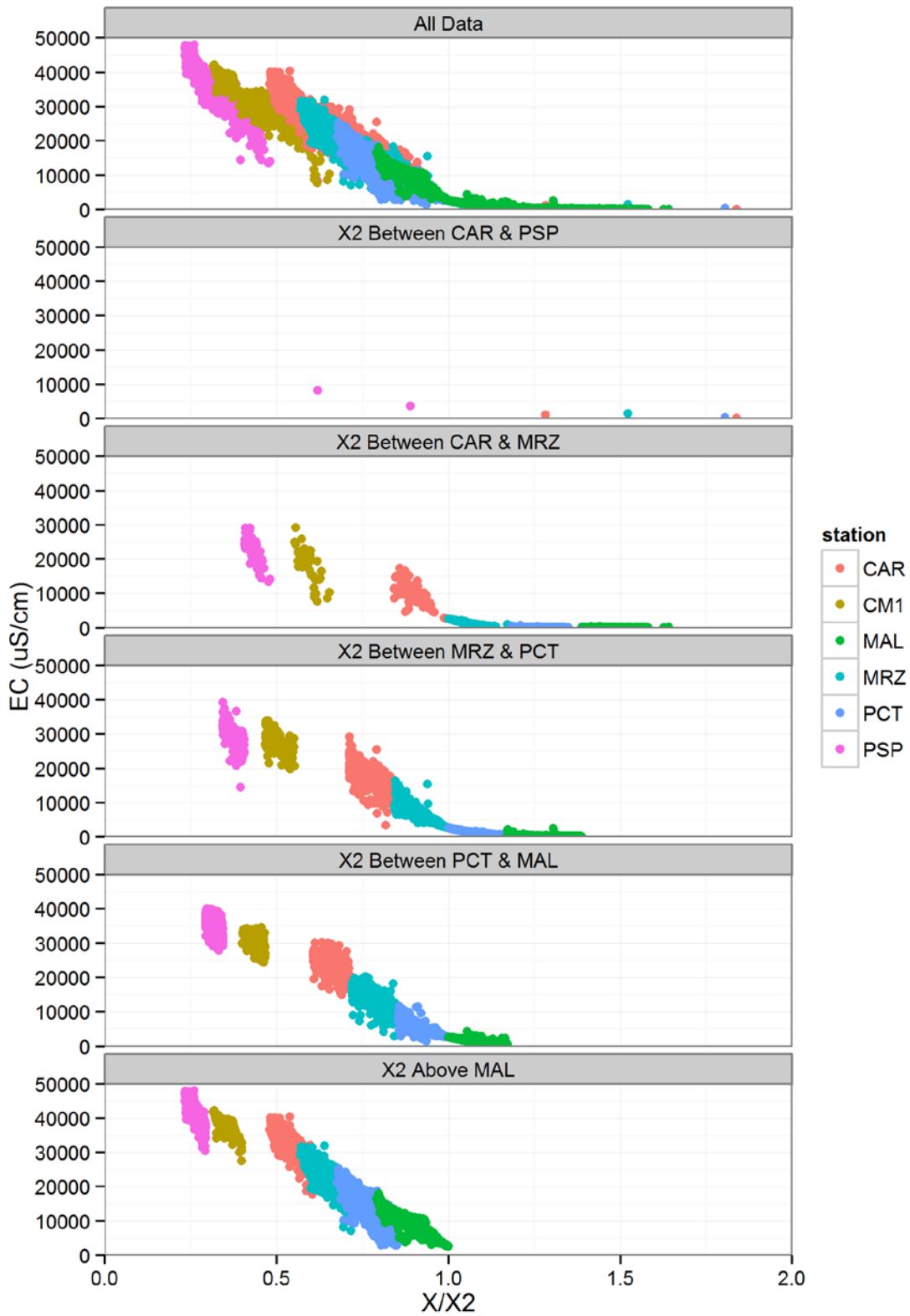


Figure 5-23 Salinity structure in Bay and Delta stations using surface salinity values as a function of station distance normalized by X2 and grouped by X2 position.

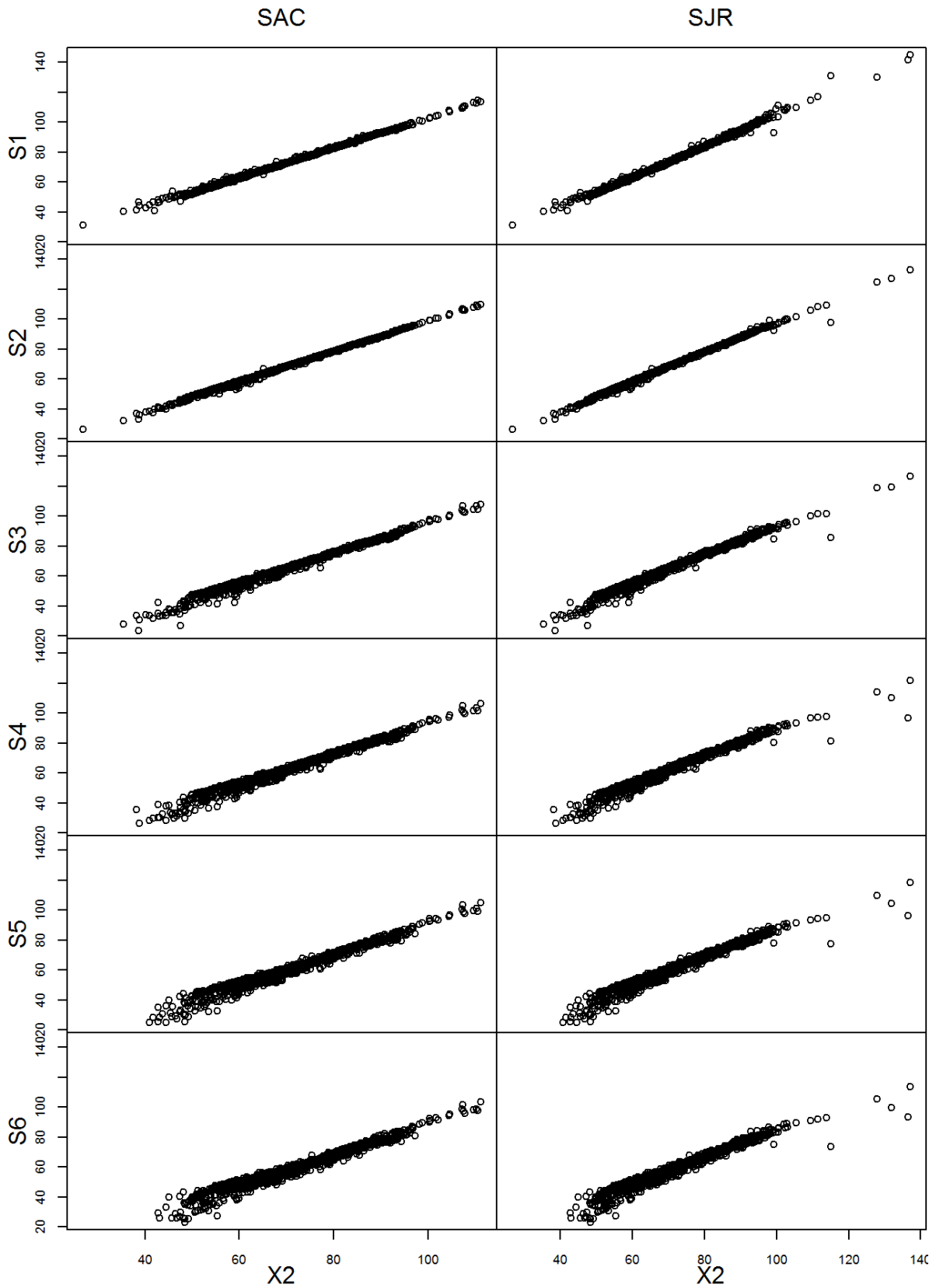


Figure 5-24 Comparison of isohaline position S1 through S6 to X2.

6. DISCUSSION

This work integrated salinity data in the Suisun Bay and western Delta from different sources over more than nine decades. Over this period there were some well-established differences in sampling and analytical methodology, such as the station locations, the sampling frequency, and the method of salinity determination. Data were converted to a monthly set of EC values using the best available information on unit conversion and tidal effects. However, other subtle variations are also possible over this extended time period, such as the location of specific stations in relation to the estuary centerline and nearby watershed effects, the limited number of data points collected using grab samples in the 1921–1967 period, and, over the last few decades, changes in protocols for conductivity sensor maintenance and cleaning. These, and other unknown variations over the period of record, were not fully resolved during this study. Recognizing that potential errors related to these causes may have occurred in the data set, we performed a cleaning effort by considering paired stations to identify potentially erroneous values. This approach was needed because, in the absence of gross errors in the data (zero values, value shifts by orders of magnitude, etc.), there is no *a priori* way to tell if a specific station value is erroneous. As described in prior sections, this procedure led to some data being rejected, but nonetheless resulted in a monthly average EC data set where the behavior of lower salinity points in particular did not always conform to the expected conceptual model of decreasing salinity with increasing distance from Golden Gate.

Despite the limitations of the data noted above, we used the cleaned salinity record to estimate daily and monthly isohaline position. This step must acknowledge that errors in the currently cleaned data may continue to exist, and potentially affect the isohaline location where lower salinity values in the more eastern stations ($<1,000 \mu\text{s}/\text{cm}$) are used in the calculation. Because there were limited data in the bay stations, another potential source of error related to the extrapolation of data in the bay, especially for high Delta outflow situations where the specific isohaline was downstream of Point Orient. While we acknowledge the limitations of the data, it is also important to highlight the benefits of using an integrated long-term data set for estimating isohalines in the estuary because it spans a much wider range of hydrologic conditions, river and Delta modifications, water exports, and watershed changes than considered in previously published data analyses (Fox et al., 1991; Enright and Culberson, 2009).

Using the X2 time series calculations for the Sacramento and San Joaquin Rivers, we found a relationship between X2 and Delta outflows with increasing X2 values at lower flows, consistent with previous observations (Jassby et al., 1995). The longer term monthly data, split up into different time intervals, were fit using an auto-regressive equation structure as used by Kimmerer and Monismith (1992). The process resulted in a set of equations with coefficients that were similar to the original work, although the fit for the entire data set was somewhat poorer than reported by Kimmerer and Monismith (1992). When the equation was fit to a limited set of data, using periods where direct EC measurements were available, the

fits improved, reflecting perhaps the greater noise in the older data. An important finding from the fitting of the longer data set using the K-M approach is that the general structure of the model holds even though there have been significant changes in the Delta and Bay over this period (changes in channel depth, Delta exports, regulatory changes, upstream land use changes, and some mean sea level rise). While it is possible that the changes in the coefficients for different time periods of fitting encapsulate this information, it is not straightforward to infer the mechanistic linkage between a coefficient and one or more of these changes. The linkage between coefficients and related changes was not explored in detail in this work. Related to the issue of coefficient identification, we could not replicate the exact X₂ values that were used by Kimmerer and Monismith, and when the fitting was performed using only X₂ values from the 1967–1991 period that was used in the original study, the resulting coefficients were not identical to those reported by Kimmerer and Monismith (1992). At this point, in the absence of the raw data used for the original analysis, it is not clear how these differences can be fully resolved. Over the long term, the availability of a cleaned master data set for salinity, as produced here, may provide the foundation for additional salinity model development and refinement.

Two different forms of the Kimmerer and Monismith model (original coefficients and re-fit coefficients) and the Delta Salinity Gradient (DSG) model (Hutton, 2013) were used for additional evaluation using the interpolated X₂ values developed in this work. Primarily we looked at the residuals between the modeled and the interpolated X₂ and how these changed as a function of X₂ and over time. The models captured major features of the interpolated X₂ but there were differences in the nature of the fit and bias. The largest systematic disagreements between modeled and interpolated X₂s occur for interpolated X₂s at the extreme ends of its range. For all three models, the change in long-term behavior of the model residuals was small compared to the disagreements between model and interpolated X₂ positions under extreme salinity conditions. For future application, we reported the linear function representing bias (function of X₂ and month) for each of the models. These linear equations can be used to correct K-M or DSG-predicted X₂ values. This evaluation of the bias between interpolated and modeled X₂ provides insight into the future use of these models, especially where inferences are to be drawn between small differences in X₂ or for conditions where X₂ values fall in extreme high or low ranges.

Aside from comparison with models, the interpolated X₂ values were subject to a variety of statistical tests. When the interpolated X₂ values were grouped by water year type and compared across the pre- and post-project periods (1921–1967 and 1968–2012), a difference in the X₂ position was noted in the wet months of drier years: X₂ was higher in the more recent period during the wet months. Similarly in the dry months of dry years, X₂ was lower in the post-project period. These visual observations were supported by a trend analysis that showed statistically significant increases in X₂ from November through May (excluding March) over the entire period, and a statistically significant decrease in X₂ in August and September. These findings were broadly true for X₂ computed along both the Sacramento and San Joaquin Rivers.

The longer data record was used to investigate the significance of the self-similarity of the data in the Bay-Delta that was previously reported for a limited time period using depth-averaged data (Jassby et al., 1995). The analysis presented here shows the limitations of self-

similarity during higher flows, especially when based only on surface salinity data. This breakdown of the structure appears to be related to the greater vertical stratification at higher flows. A parallel effort to the present analysis is focused on developing an artificial neural network for salinity in the Suisun Bay and western Delta (in progress), and the self-similarity analysis presented here supports the use of a more complex relationship between surface salinity and station location normalized by X2.

The data integration presented through this work serves as a foundation for the continuing analysis of salinity behavior in the San Francisco Bay and Delta, where the inherent variability of this constituent benefits from the use of the longest possible data record. The findings presented above, to a certain degree, are a function of the data and the cleaning procedure employed in this work. Future work may consider additional stations with grab sample salinity data, alternative strategies to improve the cleaning methodology, and reexamine the findings presented here.

7. REFERENCES

- Cleveland, R. B., Cleveland, W. S., McRae, J. E., & Terpenning, I. (1990). STL: A seasonal-trend decomposition procedure based on loess. *Journal of Official Statistics*, 6(1), 3-73.
- Contra Costa Water District (CCWD) (2010) Historical fresh water and salinity conditions in the Western Sacramento–San Joaquin Delta and Suisun Bay, Technical Memorandum WR10-001.
- Denton, R.A. and G.D. Sullivan (1993) Antecedent flow-salinity relations: Application to Delta Planning Models, report from Contra Costa Water District.
- Denton, Richard (1994) Predicting Surface 14-day EC from NDO, memo to Paul Hutton, April, 12.
- Denton, Richard (2013) Delta Salinity Constituent Analysis, Municipal Water Quality Investigation Special Study for the State Water Contractors, March, DRAFT.
- Department of Public Works, Division of Water Resources (1930 to 1955) Bulletin 23 Report of the Sacramento–San Joaquin Water Supervisor For the Period 1924–1954.
- Department of Public Works, Division of Water Resources (1931) Bulletin 27 Variation and Control of Salinity in the Sacramento–San Joaquin Delta and Upper San Francisco Bay.
- Department of Water Resources (DWR) (1956 to 1962) Bulletin 23 Report of the Sacramento–San Joaquin Water Supervisor For 1955–1961.
- Department of Water Resources (DWR) (1957) Joint Hydrology Study: Sacramento River and Sacramento–San Joaquin River Delta, Division of Planning, July.
- Department of Water Resources (DWR) (1962) Bulletin 65 Hydrologic Data 1962.
- Department of Water Resources (DWR) (1963 to 1971) Bulletin 130 Hydrologic Data 1963–1971.
- Enright, C., and S.D. Culberson (2009) Salinity trends, variability, and control in the northern reach of the San Francisco Estuary, *San Francisco Estuary and Watershed Science*, Vol. 7, No. 2.
- Feyrer, F., Nobriga, M. L., & Sommer, T. R. (2007). Multidecadal trends for three declining fish species: habitat patterns and mechanisms in the San Francisco Estuary, California, USA. *Canadian Journal of Fisheries and Aquatic Sciences*, 64(4), 723–734.

- Feyrer, F., Newman, K., Nobriga, M., & Sommer, T. (2011). Modeling the effects of future outflow on the abiotic habitat of an imperiled estuarine fish. *Estuaries and Coasts*, 34(1), 120–128.
- Finch, R. and N. Sandhu. (1995). Artificial neural networks with application to the Sacramento – San Joaquin Delta. California Department of Water Resources Delta Modeling Section, Division of Planning.
- Fox, J. P., Mongan, T. R., & Miller, W. J. (1990). Trends in freshwater inflow to San Francisco Bay from the Sacramento–San Joaquin Delta, *Journal of the American Water Resources Association*, 26(1), 101–116.
- Fox, J. P., Mongan, T. R., & Miller, W. J. (1991). Long-term annual and seasonal trends in surface salinity of San Francisco Bay. *Journal of hydrology*, 122(1), 93-117.
- Gilbert, R. 1987. *Statistical Methods For Environmental Pollution Monitoring*. Van Nostrand Reinhold Co., NY. 320 pp.
- Gross, E. S., MacWilliams, M. L., & Kimmerer, W. J. (2010). Three-dimensional modeling of tidal hydrodynamics in the San Francisco Estuary. *San Francisco Estuary and Watershed Science*, 7(2).
- Gross, E. S., Nidzieko, N. J., MacWilliams, M. L., & Stacey, M. T. (2007). Parameterization of Estuarine Mixing Processes in the San Francisco Estuary based on Analysis of Three-Dimensional Hydrodynamic Simulations. In *Estuarine and Coastal Modeling (2007)* (pp. 322–338). ASCE.
- Hill, K., Dauphinee, T., & Woods, D. (1986). The extension of the Practical Salinity Scale 1978 to low salinities. *Oceanic Engineering, IEEE Journal of*, 11(1), 109–112.
- Hutton, P.H. (2013) A New Empirical Bay-Delta Salinity Model, presentation at California Water and Environmental Modeling Forum, April 24, 2013.
- Jassby, A. D., W. J. Kimmerer, S. G. Monismith, C. Armor, J. E. Cloern, T. M. Powell, J. R. Schubel and T. J. Vendlinski. (1995). Isohaline position as a habitat indicator for estuarine populations. *Ecological Applications*, 5: 272–289.
- Kimmerer, W. and S. Monismith. (1992). An Estimate of the Historical Position of 2PPT Salinity in the San Francisco Bay Estuary. Issue Paper prepared for the fourth technical workshop on salinity, flows, and living resources of the San Francisco Bay/Delta Estuary. August 1992. Available online at: http://www.calwater.ca.gov/Admin_Record/C047938.pdf.
- Kimmerer, W. J., Gross, E. S., & MacWilliams, M. L. (2009). Is the response of estuarine nekton to freshwater flow in the San Francisco Estuary explained by variation in habitat volume? *Estuaries and Coasts*, 32(2), 375–389.
- MacWilliams, M. L., Gross, E. S., & Kimmerer, W. Simulating Salt Intrusion into Suisun Bay and the Western Delta. Undated poster.

Mierzwa, M. (2002). Chapter 4: CALSIM versus DSM2 ANN and G-model Comparisons. Methodology for flow and salinity estimates in the Sacramento–San Joaquin Delta and Suisun Marsh. 23rd Annual Progress Report. June 2002.

Monismith, S. G., Kimmerer, W., Burau, J. R., & Stacey, M. T. (2002). Structure and flow-induced variability of the subtidal salinity field in northern San Francisco Bay. *Journal of Physical Oceanography*, 32(11), 3003–3019.

Moyle, P. B., Lund, J. R., Bennett, W. A., and Fleenor, W. E. (2010). Habitat variability and complexity in the Upper San Francisco Estuary. *San Francisco Estuary and Watershed Science*, 8(3).

Schemel, L. (2001) Simplified conversions between specific conductance and salinity units for use with data from monitoring stations, IEP Newsletter, Volume 14, No. 1.

Seneviratne, S., S.Wu, and Y. Liang. (2008). Chapter 3: Impacts of Sea Level Rise and Amplitude Change on Delta Operations. Methodology for flow and salinity estimates in the Sacramento – San Joaquin Delta and Suisun Marsh. 29th Annual Progress Report. June 2008.

Shellenbarger, G. G., and Schoellhamer, D. H. (2011). Continuous Salinity and Temperature Data from San Francisco Estuary, 1982–2002: Trends and the Salinity-Freshwater Inflow Relationship. *Journal of Coastal Research*, 27(6), 1191–1201.

Stahle, D. W., Therrell, M. D., Cleaveland, M. K., Cayan, D. R., Dettinger, M. D., and Knowles, N. (2001). Ancient blue oaks reveal human impact on San Francisco Bay salinity. *Eos, Transactions American Geophysical Union*, 82(12), 141–145.

State Water Resources Control Board (1999) Water Right Decision 1641, on the Internet at: http://www.swrcb.ca.gov/waterrights/board_decisions/adopted_orders/decisions/d1600_d1649/wrd1641.pdf.

Suits, R. (2002) Calibrating DSM2-QUAL dispersion factors to practical salinity, Chapter 6 in DWR 23rd Annual Progress Report, Methodology for Flow and Salinity Estimates in the Sacramento–San Joaquin Delta and Suisun Marsh, Delta Modeling Annual Report to the California State Water Resources Control Board.

U.S. Environmental Protection Agency (USEPA) (2012) Water Quality Challenges in the San Francisco Bay/Sacramento–San Joaquin Delta Estuary: EPA’s Action Plan.

U.S. Fish and Wildlife Service (USFWS) (2008) Formal Endangered Species Act Consultation on the Proposed Coordinated Operations of the Central Valley Project (CVP) and State Water Project (SWP), on the Internet at: http://www.fws.gov/sfbaydelta/documents/SWP-CVP_OPs_BO_12-15_final_OCR.pdf.

Venables, W. N. & Ripley, B. D. (2002) *Modern Applied Statistics with S*. Fourth Edition. Springer, New York. ISBN 0-387-95457-0.